

INFORMATION TO USERS

This dissertation was produced from a microfilm copy of the original document. While the most advanced technological means to photograph and reproduce this document have been used, the quality is heavily dependent upon the quality of the original submitted.

The following explanation of techniques is provided to help you understand markings or patterns which may appear on this reproduction.

1. The sign or "target" for pages apparently lacking from the document photographed is "Missing Page(s)". If it was possible to obtain the missing page(s) or section, they are spliced into the film along with adjacent pages. This may have necessitated cutting thru an image and duplicating adjacent pages to insure you complete continuity.
2. When an image on the film is obliterated with a large round black mark, it is an indication that the photographer suspected that the copy may have moved during exposure and thus cause a blurred image. You will find a good image of the page in the adjacent frame.
3. When a map, drawing or chart, etc., was part of the material being photographed the photographer followed a definite method in "sectioning" the material. It is customary to begin photoing at the upper left hand corner of a large sheet and to continue photoing from left to right in equal sections with a small overlap. If necessary, sectioning is continued again - beginning below the first row and continuing on until complete.
4. The majority of users indicate that the textual content is of greatest value, however, a somewhat higher quality reproduction could be made from "photographs" if essential to the understanding of the dissertation. Silver prints of "photographs" may be ordered at additional charge by writing the Order Department, giving the catalog number, title, author and specific pages you wish reproduced.

University Microfilms

300 North Zeeb Road
Ann Arbor, Michigan 48106
A Xerox Education Company

73-4293

SNYDER, Jr., Arnold Lee, 1937-
THE AURORAL OVAL AND THE HIGH LATITUDE
IONOSPHERE.

University of Alaska, Ph.D., 1972
Geophysics

University Microfilms, A XEROX Company, Ann Arbor, Michigan

THIS DISSERTATION HAS BEEN MICROFILMED EXACTLY AS RECEIVED.

THE AURORAL OVAL AND THE HIGH LATITUDE IONOSPHERE

A

DISSERTATION

Presented to the Faculty of the
University of Alaska in Partial Fulfillment
of the Requirements
for the Degree of
DOCTOR OF PHILOSOPHY

By

Arnold Lee Snyder, Jr., B.C.E., M.S.

Fairbanks, Alaska

May 1972

THE AURORAL OVAL AND THE HIGH LATITUDE IONOSPHERE

APPROVED:

Eugen M. Wesscott

Howard F. Bode

Mc M. Stenley

Spudis Mearns
Chairman

Rog Sheridan
Department Head

APPROVED:

C. Bulkh

Date May 9, 1972

Dean of the College of Mathematics,
Physical Sciences and Engineering

C. Lee

Vice President for Research and Advanced Study

PLEASE NOTE:

Some pages may have

indistinct print.

Filmed as received.

University Microfilms, A Xerox Education Company

ABSTRACT

(I) The overall purpose of this work is to examine the morphology of the high latitude winter ionosphere during magnetospheric substorms. Recent studies have shown that the large-scale structure of the high latitude ionosphere is characterized by pronounced circumpolar features that are closely associated with the auroral oval. Therefore, it is hypothesized that there exist relationships between the variations of the high latitude ionosphere and the dynamics of the auroral oval during magnetospheric substorms.

(II) Ionograms from ground and airborne ionosondes form the ionospheric data base for these studies. Auroral all-sky camera data and auroral zone magnetograms reliably define the occurrence of magnetospheric substorms. These latter two data types form the majority of the associated observational material for the interdisciplinary study of the morphology of the high latitude ionosphere.

(III) As a first step, all-sky camera data from the Alaskan meridian chain of observatories are studied to determine the meridional distributions and motions of auroras that comprise the auroral oval. A magnetic meridian observing chain is similar to an azimuth scan radar that 'scans' the auroral oval once per day. The results of this investigation reveal several new morphological features of the auroral substorm: (i) An enhanced equatorward drift of auroral forms and the 'clearing' of the poleward sky result in an equatorward 'thinning' of the auroral oval prior to the onset of the expansive phase of the substorm. These phenomena may possibly indicate the growth phase of a magnetospheric substorm.

(ii) During worldwide magnetoquiet, intense auroral substorms occur on the contracted auroral oval. Such substorms may occur beyond the poleward horizon of an auroral zone observatory. This fact emphasizes the importance of data from a meridian chain of observatories for morphological studies of auroras. (iii) All-sky camera data from the Alaskan meridian chain confirm the earlier statistical results which indicate that equatorward auroral motions in the night sector are more frequent than poleward motions. Sunlight precludes comprehensive day sector observations by the Alaskan meridian chain. For this reason, southern hemisphere all-sky camera data are used to determine that poleward motions of day sector auroras occur statistically more frequently than equatorward motions.

(IV) An investigation of ionospheric disturbances depends upon a detailed knowledge of the behavior of the ionosphere during magnetoquiet periods. Data from airborne and ground based ionosondes are combined to deduce the macroscale patterns of the magnetoquiet high latitude ionospheric E-region and the F2-layer. (i) During such periods, the auroral E-layer and retarded type sporadic E occur in a circumpolar band bounded by approximately 68° and 75° CGL; non-retarded type sporadic E, with top frequencies above two megahertz does not occur equatorward of approximately 68° CGL. (ii) The magnetoquiet night sector F2-layer is characterized by the main trough, with critical frequencies of approximately one megahertz; the main trough is bounded on the poleward side (~67° CGL) by a well defined

wall and a plateau of F-region ionization that extends poleward to the instantaneous auroral oval.

(V) Night sector ionospheric disturbances are closely associated with the occurrence of magnetospheric substorms.

(i) At approximately 65° CGL in the night sector, sporadic E with top frequencies greater than two megahertz occurs in conjunction with substorms. The top frequency of sporadic E decreases below two megahertz during the recovery phase of the substorm. At times, the blanketing frequency of sporadic E increases prior to the onset of accepted substorm phenomena. (ii) The night sector poleward trough wall is displaced equatorward during the development of a substorm. From these limited studies, it appears that the displacement occurs during the expansive phase of the auroral substorm. Normally once the poleward trough wall is displaced equatorward, it remains equatorward of its magnetoquiet position for the remainder of the night.

(VI) Day sector disturbances are recognized by ionospheric characteristics closely associated with auroral phenomena. (i) The day sector F-layer irregularity zone and the discrete auroras move equatorward and then poleward with the development and decay of a magnetospheric substorm. (ii) Increased non-deviative ionospheric absorption of high frequency radio waves is associated with the formation of midday auroral patches that occur in conjunction with substorms.

(VII) This work illustrates the advantages of an interdisciplinary study of the high latitude ionosphere. It also demonstrates the

need for a meridian chain of geophysical observatories equipped with ionosondes, as well as all-sky cameras, magnetometers and riometers. Such a chain would provide the data necessary for the refinement and expansion of the studies presented here.

ACKNOWLEDGEMENTS

The research for this dissertation was supported in part by the National Science Foundation, Atmospheric Sciences Section, through grants GA-31700 and GA-28101 and in part by the United States Air Force through grant number F-19628-C-0182. The author attends the University of Alaska as a member of the United States Air Force and is sponsored by the Air Force Institute of Technology Civilian Institutions Programs.

I extend my sincere appreciation to Dr. Syun-Ichi Akasofu for his patient guidance and most of all for his inspiration that led to the completion of this work. One cannot help but be inspired by Dr. Akasofu's deep understanding, interest, and enthusiasm for the work of others as well as for his own.

I express my deep gratitude to Professor Glenn M. Stanley for his many helpful suggestions and discussions as well as for his careful reading of the manuscript as it was being prepared.

I extend my deep appreciation to Dr. George Gassmann of the Air Force Cambridge Research Laboratories for providing me the ionograms and all-sky camera data from numerous airborne surveys of the arctic ionosphere. I also extend my thanks to him, as well to his close colleagues, Dr. James Whalen, Mr. Charles Pike, Mr. Jurgen Buchau, and Mrs. Rosemarie Wagner for their helpful discussions.

I also acknowledge that Dr. Charles Wilson provided the Inuvik magnetograms and Dr. Thomas Berkey obtained the Asian sector riometer data for one of the events considered in this dissertation.

All-sky camera films, magnetograms and ionograms were generously provided by the Geophysical Institute Archives. The Allakaket ionosonde

was operated under a contract with NASA. The Anchorage, Barrow and College ionosondes were operated under contracts with NOAA.

I am especially grateful to Mrs. Linda Fredrick for her personal pride in carefully typing the final manuscript.

I also gratefully acknowledge the timely and excellent work provided by the Drafting Office and the Photographic Services in the preparation of the illustrations used in this dissertation.

To my wife Pat, I express my thanks for sharing her life with me during the often difficult periods that have preceded the completion of this work.

TABLE OF CONTENTS

	Page
ABSTRACT	iii
ACKNOWLEDGEMENTS	vii
TABLE OF CONTENTS	ix
LIST OF ILLUSTRATIONS	xiii
LIST OF TABLES	xix
PREFACE	xx
CHAPTER 1 INTRODUCTION	1
1.1 Spatial and Temporal Distributions of Auroras	1
1.1.1 The Auroral Oval	1
1.1.2 The Auroral Substorm	5
1.1.3 General Dynamics of the Auroral Oval	7
1.2 Synoptic Pattern of the High Latitude Ionospheric F2-Layer	9
1.2.1 Synoptic Studies from Satellite Data	9
1.2.2 Contributing Studies of Bottomside Ionosonde Data	13
CHAPTER 2 MAGNETIC MERIDIAN OBSERVATIONS OF AURORAS	17
2.1 Magnetic Meridian Observing Chains	17
2.2 Alaskan Meridian Observing Chain	19
2.2.1 Observing Site Locations and Instrumentation	19
2.2.2 The Analysis and the Limitation of All-Sky Camera Data	21
2.3 Meridional Motions and Distributions of Auroras	27
2.3.1 Introduction	27

2.3.2	Meridional Motions Related to Auroral Oval Geometry and Size	29
2.3.3	Meridional Motions Related to the Auroral Substorm	34
2.3.3.1	The Growth Phase of Magnetospheric Substorms	34
2.3.3.2	Foleward Motions and the Expansive Phase	46
2.3.3.3	Recovery Phase	49
2.3.4	Summary	50
2.4	Auroral Substorms on the Contracted Auroral Oval	52
2.4.1	Introduction	52
2.4.2	January 5, 1970 Auroral Substorm	53
2.4.3	January 8, 1970 Auroral Substorm	54
2.4.4	Discussion	55
2.5	Continuous Auroral Observations	55
2.5.1	Limiting Factors for Continuous Auroral Observations	55
2.5.2	A Southern Hemisphere Auroral Observing Chain	57
2.5.3	Continuous Auroral Observations for May 30, 1960	58
2.5.4	Day-Sector Meridional Auroral Motions	61
CHAPTER 3	THE HIGH LATITUDE IONOSPHERE DURING MAGNETOQUIET	85
3.1	Introduction	85
3.2	Airborne Surveys	87
3.2.1	High Latitude Ionospheric E-Region	88
3.2.1.1	Ionogram Interpretation	88
3.2.1.2	Results	91
3.2.2	High Latitude Ionospheric F2-Layer	95

	3.3 F2-Layer Synoptic Pattern Deduced from Ground Ionosondes	100
CHAPTER 4	THE HIGH LATITUDE IONOSPHERE DURING MAGNETOSPHERIC SUBSTORMS	112
	4.1 The Day Sector F-Layer During a Magnetospheric Substorm	112
	4.1.1 Introduction	112
	4.1.2 Aircraft Instrumentation and Flight Track	114
	4.1.3 Magnetic Activity	114
	4.1.4 Auroral Activity	116
	4.1.5 Ionogram Interpretation	116
	4.1.6 Discussion	119
	4.1.7 Summary	122
	4.2 Midday Auroral Patches and Related Ionospheric Phenomena	123
	4.3 The Night Sector Ionosphere During Magnetospheric Substorms	127
	4.3.1 Introduction	127
	4.3.2 Data Presentation	129
	4.3.3 Discussion of the Observed Ionospheric Variations	130
	4.3.3.1 December 4, 1965	131
	4.3.3.2 January 2, 1966	134
	4.3.3.3 January 18, 1966	135
	4.3.3.4 March 3, 1966	137
	4.3.4 Summary and Discussion of Results	138
CHAPTER 5	SUMMARY	163
	5.1 The Auroral Oval and Auroral Substorms	164

5.2	The High Latitude Ionosphere During Magnequiet	166
5.3	The High Latitude Ionosphere During Magnetospheric Substorms	167
5.4	High Latitude Ionogram Interpretation	169
5.5	A Magnetic Meridian Observing Chain for Continued Studies	170
	APPENDIX I	171
	REFERENCES	172

LIST OF ILLUSTRATIONS

	Page
Figure 1. Location of the Alaskan meridian observatories with respect to the $Q = 3$ auroral oval and Universal time during the winter solstice. The circles are from the innermost one, 80°N , 70°N and 65°N CGL .	64
Figure 2. Representative calibration curve relating radial distance, on a projected image of 35mm. all-sky camera film, to zenith angle. Also shown are ground projection distance curves as a function of zenith angle and radial distance for assumed auroral lower border heights of 100, 110 and 120 kilometers.	65
Figure 3. Azimuth and zenith angle grid for analysis of 35mm all-sky camera data recorded by the AFCRL NKC-135 Flying Ionospheric Laboratory. Zenith angle circles are shown for increments of five degrees beginning with $Z = 10^{\circ}$ (innermost) and ending with $Z = 80^{\circ}$ (outermost). Radial lines are shown for each five degrees of azimuth.	66
Figure 4. The upper part of the figure is a cross section of the auroral oval as observed by the Alaskan meridian chain of stations for the first 16 hours (UT) of December 5, 1969. See the text, section 2.3.1, for a description of the different lines, shading and hatching. The lower part of the figure presents the corresponding AU and AL indices with the Inuvik H component magnetogram superposed. Magnetograms from the following stations were used to construct the AU/AL indices: College, Barrow, Dixon, Murmansk, Abisko, Leirvogur, Narsarsuaq, Great Whale River, Fort Churchill, Baker Lake and Meanook.	67
Figure 5. January 5, 1970, the format of the figure is similar to that of Figure 4. Magnetograms from the following stations were used to construct the AU/AL indices: College, Barrow, Cape Wellen, Tixie Bay, Cape Chelyuskin, Kiruna, Leirvogur, Great Whale River, Fort Churchill, Baker Lake and Meanook.	68
Figure 6. January 6, 1970, the format of the figure is similar to that of Figure 4. Magnetograms from the following stations were used to construct the AU/AL indices: College, Barrow, Cape Wellen, Tixie Bay, Cape Chelyuskin, Kiruna, Leirvogur, Great Whale River, Fort Churchill, Baker Lake and Meanook.	69

	Page
Figure 7. January 8, 1970, the format of the figure is similar to that of Figure 4. Magnetograms from the following stations were used to construct the AU/AL indices: College, Barrow, Cape Wellen, Tixie Bay, Cape Chelyuskin, Kiruna, Leirvogur, Great Whale River, Fort Churchill, Baker Lake and Meanook.	70
Figure 8. February 14, 1970, the format of the figure is similar to that of Figure 4. Magnetograms from the following stations were used to construct the AU/AL indices: College, Barrow, Cape Wellen, Tixie Bay, Cape Chelyuskin, Dixon, Kiruna, Narssarsuaq, Great Whale River, Fort Churchill Baker Lake and Meanook.	71
Figure 9. The Tromsø magnetic record (the H component) on February 14, 1968.	72
Figure 10. An auroral display observed at Mould Bay during a DP-2 variation on December 1, 1965. From the top, the angle θ of the interplanetary magnetic field, the Alert Y component magnetogram, the AL index and selected all-sky photographs from Mould Bay.	73
Figure 11. An auroral display observed at Fort Yukon on December 22, 1967 during the growth phase defined on the basis of magnetic records.	74
Figure 12. Auroral displays observed at College during DP-2 variations on October 2, 1965. The format of the figure is similar to that of Figure 10.	75
Figure 13. The upper part of the figure is a cross section of the auroral oval as observed by Byrd Station and South Pole Station on May 30, 1960. The lower part of the figure presents the corresponding AU, AL, AE and D_{st} indices. The capital letters are for cross reference with Figures 14 and 15.	76
Figure 14. Selected all-sky camera photographs (in negative) from Byrd Station and South Pole Station during the first part of May 30, 1960. The 's' prefix indicates photographs taken from the South Pole Station. The capital letters are for cross reference with Figure 13.	77
Figure 15. Selected all-sky camera photographs (in negative) from Byrd Station and South Pole Station during the latter part of May 30, 1960. The 's' prefix indicates photographs taken from the South Pole Station. The capital letters are for cross reference with Figure 13.	78

	Page
Figure 16. The H component magnetic records from College, Barrow and Cape Wellen on February 13, 1968.	79
Figure 17. The H component magnetic records from Inuvik, Bar I, Fort Yukon and College on January 5, 1970.	80
Figure 18. Magnetic records from Inuvik, Bar I, Fort Yukon, College and Anchorage on January 8, 1970.	81
Figure 19. Selected all-sky camera photographs from the Alaskan meridian observatories for January 8, 1970.	82
Figure 20. Equatorward boundary, for selected northern hemisphere fall and winter dates, poleward of which the earth's shadow height is greater than or equal to 50 kilometers at local solar noon. The outline of the land areas is shown as transformed into the corrected geomagnetic coordinate system.	83
Figure 21. Meridional distributions of day sector discrete auroras observed from South Pole Station on nine days in 1962.	84
Figure 22. The H (or X) component magnetic records from aurora zone stations for a 14 hour period on December 13-14, 1969.	104
Figure 23. The H (or X) component magnetic records from auroral zone stations for a 14 hour period on November 30, 1970.	105
Figure 24. The H (or X) component magnetic records from auroral zone stations for a 14 hour period on December 1, 1969.	106
Figure 25a. Flight paths for five airborne surveys of the magnetoquiet high latitude ionosphere. The flight paths are shown in the corrected geomagnetic latitude-time (CGL-CGLT) coordinate system.	107
Figure 25b. CGL-CGLT positions of E-region parameters and discrete auroras observed on the five airborne survey paths shown in Figure 25a.	107
Figure 26. Synoptic pattern of the magnetoquiet F2-layer critical frequencies deduced from the data from three airborne surveys of the Alaskan sector ionosphere. The flight paths and data are presented in the CGL-CGLT coordinate system.	108

	Page
Figure 27. Typical ionograms from the airborne ionosonde showing examples of an equatorward crossing beneath the F-layer poleward trough wall, the auroral E-layer, retarded type sporadic E and non-retarded type sporadic E.	109
Figure 28. The H (or X) component magnetic records from auroral zone stations for a 24 hour period on September 14-15, 1964.	110
Figure 29. Synoptic pattern of the magnetoquiet F2-layer critical frequencies deduced from the Barrow, College and Anchorage ionosonde data for a 24 hour period on September 14-15, 1964.	111
Figure 30. Aircraft flight path (CGL-CGLT) for December 5-6, 1969. Universal times are given for representative flight path locations. Superimposed is the $Q = 3$ statistical auroral oval for moderately disturbed magnetic conditions.	144
Figure 31a. The AE, AU, AL and D_{st} indices for 0000-0700 UT, December 6, 1969. Magnetograms from the following stations were used to construct the AE, AU and AL indices: College, Barrow, Dixon Island, Abisko, Isivogur, Narsarsuaq, Great Whale River, Fort Churchill, Baker Lake, Meanook and Inuvik.	145
Figure 31b. Flight path in corrected geomagnetic latitude and Universal time for December 6, 1969, 0000-0700 UT. Also shown are representative auroral and FLIZ positions. The lower case letters are for cross reference with Figure 32.	145
Figure 32. Representative ionograms and all-sky camera photographs for the times identified by the lower case letters in Figure 31b. The following abbreviations are used to identify F-layer characteristics; (1) polar cavity F-layer - PC, (2) F-layer irregularity zone - FLIZ, and (3) subauroral F-layer - SF.	146
Figure 33. Schematic drawing that illustrates the meridional motions of the day sector polar F-layer that occur during a magnetospheric substorm. The subauroral F-layer is denoted as the 'solar F-layer' in the upper part of the figure.	147
Figure 34. Night sector auroral zone magnetic records (H or X component) for December 9, 1969, 0000 to 0800 UT.	148

	Page
Figure 35. Aircraft flight path (CGL-CGLT) for December 9, 1969. Universal times are given for representative flight path locations. Superimposed is the $Q = 3$ statistical auroral oval for moderately disturbed magnetic conditions.	149
Figure 36. Representative auroral positions and orientations of discrete auroral arcs observed on the flight of December 9, 1969. All times are UT.	150
Figure 37. All-sky camera photograph of midday auroral patches observed on December 9, 1969, 0445 UT and compared with a similar photograph without the auroral patches. (Both photographs are ground projections).	151
Figure 38. Asian sector riometer absorption data shown in relation to the observed location of midday auroral patches and to the aircraft flight path (CGL) for December 9, 1969, 0300-0700 UT. Also shown are the corresponding corrected geomagnetic local times (CGLT) for each ground station.	152
Figure 39. Ionosonde observed minimum frequencies associated with the midday auroral patches, December 9, 1969. Minutes without data are due to ionosonde calibration. 'v' indicates that f_{\min} was lower than 2.0 MHz, the low frequency limit of the ionosonde.	153
Figure 40. Partial f-plot for Allakaket, 'AU' and 'AL' indices and riometer absorption data for Allakaket and College for a 10 hour period on December 4, 1965. The 'AU' and 'AL' indices were derived from the superposition of the night sector H (or X) component magnetic records shown in Figure 41. The lower case letters are for cross reference with Figure 42.	154
Figure 41. Auroral zone magnetic records (H or X component) for December 4, 1965, 0400 to 1900 UT.	155
Figure 42. Representative ionograms for Allakaket, College and Anchorage for the night of December 4, 1965 (Universal times and date). Also shown are the corresponding all-sky camera photographs from College. The lower case letters are for cross reference with Figure 40.	156
Figure 43. Partial f-plots for Allakaket and College and the 'AU' and 'AL' indices for a 10 hour period on January 2, 1966. The 'AU' and 'AL' indices were derived from the superposition of the night sector H (or X) component magnetic records shown in Figure 44.	157

	Page
Figure 44. Night sector auroral zone magnetic records (H or X component) for January 2, 1966, 0700 to 1700 UT.	158
Figure 45. Partial f-plots for Allakaket and College and the 'AU' and 'AL' indices for a 10 hour period on January 18, 1966. The 'AU' and 'AL' indices were derived from the superposition of the night sector H (or X) component magnetic records shown in Figure 46.	159
Figure 46. Night sector auroral zone magnetic records (H or X component) for January 18, 1966, 0700 to 1700 UT.	160
Figure 47. Partial f-plot for College and the 'AU' and 'AL' indices for a 10 hour period on March 3, 1966. The 'AU' and 'AL' indices were derived from the superposition of the night sector H (or X) component magnetic records shown in Figure 48.	161
Figure 48. Night sector auroral zone magnetic records (H or X component) for March 3, 1966, 0700 to 1700 UT.	162

LIST OF TABLES

		Page
TABLE 1	ALASKAN SECTOR OBSERVATORIES (1969-1970)	63a
TABLE 2	AIRBORNE SURVEYS OF THE HIGH LATITUDE IONOSPHERE DURING MAGNETOQUIET	103a

PREFACE

Accurate knowledge of the behavior of the high latitude ionosphere is vital for understanding the environmental effects upon the communication of information via or through the polar ionosphere.

The ionosphere forms the base of the magnetosphere. As such, the polar ionosphere is subject to the continuous bombardment of energetic particles that populate the outer magnetosphere and precipitate along the auroral oval. Electric fields, which are an integral part of the description of the magnetosphere and its variations, also effect the ionosphere.

The purpose of the work presented here is to morphologically examine the morphological large-scale changes in the structure of the high latitude ionosphere during magnetospheric substorms. The distribution of auroras (the only "visible" phenomenon in polar aeronomy) is closely related to the structure of the high latitude ionosphere and is also an excellent indicator of substorm variations. Thus, the characteristics of the high latitude ionosphere have been jointly considered with auroral phenomena. It is for this reason that auroral substorms and associated polar magnetic substorm activity have been studied in the first part of the thesis.

The meridional distribution of auroras during magnetospheric substorms is studied in detail with data from the Alaskan meridian chain of geophysical observatories (Chapter 2). This observing

chain systematically observes the auroral oval once-per-day like an azimuth scan radar. The study of these systematically acquired data has revealed several new features of auroral substorms:

1. There seems to be an enhanced equatorward drift of night-sector auroral forms one to two hours prior to the onset of the expansive phase of an auroral substorm. The equatorward drift and the "clearing" of the poleward sky result in an equatorward thinning of the auroral oval. These auroral phenomena may be indicators of the growth phase of magnetospheric substorms.

2. Auroral substorms occur on the contracted auroral oval during general worldwide magnetoquiet. The features of these auroral substorms are identical, with the exception of their latitude of occurrence, to those that occur at typical auroral zone latitudes.

In the second part of the thesis, the synoptic pattern of the magnetoquiet ionosphere has been established (Chapter 3) and identification of ionospheric disturbances as deviations from the magnetoquiet patterns have been made (Chapter 4). These ionospheric disturbances have been related to several major features of auroral and magnetospheric substorms. Data from the Flying Ionospheric Laboratory, an Air Force Cambridge Research Laboratories NKC-135 jet aircraft, instrumented with an ionospheric sounder and an all-sky camera, have also been used for these studies.

Several new results from the interdisciplinary study

of the high latitude ionosphere include the following:

1. There are F2-layer variations in latitude that are closely associated with magnetospheric substorms. The day-sector F-layer irregularity zone and auroras both move equatorward and then poleward with the development and decay of a magnetospheric substorm. In the night-sector the poleward trough wall moves equatorward with the development of a substorm.

2. The ionospheric absorption substorm in the day-sector is related to the formation of midday auroral patches.

3. Occurrences of night sector sporadic E, at approximately 65° corrected geomagnetic latitude and with blanketing frequencies greater than two megahertz, are associated with magnetospheric substorms. The blanketing frequency of sporadic E is often observed to increase prior to the onset of other substorm phenomena.

It is recommended, on the basis of the studies presented here, that a meridian chain of ionospheric sounders be established in association with a high latitude observing chain such as now exists in Alaska.

Such an interdisciplinary and systematic observing approach would provide the data necessary for refinement of the studies presented here and for examination of the possibilities of providing warning for the occurrence of magnetospheric substorms. Such studies are essential for a better understanding of the ionospheric environment and its effect upon the communication of information via or through the polar ionosphere.

CHAPTER I

INTRODUCTION

This chapter reviews the previous work in the fields of auroral and ionospheric morphology as a background for the topics treated in the final three chapters. The first half of this chapter considers the auroral oval and its dynamics including the auroral substorm. The latter half of the chapter discusses the known large-scale synoptic features of the high latitude ionospheric F2-layer.

1.1 SPATIAL AND TEMPORAL DISTRIBUTIONS OF AURORAS

1.1.1 The Auroral Oval

The world-wide distribution and occurrence frequency of auroras has been refined and clarified greatly during the past decade. However the history of this scientific endeavor dates to the mid-19th century.

Loomis (1860) collected many early northern hemisphere auroral observations dating back to the time of Aristotle. Loomis's contribution was the recognition that the occurrence frequency of auroras maximizes in a roughly circular band. The center of this band was shifted from the geographic pole by about ten degrees of latitude toward Greenland. Fritz (1881) cataloged auroral records for the preceding 2300 years and determined isochasms of auroral occurrence. An isochasm is an isocontour line of auroral occurrence frequency commonly

expressed in nights per year. Vestine (1944), using Fritz's data and observations of the aurora from the First and Second International Polar Years, expanded Fritz's work and refined the concept of the auroral zone. The auroral zone is the region in the vicinity of the maximum value isochasm. Vestine also made an analysis improvement by considering only those nights on which auroras could be observed.

Evidence for the auroral zone was pieced together from data that consisted of observing notes made from visual sightings of auroras. The development of the all-sky camera for auroral photography (Davis and Elvey, 1955) provided a dramatically improved capability for the systematic gathering of auroral data. The operation of many auroral all-sky cameras during the International Geophysical Year provided the necessary data base for two significant morphological results.

The first of these results was the determination that auroras occur statistically within an oval belt, called the auroral oval, which encircles the polar regions and which is fixed approximately with respect to the sun (Feldstein, 1960, 1963; Khorosheva, 1962; Feldstein and Starkov, 1967). The auroral oval is eccentric with respect to the dipole pole and coincides with the auroral zone only near the local magnetic midnight time sector.

The concept of the auroral oval was developed through the statistical smoothing of a great amount of all-sky camera data. However, even the combined field-of-view of the IGY all-

sky camera network was insufficient to determine the instantaneous distribution of auroras over the entire polar region. Largely for this reason, the question has remained as to the instantaneous distribution of the auroras that statistically produces the oval configuration.

There are many observational facts that favor strongly the concept of the auroral oval as a physical entity. Khorosheva (1963) and Akasofu (1964) presented specific first case evidence that auroras are located in an oval configuration that extends from high geomagnetic latitudes ($\sim 75^\circ$ to 80° corrected geomagnetic latitude, CGL) during the day to auroral zone latitudes ($\sim 65^\circ$ to 70° CGL) at night. The corrected geomagnetic coordinate system (Huitquist, 1958; Hakura, 1965) will be used throughout this thesis.

Even with an all-sky camera network with the required field-of-view, cloud, lunar, and solar lighting interference would reduce the probability of the determination of the instantaneous polar distributions of auroras to a minuscule value. Photography or television imaging from a polar orbiting satellite will provide, in time, the data to resolve the continuity question.

However, in the absence of such data, the continuity of the auroral oval has been examined, with reasonable certainty, by using a high speed jet aircraft as an observing platform (Buchau et al., 1970). These unique auroral data reveal that under moderately disturbed magnetic conditions ($\sum_{24 \text{ hr}} K_p > 10$) visible auroral arcs form a continuous band around the geomagnetic

pole; under quiet magnetic conditions ($\Sigma_{24\text{hr}} K_p < 10$) temporal and/or spatial gaps were found in the morning, noon and evening time sectors of the instantaneous auroral oval (Buchau et al., 1970). Further studies have shown that these gaps are bridged by subvisual bands of auroral emissions (Buchau et al., 1972).

The subvisual emissions that bridge the gaps in the discrete auroras suggest that the rather discontinuous statistical auroral distribution obtained by Lassen (1969) for the evening and morning time sectors may be a visual threshold problem and not a physical reality as suggested by Mishin et al. (1970).

The alignment of auroral arcs has been studied in detail since the IGY (Denholm, 1961; Davis, 1962; Feidstein, 1963; Stringer and Beion, 1967; Gustafsson, 1967; Lassen, 1970). In the most recent study, auroral data acquired from an aircraft observing platform were used by Akasofu et al., (1972) to show a continuous pattern of quiet auroral arc positions and alignments that are consistent with the Feldstein and Starkov (1967) $Q = 3$ statistical auroral oval. Akasofu et al., (1972) conclude that their auroral arc position and alignment data agree with the concept of a continuous auroral oval.

Ground-based auroral observations through the visual atmospheric radiation window will always be hampered at times by weather, direct sunlight, twilight and moonlight. Bates et al., (1966, 1959) have shown a close correspondence between sweep frequency HF auroral backscatter radar echoes and visual auroras. Bates (1966) suggested the installation of an auroral

radar at each magnetic pole to permit a comprehensive study of the auroral oval, thus circumventing unfavorable weather and lighting conditions. The radars are now operating at Resolute Bay in the northern hemisphere and at McMurdo Station in the southern hemisphere. First results (Bates, 1972) show that the auroral radar data yield the location of the instantaneous auroral oval with a reasonable temporal and spatial resolution.

The main purposes of the work described in Chapters 2, 3 and 4 are to examine the dynamics of the auroras that comprise the auroral belt and to demonstrate the value in ordering high latitude ionospheric phenomena relative to this belt. Nevertheless, certain aspects of these studies border on the question of the continuity of the auroral oval; where appropriate, comments will be made and then summarized in Chapter 5.

1.1.2 The Auroral Substorm

As mentioned in Section 1.1.1, the IGY all-sky camera network provided the data base for two significant results. The second of these two results was the development of the concept of the auroral substorm. This concept has ordered the different and complex auroral forms and displays into a substorm and local-time coordinate framework within the auroral oval (Akasofu, 1964; Feldstein and Starkov, 1967).

Prior to the post-IGY period it was recognized that a close relationship existed between auroral displays and polar magnetic disturbances (cf. Harang, 1951; Heppner, 1954). However, at that time the understanding of the large-scale auroral display

over the entire polar region was dominated by the concept of a fixed pattern of auroral activity under which the earth rotates once-per-day. This concept evolved from the finding that characteristic auroral forms statistically dominate specific local time sectors: quiet homogeneous arcs in the evening, active rayed arcs and bands near midnight and diffuse auroral surfaces or patches in the morning.

Analysis of simultaneous all-sky camera photographs taken from a number of IGY observations revealed (Akasofu, 1964) that the statistical treatment of auroral data to determine the large scale morphology of auroral displays was incorrect. Akasofu determined that quiet auroral forms could be found, during magnetoquiet, in all time sectors of the night half of the auroral oval. He further found that the breakdown of the quiet auroral condition begins near local magnetic midnight and expands in all directions. The result of this expansive activity is the westward traveling surge of the evening sector (Akasofu et al., 1965) and the active auroral forms of the midnight and morning sectors that were identified previously and incorrectly with a fixed pattern of auroral activity. Following the transient auroral disturbance, quiet auroral conditions return to the auroral oval. This sequence of auroral activity was termed by Dr. Sydney Chapman (cf. Akasofu, 1968) as the "auroral substorm". A full summary of the night sector auroral substorm may be found in Akasofu (1965, 1966). More recently the auroral substorm concept has been extended to the day sector of the auroral

oval by Starkov and Feldstein (1967a) and Feldstein and Starkov (1967).

There are several considerations and facets of the auroral substorm that are important to mention for their connection with the discussions that follow. First, the occurrence of an auroral substorm is independent of local time; however, the nature of the substorm auroras is strongly dependent upon local time (cf. Akasofu, 1968). Second, while an auroral substorm does alter the dynamics of the auroras, the substorm occurs within the concept of the auroral oval (Feldstein and Starkov, 1967).

1.1.3 General Dynamics of the Auroral Oval

The characteristics of the auroras that comprise the auroral oval are described well in the substorm concept. However, because of the lack of comprehensive data, there is insufficient evidence available to undertake case studies of the dynamic character of the entire auroral oval or even a significant fraction thereof. For this reason the general dynamics of the auroral oval have been assembled from case studies in narrow time sectors or through the statistical collation of auroral data from all local times.

Russian scientists have been leaders in the statistical study of the variations in the space-time distribution of auroras. Feldstein and Starkov (1967), in their classic work, determined from IGY data the mean position of the boundaries of the auroral oval for different time sectors and for different levels of

the midnight sector Q index (Bartels, 1957). Their basic work has been followed by several refinements. Starkov and Feldstein (1968) determined from IGY data the midnight sector boundaries of the auroral oval as a function of Q and D_{st} . Starkov and Feldstein (1968) compared the midnight sector auroral oval boundaries during the IGY and the IQSY; their results revealed approximately a two degree poleward latitude shift of the IQSY oval boundaries for $Q > 1$.

The results of the statistical studies of auroral distributions during varying levels of magnetic activity have shown the following:

- 1). The spatial distribution of auroras, in an oval belt, is preserved for all levels of magnetic activity.
- 2). The low latitude boundary of the auroral oval moves equatorward with an increase in the magnetic disturbance level.
- 3). The latitudinal width of the night sector auroral oval increases with increasing Q; however, the poleward boundary moves equatorward with an increase in D_{st} (more negative).

Numerous case studies (e.g., Akasofu and Chapman, 1963; Stringer et al., 1965; Stringer and Belon, 1967; Chubb and Hicks, 1970), but limited in local time, have considered the "geometry" or the position of the auroral oval in relation to various geomagnetic indices (D_{st} , K_p , and local K). The case studies in general agree with the statistical results; as magnetic activity increases, visual auroras occur at progressively lower latitudes.

The prime interest in auroral morphology during the past 15 years has been in the determination of general substorm characteristics, occurrence frequency, spatial distribution, and variations in the general spatial distributions with changes in magnetic activity. The same 15 year period has been marked by the rapid development of the interdisciplinary science of magnetospheric physics. Undoubtedly the extension of the observational domain by satellites has been instrumental in this rapid progress. However the concepts of the auroral oval and the auroral substorm have also contributed significantly. Because of the close relationship that exists between the aurora and the upper atmosphere and its extension into the magnetosphere, the continuing detailed study of auroral morphology will aid in the further understanding of the dynamics of the magnetosphere.

1.2 SYNOPTIC PATTERN OF THE HIGH LATITUDE IONOSPHERIC F2-LAYER

1.2.1 Synoptic Studies from Satellite Data

The International Geophysical Year and the International Years of the Quiet Sun included a great emphasis on the determination of a self-consistent synoptic pattern of the high latitude ionosphere. Toward this end, many ground-based ionosondes were operated. Although an astonishing amount of data was recorded, a unified pattern of the high latitude ionosphere was not determined from these data. Rather, the results from the higher density of observatories revealed frequent and significant dissimilarities among data from adjacent stations.

However, even prior to the IQSY, data were being acquired that would provide a new conceptual understanding of the high latitude ionospheric F-region. On September 29, 1962, the Alouette I satellite (Canadian built and American launched) was injected into a near polar circular orbit 1000 kilometers above the earth. Satellite instrumentation included a topside ionospheric scander that operated from 0.5 to 11.5 MHz (Nelms, 1964). Data from this satellite and follow-on satellites of the Alouette and the ISIS series have defined the general structure of the topside ionosphere as a function of latitude, local time and season.

In retrospect, the Alouette ionospheric data have also provided the necessary insight to understand the original difficulties in the interpretation of ground acquired ionograms (Thomas and Andrews, 1969). First, the spacing between the ionosondes was too great to determine the fine structure of the ionosphere; and second, the data that might have identified the large scale, rather sharply defined, east-west aligned troughs and ridges of F-region ionization were generally overlooked -- again because of the lack of corroboratory evidence from adjacent stations.

Alouette's polar orbit and its data gathering rate of one ionogram per degree of latitude provided the spatial resolution and the latitude profiles necessary for the discovery of the main F-layer trough. Muldrew (1965) in the first major investigation concluded that the trough was an annular region of relatively low F-layer ionization that is aligned approximately in a magnetic

east-west direction. Muldrew (ibid) was able to identify the trough between approximately 1400 hours and 0700 hours local time and to show that it characteristically shifts from $\sim 74^\circ$ CGL at 1400 hours to $\sim 60^\circ$ at 0000 hours and shifts back poleward to $\sim 63^\circ$ at 0700 hours; he also showed that the trough shifts equatorward with increasing K_p .

Tulunay and Sayers (1971), in an extensive statistical treatment of the main trough data obtained by Ariel III, verified and refined the work of previous studies (e.g., Muldrew, 1965; Sharp, 1966; Calvert, 1966; Hagg, 1967; Carpenter, 1966). Several results (Tulunay and Sayers, 1971) are important to note for their connection with the material presented in Chapters 3 and 4:

1. Seasonally, the trough occurrence is most frequent in winter.
2. Diurnally, the trough occurrence is most pronounced in the early morning hours.
3. The gradient of electron density is normally greater on the poleward side of the trough than on the equatorward side.
4. The trough width decreases with increasing K_p and is dependent upon local time - being greatest in the early morning and the late evening hours.

Thomas and Dufour (1965) suggested that the equatorward edge of the main trough represents the termination of the normal solar-produced ionospheric F-layer and that the poleward trough

"wall" is formed by auroral ionization. The characteristics of the poleward trough wall are also of special interest in connection with the topics of Chapters 3 and 4.

Thomas and Andrews (1969) showed that the general latitudinal decrease in the maximum electron density of the F-layer is interrupted in winter by a superposition of ionization enhancements that are extended in longitude with a latitudinal width of approximately five to ten degrees. The combination of the general decrease of ionization and the auroral ionization enhancements results in a meridional distribution of ionization which has a sharp minimum that corresponds to the main trough. To a first approximation, the poleward trough wall is formed by a quasi-stationary, circumpolar "plasma ring" of higher density under which the earth rotates (Thomas and Andrews, 1969; Andrews and Thomas, 1969). As in the case of the main trough, the plasma ring's latitudinal position is associated with the geomagnetic disturbance level. The low latitude boundary of the plasma ring moves equatorward with increasing magnetic activity; the position of the poleward boundary, while more variable, moves also to lower latitudes with increasing K_p for moderate geomagnetic activity (Thomas and Andrews, 1969). Poleward of the plasma ring is another low electron density F-region sector called the polar cavity (ibid).

While not of prime interest for the following considerations, a Universal time effect has been observed in the high latitude ionosphere (e.g., Duncan, 1962; Thomas et al., 1966, Maehlum,

1968, 1969). Mashlum (1968) has suggested that the Universal time effect may be due to the "wobble" of the geomagnetic axis with respect to the solar wind. This wobble may also account partially for seasonal effects observed in the polar ionosphere (ibid). The Universal time effect alters the degree but not the character of the synoptic pattern of the high latitude ionosphere. This effect is a second order consideration for the present studies of the substorm time variations of the ionospheric F-region.

In summary, the topside ionospheric observations from satellites have identified three gross features that comprise the synoptic pattern of the high latitude ionospheric F-layer:

1. The F-layer plasma ring -- associated spatially and temporally with the auroral precipitation region.
2. The main F-layer trough -- equatorward of the plasma ring.
3. The F-layer polar cavity -- poleward of the plasma ring.

1.2.2 Contributing Studies of Bottomside Ionosonde Data

As mentioned in the previous section, the synoptic interpretation of ground acquired ionosonde data was virtually impossible prior to the "discoveries" that were made with the topside satellite data. New observational techniques (e.g., incoherent backscatter and high frequency backscatter) can also provide detailed measurements of ionospheric parameters. But, the vast amount of ground acquired ionosonde data, the number of ionosondes still being

operated coupled with several recent studies completed with these data may again given interest in the ionosonde as an effective probe of the ionosphere, the aurora and the magnetosphere.

The recent airborne ionospheric and auroral studies by the Air Force Cambridge Research Laboratories group (cf. Whalen *et al.*, 1971; Pike, 1971b; Wagner and Pike, 1971; Buchau *et al.*, 1972) have gone far to direct attention toward ionosonde data for the interdisciplinary study of the high latitude ionosphere and interrelationships between the ionosphere, the aurora and the magnetosphere. The work of this group has identified the topside observed F-layer plasma ring on bottomside ionograms and has established that the F-layer polar cavity is common to both observations. They have further established several relationships between ionospheric and auroral parameters. These aspects will be considered in later chapters.

The mobility of the aircraft and the rapid areal coverage by the satellite are advantages that render these platforms useful for gathering high latitude ionospheric data. But, the ground-based ionosonde and the insight of the workers who have studied these data have been essential to the greater understanding of the high latitude ionosphere that is now evolving.

Burkard (1948), in a little recognized but significant research note, discussed what he called the "sporadic F-layer" observed at Tromsø (67.1°N CGL). In the context of the current terminology and understanding, Burkard observed during winter nights the frequent encroachment of the poleward wall of the main F-layer trough over Tromsø. He also suggested that a possible

relationship between the appearance of this layer and magnetic activity should not be dismissed. However, the possible relationship with meteor showers, suggested by other workers, was not supported by his data (ibid).

Meek (1953, 1954b) studied the relationships between magnetic, auroral and ionospheric variations at Saskatoon (61.5°N CGL). He concluded that the critical frequency of the ionospheric F-layer decreases regularly through a quiet night; however, when there is magnetic disturbance, the critical frequency of the F-layer is higher than normal. Meek's observations are compatible with the interpretation given to Burkard's. Meek's work was one of the first efforts to study in detail the high latitude F-layer variations associated with auroral and polar magnetic disturbances.

In a study similar to those of Burkard (1948) and Meek (1953, 1954), Bellchambers et al., (1962) considered Halley Bay (61.4°S CGL) ionospheric data; they noted the same F-layer phenomena as were observed at Tromsø and Saskatoon. Bellchambers et al., (1962) noted that on disturbed days a new ionospheric F-layer appeared in the early evening and "replaced" the old layer; however, on quiet days the "replacement-layer" remained poleward of Halley Bay throughout the night.

Stanley (1966) was one of the first workers to interpret winter night auroral zone F-layer ionograms in the context of the main F-layer trough; he showed that oblique F-layer echoes from the poleward wall of the main F-layer trough move

toward auroral zone latitude stations in a regular manner almost every night. Stanley (ibid) also showed that typical winter night IQSY values of the F-layer critical frequency at College were near and at times less than one megahertz.

Bowman (1969) noted, from his studies of Ellsworth (62.6°S CGL) ionosonde data that in the night hours before 2200 (magnetic time) the rotation of the earth seemed to produce an apparent equatorward movement of the main F-layer trough relative to a stationary observer.

Together the prior studies of satellite, aircraft and ground-acquired data support the conclusion that the synoptic pattern of the high latitude ionospheric F-layer consists of a circumpolar ring of enhanced electron density bounded on the equatorward side by the main F-layer trough (ill-defined under sunlit conditions) and on the poleward side by the polar cavity. Further, these ionospheric features are approximately fixed with respect to the sun, and they exhibit temporal and spatial variations associated with changing magnetic conditions.

CHAPTER 2

MAGNETIC MERIDIAN OBSERVATIONS OF AURORAS

A high latitude magnetic meridian chain of observatories permits a systematic examination of the auroral oval. The first part of this chapter considers the concept of a magnetic meridian observing chain for auroral observations, the Alaskan meridian chain in particular, and the analysis and the limitations of auroral all-sky camera data. The second part of the chapter discusses the meridional distributions and motions of auroras that were obtained from the detailed studies of the Alaskan all-sky camera data as well as from similar data from the southern hemisphere. The major results of these investigations are presented in sections 2.3.4, 2.4.4, 2.5.3, and 2.5.4.

2.1 MAGNETIC MERIDIAN OBSERVING CHAINS

The distribution of the all-sky camera observatories has limited the number of comprehensive case studies of auroral phenomena. As mentioned in the previous chapter, the auroral oval, within which the auroral substorms occur, is eccentric with respect to the dipole pole and coincides with the auroral zone only in the midnight sector. This means that even a large number of observatories distributed along the auroral zone ($\sim 67^\circ$ CGL) cannot effectively monitor auroral activity.

There were a great number of IGY all-sky camera observatories. However, these sites were located with only the a priori concept of the auroral zone and the desire for as dense a network as

possible. The IGY data provided an adequate base for statistical studies of auroral occurrences and spatial distributions as well as for the development of the auroral substorm concept. But the random scatter of observatories has limited the value of the IGY data for comprehensive case studies to only several auroral disturbances.

To determine the distribution of phenomena that occur spatially more or less at random requires a matrix array of observatories. Yet to observe phenomena that occur spatially in some known geometry requires only a network of observatories to monitor the changes to the nominal geometry. For this reason, the most efficient auroral oval observing network is one comprised of several magnetic meridian 'chains' of observatories. Each chain in order to observe the majority of the auroras within the instantaneous auroral oval, should gather data over the latitude range of 60° to approximately 85° CGL. It is noted however that auroral disturbances that occur during infrequent great world-wide magnetic storms will extend equatorward of 60° CGL.

Auroras that comprise the auroral oval can be systematically monitored with magnetic meridian observing chains, but the present lack of a synoptic understanding of polar cap auroras would require a matrix array of observatories for initial comprehensive investigations. There are, however, certain features of polar cap auroral distributions that could be studied systematically with meridian observing chains. The preferential earth-sun orientation and the greater occurrence frequency of

polar cap auroras in the morning hours (cf. Danielsen, 1969 and Lassen, 1972) would favor a meridian chain.

In the midnight or the midday time sectors a meridian chain would not be helpful. In these time sectors, the auroral forms would be preferentially oriented parallel to the meridian observing chain and possibly simultaneously out-of-view of all sites.

Polar cap auroras occur over mostly uninhabited areas. This fact alone may preclude a systematic observing array unless a reliable automatic all-sky camera is developed or auroral imaging is undertaken from polar orbiting satellites.

2.2 ALASKAN MERIDIAN OBSERVING CHAIN

2.2.1 Observing Site Location and Instrumentation

Akasofu recognized the observational deficiencies of the random scatter of the IGY auroral observing network, and he established a magnetic meridian chain of auroral observatories in the Alaskan sector.

The Alaskan meridian chain as operated in 1969-1970, consisted of five all-sky camera sites with several additional supporting locations where other monitoring instruments were operated. Table I provides the location data for each site and the instruments operated. While lesser scale observing chains were operated in prior years along the Alaskan meridian, the 1969-1970 observing season was the first period with five all-sky camera locations. Figure I shows the location of the chain stations with respect to the $Q = 3$ statistical auroral oval (Feldstein and Starkov, 1967) and Universal time during the

winter solstice.

Each all-sky camera was fundamentally of Davis and Elvey (1955) design. A modified Kodak 16mm K-100 movie camera body controlled by an auxiliary timer, provided the film management. Photographs were taken during darkened hours and nominally at a rate of one six to eight second exposure per minute. The Soligar lens opening was $f0.95$, and the exposures were made on Kodak Tri-X or 4-X movie film that was developed for maximum speed and contrast. A combination of 60 Hz AC powered digital clocks and large face battery powered Accutron clocks provided times internally accurate to within at least two or three minutes depending upon the diligence of the camera operators.

From Table I it is noted that the Alaskan magnetic meridian chain of stations has a geographic northeast-southwest orientation. The orientation is roughly parallel to the tilt of large-scale weather patterns. The result is that similar weather conditions often prevail along the magnetic meridian. It is not exceptional for the magnetic meridian to have favorable sky conditions for the photographic recording of auroral forms throughout a 16-hour winter night.

Data from a magnetic meridian auroral observing chain is ideal for the systematic study of meridional motions and distributions of auroras as a function of local and substorm time. The following section will outline the analysis and limitations of all-sky camera data to be used for the specific

purpose of meridional motion and distribution studies.

2.2.2 The Analysis and the Limitations of All-Sky Camera Data

The purpose of this section is twofold:

1. A description is given of how the all-sky camera data were analyzed to determine the meridional distributions and motions of auroral forms.
2. A discussion is also presented to outline the difficulties and the limitations in the use of all-sky camera data for the determination of auroral position and character.

With a multi-station all-sky camera network, it is possible within overlapping fields-of-view to triangulate upon auroral forms to determine their ground projection position and their height. The station spacing (minor overlap) and the small 16mm film format have precluded such a detailed analysis for the Alaskan meridian data.

To obtain the ground projection position a 110 kilometer lower auroral border height was assumed throughout the analysis. While the work of Boyd et al. (1971) illustrates that significant and systematic auroral height variations do occur as a function of local time and latitude, the substorm auroras that Boyd et al. (1971) purposely avoided depart widely from their results. For this reason the very simple assumption of 110 kilometer lower auroral border height was used for all latitudes and local and substorm times.

Each all-sky camera film was scaled to obtain the temporal variation of the ground projection position of the auroras

along the local magnetic meridian through each station. Where possible, an attempt was made to keep track of individual auroral forms in their meridional motions.

When two or more cameras recorded auroral forms to be at approximately the same latitude along the meridian, the final analysis was based on the data from the station nearest to the auroral form. At times when an auroral form passed from the proximity of one station to another, slight 'smoothing' of the position data may have been required to join the motion of the form along the meridian. Such joining errors can result from any one or a combination of five factors:

1. An auroral form may deviate from a magnetic east-west orientation.
2. An auroral form may not have a lower border height of 110 kilometers.
3. There may be timing errors between observatories.
4. Individual stations may depart from a common magnetic meridian.
5. There are greater uncertainties in the ground projection distances for large zenith angles.

The last consideration is especially important for observing networks with large station separations. The geometrical conversion from zenith angle to ground projection distance is a non-linear function:

$$D = R_e \left[Z - \sin^{-1} \left(\frac{R_e + h'}{R_e + h} \sin Z \right) \right]$$

where

D = ground projection distance

Z = measured zenith angle

R_e = radius of the earth

h' = elevation of the observatory

h = height of the auroral lower border

A small change in a large zenith angle corresponds to a relatively large change in the ground projection distance compared to the ground projection distance change related to the same small change in a small zenith angle.

The joining errors were largest for the greater station separations in which the zones of overlap occurred at larger zenith angles. Joining errors were approximately one-half to one degree of latitude for forms that moved rapidly along the meridian from the proximity of one station to another. Position uncertainties were generally less than one-half a degree of latitude for those forms that persisted at a constant latitude or drifted slowly along the meridian. 'Smoothing' was limited to auroral forms that were oriented approximately east-west and had an arc or band-like appearance.

In the 1800 to 0600 hours local time (corrected geomagnetic local time, CGLT) sector during quiet periods, homogeneous (inactive) arcs are the common auroral forms. Within approximately 10 to 30 minutes after the onset of an auroral substorm in the midnight sector, diffuse patches and irregular folds develop to the equatorward side of discrete auroral arcs and bands that

lie in the midnight and the morning time sectors (Akasofu et al., 1966b). The extension of patchy auroras into the day sector will be discussed in section 4.2.

Auroral patches are aspect sensitive. That is, they may appear as arc-like when photographically recorded at large zenith angles. But when they are seen in the zenith, they appear as patchy diffuse auroral forms. Akasofu et al. (1966b) noted that the formation of patches, in the early morning time sector (0000 to 0600 hours CGLT), decreases in occurrence frequency at dipole latitudes greater than 65° . The Alaskan meridian station spacing is inadequate for the accurate determination of the precise boundaries of regions of auroral patches. In the analyses that follow, it was assumed that when patches were observed at College and possibly near the zenith at Fort Yukon that the southern boundary of auroral luminosity was comprised of diffuse auroras even though the auroral luminosity may have had an arc-like appearance when viewed from a distance. An obvious exception to this assumption occurs when an arc-like form moves from a distance to a position in or near the zenith amidst or replacing the diffuse auroras. Also in the analyses that follow, the indicated poleward boundary of the diffuse auroras is meant only to show that such auroras were equatorward or poleward of an observing station.

The arc-like appearance of the diffuse auroras, when photographically recorded at large zenith angles is due to several integration effects:

1. The line-of-sight may have passed through several auroral forms.
2. The rapid motion of these forms coupled with the six to eight second camera exposure time may have resulted in a blurred film image.

Several additional factors contribute to the uncertainties in the analyses of all-sky camera films. One of the most important of these is the zenith angle calibration of the optical system. The calibration requires the determination of zenith angles for representative stars. A comparison is made of the known zenith angles of the stars with the measured radial distances to the stars from the center of the all-sky camera circle (assuming camera level). The result of such a calibration is a best fit curve of a series of data points that define the zenith angle for a known radial distance from the center of the all-sky camera circle. Belon (1971) supplied the calibration shown in Figure 2. For very precise work, each all-sky camera system must be calibrated; for triangulation studies, the film should be scaled directly from the star field.

The following assumptions were made for the analysis of the 16mm Alaskan meridian all-sky camera data:

1. The camera was level
2. The camera maintained a constant azimuth orientation.
3. The camera was operated at sea level on a circular earth of polar radius 6356.79 kilometers (Allen, 1955).
4. The calibration data shown in Figure 2 are valid for all the cameras operated.

Thirty five millimeter auroral all-sky camera film, recorded aboard a jet aircraft, provided a part of the auroral data base. The analyses of aircraft acquired all-sky camera data present several problems peculiar to these data sources. The obvious and the most important additional factor is the motion of the aircraft. Again for very precise work, the data should be scaled directly from the star field. Such an analysis will account for the three dimensional motions of the aircraft.

The following assumptions were made for the analysis of the 35mm aircraft acquired all-sky camera data:

1. The camera was level.
2. The camera was operated at a nominal elevation of 10 kilometers above a circular earth.
3. The aircraft maintained a constant speed and geographic heading between navigator log entry times.
4. The calibration data (Wagner, 1971) shown in Figure 3 are valid for the data analyzed.

The determination of the ground projection position from either the aircraft or the ground acquired data is first in the geographic coordinate system. This determination is transferred into a geomagnetic coordinate system. Whalen (1970) has developed a useful nomograph for performing the transformation from high latitude geographic positions in the northern hemisphere into the corrected geographic latitude, longitude and time coordinate system. The nomograph was used throughout these analyses.

2.3 MERIDIONAL MOTIONS AND DISTRIBUTIONS OF AURORAS

2.3.1 Introduction

A meridian chain of auroral all-sky camera observatories is aligned at approximately right angles to the circumpolar auroral belt and as such is ideal for the study of meridional auroral motions and for determining the instantaneous meridional distribution of auroras that comprise the auroral oval.

The upper part of Figures 4-8 present cross sections through the instantaneous auroral oval as observed by the Alaskan magnetic meridian chain of stations during five nights of the 1969-1970 auroral season. The heavy solid line of the upper part of Figures 4-8 represents the position and continuity of auroral forms. The heavy dashed line defines the approximate boundary of the auroral oval when it is not defined by the continuous presence of an auroral form. The shading defines the latitudinal extent of the auroral oval when it is defined clearly by multiple auroral forms. The light hatching, as indicated, represents the approximate location of the patchy diffuse auroras. As mentioned previously, the northern extent of these diffuse auroras cannot be defined well with the data from the station spacing used. The boundaries of the $Q = 3$ statistical auroral oval (Feldstein and Starkov, 1967) are also shown for comparison. The lower portions of Figures 4-8 are the corresponding auroral zone magnetic indices in the form of AU and AL. The AU and AL indices provide a measure of the eastward and westward electrojet currents

flowing along the auroral zone (Davis and Sugiura, 1966). The figure captions list the stations that were used to develop the AU and AL indices. Superposed on the AU/AL indices are the H component magnetograms from Inuvik (71.1°N CGL).

The 'scanning' speed around the auroral oval by a single chain of observatories is too slow (one 'scan' per day) to depict the instantaneous azimuthal display of the auroral oval. Nevertheless, it is interesting to see that a gross oval pattern does emerge from the 'scan' (Figures 4-8).

The horizontal motions of visual auroral forms have been treated specifically by numerous authors (e.g. Meinel and Shulte, 1953; Meek, 1954b; Kim and Currie, 1958; Nicols, 1959; Evans, 1959, 1960; Davis and Kimball, 1960; Davis and Dewitt 1963; Akasofu et al., in the "Dynamics of the Aurora" series that appeared in *Journal of Atmospheric and Terrestrial Physics*, 1965-1966, and Davis, 1971). Previous observations agree that the east-west component of auroral motion is generally an order of magnitude greater than the north-south component (cf. Kim and Currie, 1958); possibly because of this asymmetry, the meridional motions have not been studied extensively.

Akasofu and his co-workers have found that the meridional motions of the auroras have five basic components within two general categories:

- A. Meridional motions related to auroral oval geometry and size:
 1. The earth's rotation beneath the quasi-stationary auroral oval results in even equatorward and morning

poleward motions.

2. Equatorward and poleward motions are associated with the interdependence of the geometrical configuration of the auroral oval and the general level of magnetic activity.
- B. Meridional motions related to the auroral substorm:
1. Poleward motions occur during the expansive phase.
 2. An equatorward 'spread' of irregular bands also occurs during the expansive phase.
 3. Equatorward motions occur during the recovery phase.

The auroral substorm related meridional motions are seen easily from a small network or, even in ideal situations, by a single station. However, there have been almost no case studies that have documented all of the motions described.

Davis and Kimball (1960) concluded from a statistical study of night sector auroras that equatorward motions occur more frequently than poleward motions. These considerations as well as the present interest in the early phase of magnetospheric substorms suggest that the case history study of meridional auroral motions with comprehensive data is relevant. In the following subsections, the results shown in Figures 4-8 will be discussed with respect to the five listed meridional motions; comments will be made where appropriate on the Davis and Kimball (1960) study, and a discussion will be presented on a possible growth phase of magnetospheric substorms.

2.3.2 Meridional Motions Related to Auroral Oval Geometry and Size

The following discussion will treat observed (actual plus

apparent) motions of auroral forms. The spatial configuration of the auroras occupies an oval band that is offset from the rotational pole of the earth. This means that if auroral forms are stationary within a static oval that an observer fixed on the earth will observe apparent motions of auroral forms. To aid in the visualization of the magnitude and direction of these apparent motions, the $Q = 3$ statistical auroral oval is superposed on the upper part of Figures 4-8.

The apparent meridional motion of the aurora due to the earth's rotation beneath the auroral oval should be observed during periods of non-varying magnetic activity to be sure that other factors are not the cause of the observed motions. Of the days analyzed certain periods of January 6 and 8, 1970 satisfy the magnetic criteria. From 0200 to 1000 UT on January 6, the AU/AL indices were low and fairly uniform (Figure 2). Note the equatorward drift of auroras that occurred during this period, in particular, the fact that neither boundary of the instantaneous auroral oval was defined for more than 90 minutes by a continuous auroral form.

In general the individual auroral forms moved equatorward at a faster rate than either boundary or the statistical auroral oval even though the envelope of all the observed auroras moved roughly parallel to the statistical oval.

On January 8 from 1300-1600 UT, the AU/AL indices were enhanced but relatively constant (Figure 7). We observed that the equatorward auroral form that was present for the entire period did not move poleward as expected. The poleward

boundary of the instantaneous oval was ill-defined by forms that moved rapidly equatorward and disappeared while new forms reappeared at higher latitudes.

In each of the cases studied, the envelope of all auroral forms behaves in agreement with the gross motions expected from the statistical oval, i.e. pre-midnight equatorward drift and post-midnight poleward drift of the envelopes that bound the instantaneous auroral oval. However, the individual auroral forms often move equatorward between the envelopes. This finding verifies the statistical result of Davis and Kimball (1960) that equatorward motions are dominant throughout the night.

Akasofu and Chapman (1963) using D_{st} , Feldstein and Starkov (1967) using Q , Feldstein (1969) using Q and D_{st} , Stringer et al. (1965) using K_p and local K , Stringer and Belon (1967) using K_p and local K and Chubb and Hicks (1970) using K_p , have all discussed the 'geometry' or position of the auroral oval in relation to magnetic activity as defined by the forementioned magnetic indices. These studies agree that as magnetic activity increases visual auroras occur at progressively lower latitudes. Feldstein and Starkov (1967) have shown for the night sector that discrete auroral forms are found over a wider range of latitudes as well as at lower latitudes during increased magnetic activity in the auroral zone. These previous studies suggest that as the general level of magnetic activity changes, one should observe meridional motions as the oval size expands or contracts. This discussion will concentrate on the meridional

motions associated with the equatorward boundary of the instantaneous auroral oval, thus avoiding the difficult consideration of the motions that may be related to the thickening and the thinning of the oval band itself.

Stringer et al. (1965) present several cases in which the expansion equatorward and the contraction poleward could and could not be followed with changes in magnetic activity. They note that at times an abrupt change in the latitude of the auroras occurred with a change in the local magnetic disturbance index. A similar latitude change occurs in the case studies reported here; however, AU/AL and the Inuvik H component magnetogram were used as the indicators of magnetic activity. Notice at ~0520 UT on December 5, 1969 the abrupt appearance of auroras near the Inuvik zenith in the evening sector following, but associated with, the increased magnetic activity in the midnight sector (AL). On February 14, 1970 another similar and striking example occurred in the afternoon sector at approximately 0300 UT. In this case the aurora could be followed south during the development of an intense negative bay in the midnight sector that was also associated with a significant decrease in D_{st} (Sugiura and Poros, 1970). As the bay recovered, the aurora also showed a tendency to retreat poleward prior to another increase in activity about 0500 UT. As auroral zone magnetic activity decreased again after 0600 UT, the equatorward auroras disappeared from south of Inuvik and auroras were seen well to the north of Inuvik.

It can be seen also that the examples cited do not include the meridional auroral motions associated with abrupt changes in magnetic activity near local magnetic midnight (~ 1100 UT along the Alaskan meridian for the dates considered). Here, the substorm related motions are dominant, and studies to separate the substorm motions from the motions related to the auroral oval geometry and size are not feasible. An exception to the last statement may exist in a possibly pre-expansive phase meridional motion that will be discussed in the next subsection. In the cases studied, there were no isolated changes in magnetic activity during the local morning hours that could be used to study the association of the morning sector oval geometry with changes in magnetic activity.

Another aspect of this general problem of auroral oval geometry is the association of the 'size' of the oval, as defined by the latitude indices at different levels of solar activity. The days selected for this study were days of relatively low ring current activity; $|D_{ST}|$ was less than or equal to 18 gammas (Sugira and Poros, 1970). The contribution of ring current activity to the auroral oval size for the days of this study should be minimal (Feldstein, 1969). Polar magnetic substorms with an AL index of more than 500 gammas (Q index of 7 (Bartels, 1957)) occurred on December 5, 1969 and on February 14, 1970. The equatorward boundary of the discrete auroras on both of these days, with minor exceptions, was poleward of the equatorward boundary of the statistical

auroral oval (Feldstein and Starkov, 1967) defined for $Q = 3$ (an AL index of about 60 gammas) for the IGY solar maximum. However, the observed sunspot number for the period of these analyses was approximately one-half that of the IGY period (Solar Geophysical Data, Jan., 1972). These observations illustrate, by case study, the contraction of the auroral oval associated with a decrease in solar activity (Starkov and Feldstein, 1967).

2.3.3 Meridional Motions Related to the Auroral Substorm

2.3.3.1 The Growth Phase of Magnetospheric Substorms

There are two general purposes for the discussion that follows in this section:

1. Several examples will be given to illustrate the difficulties that other workers have had in successfully identifying the growth phase from surface and satellite observed magnetic field variations.
2. The Alaskan meridian all-sky camera data will be examined for a possible identification of the growth phase.

Recently there has been considerable interest in a very early phase of magnetospheric substorms. A number of works (Pudovkin, 1968, McPherron, 1970, Kokobun, 1971, Nishida and Kokobun, 1971, and Iijima and Nagata, 1971) have suggested that there is a distinct phase, called the growth phase, which precedes the expansive phase of magnetospheric substorms. The onset of the latter phase, defined by Akasofu (1964), is characterized by a rapid poleward expansion of the midnight sector auroral oval. Pudovkin, Shumilov and Zaitzeva (1968), Feldstein (1971), Kelley, Starr, and Mozer (1971), and Mozer (1971)

have noted an equatorward motion of auroras before the onset of the expansive phase of a substorm.

Unfortunately, in some of the referenced studies, the growth phase was determined on the basis of geomagnetic field variations without an examination of the corresponding all-sky camera photographs. From the Davis and Kimball (1960) study and also from the material discussed in previous sections of this chapter, it is apparent that equatorward auroral motions are not unusual at any local time of the night or, with the exception of the early expansive phase, at any substorm time. For an equatorward auroral motion to define the growth phase, there must be one or more additional characteristics which can provide the onset time of the growth phase.

It is believed commonly that several geomagnetic observatories scattered along the auroral zone can monitor the intensity of the auroral electrojet. As pointed out by Feldstein and Starkov (1967), Stringer and Belon (1967) and Akasofu (1969), the auroral oval contracts poleward during quiet periods to about dp latitude 70° or higher and expands equatorward during disturbed periods (see also Akasofu and Chapman, 1963). Care must be exercised to interpret geomagnetic variations for substorms which are preceded by a few hours of magnetoquiet (both the AE and D_{st} indices are small). This is especially true for the so-called 'isolated' substorms. Such substorms tend to occur along the contracted oval, and their 'magnetic signature' along the auroral zone can be quite different from that for

successive substorms. In this situation, since the oval is located well poleward of auroral zone stations in the midnight sector, a typical auroral zone station temporarily 'becomes' a subauroral station. Examples of two such substorms are discussed in section 2.5 on the basis of the records taken from the Alaska meridian chain of stations; such substorms, on the contracted oval, occurred almost beyond the field of view of the College all-sky camera.

In such situations the AE index is not proportional to the total intensity of the auroral electrojet. Indeed, it is possible that when successive substorms occur after a few hours of magnetoquiet, the first substorm begins along the contracted oval, and the oval expands equatorward as a whole as the subsequent substorms occur. During the first of several successive substorms, the H component magnetic records from auroral zone stations in the midnight sector may show a weak negative bay (or sometimes even a positive bay). Subsequent substorms are defined more clearly as negative bays with a sharp onset. McPherron (1970) and Kokubun (1971) noted that a sharp growth of negative bays is preceded by a gradual growth of negative bays which last for 1-2 hours. They call this initial slow growth the 'growth phase'. However, their growth phase fits with the pattern of the described magnetic variations. Such an inference cannot be proved easily without having magnetic and/or all-sky records from a meridian chain of stations. The following example, supplemented with magnetic and all-sky

camera data from the Alaskan meridian, will serve to illustrate the sequence of events just described.

The lower half of Figure 8 shows the AU and AL indices on February 14, 1970. Superposed on the AL index is the simultaneous magnetic record from Inuvik (71.1°N CGL), located about 680 km poleward of College (64.9°N CGL).

In the AL index, a weak negative bay began at about 0850 UT and gradually developed until about 1025 UT when an intense negative bay began at College; this portion of the AL index is identical to the College records. Such a gradual growth of the negative bay fits with the description of the growth phase. However, the Inuvik magnetic record superposed on the AL index shows a fairly well defined negative bay during this period as well as at 0830 UT. At 1000 UT, the center line of the oval was located at about 68.5°N CGL , about 270 km south of Inuvik, and its all-sky camera recorded clearly active auroras. Thus, on the basis of both the magnetic and auroral records from Inuvik, it is concluded that the 'slow' growth negative bay in the AL index is misleading if this 'slow' growth is interpreted as a growth phase.

It is important to note that such auroral activity is not observable from a typical auroral zone station (like College), except for an equatorward motion associated with the expansion of the oval. The absence of auroral displays near the zenith of a typical auroral zone station does not necessarily mean the absence of substorms. A single auroral zone all-sky camera

will often be inadequate to identify the expansive phase.

Another complication occurred also on the same day. The AL index began to increase at 1315 UT and suddenly increased at 1440 UT after a slight decrease between 1415 and 1440 UT. The all-sky photographs taken from College show the formation of patches near the equatorward boundary of the oval at 1315 UT. The patches faded between 1415 and 1440 UT and reappeared at 1440 UT. Since the formation of patches is one of the major features of auroral substorms, we can conclude that both the gradual and sudden increases of the AL index indicated the occurrence of two substorms. It should be noted that the formation of the patches was not visible from Fort Yukon, since it occurred near the equatorward horizon there.

As mentioned earlier, it is difficult to detect the occurrence of substorms from sub-auroral zone stations during fairly quiet periods. For example, examining magnetic records from Sodankyla, Leirvogur, Great Whale River, Meanook, Sitka and College on February 14, 1968, Aubry and McPherron (1970) claimed that no distinct substorm could be identified. However, the magnetic record from Tromsø showed clearly a negative bay of magnitude of more than 100 γ (Figure 9), thus casting doubt on some of their conclusions.

Kokubun (1971) and Nishida and Kokubun (1971) noted that the equivalent current system for the growth phase consists of two vortices of currents and that it is similar, or essentially identical, to the current system for the DP-2 variation (cf. Nishida and Kokubun, 1971). All-sky camera data are available for several

prior determinations of the growth phase and DP-2 variations. These examples were studied to determine if growth phase and DP-2 conclusions are valid with respect to the known auroral substorm phenomena.

Figure 10 shows, from the top, the angle θ (Ness *et al.*, 1964) of the interplanetary magnetic field, the Y component magnetic record from Aiert, the AL Index, and selected all-sky camera photographs from Mould Bay (80.9°N, CGL, 1600 km. poleward of College) on December 1, 1965. This example was examined in detail by Nishida (1971) who identified the disturbance between 1240 and 1310 UT to be the DP-2 variation and the disturbance 1310 UT to 1510 UT to be the DP-1 (auroral electrojet) variation. The Mould Bay all-sky records show clearly, however, that a violent poleward expansive motion began at about 1230 UT. Active auroras crossed the zenith about 1254-1255 UT and went further poleward. In this case, the poleward expansive motion of auroras occurred during the DP-2 variation which is supposed to be distinct from the DP-1 variation.

Figure 11 shows the AL index and the growth phases determined by Iijima and Nagata (1971) and also the corresponding all-sky photographs from Fort Yukon. Again, an intense poleward motion is seen clearly during the initial slow growth or their 'growth phase'.

Figure 12 shows another example of similar incorrect identification. The format of the upper part is the same as that of Figure 10, and the lower part shows selected all-sky

photographs from College on October 2, 1965. Nishida (1971) identified three successive DP-2 variations which were followed by a DP-1 variation and then two other DP-2 variations. The College all-sky photographs show, however, that during the first three DP-2 variations all the major characteristics of auroral displays during auroral substorms occurred. First of all, there were two westward traveling surges (1132-1147 UT), the subsequent poleward expansive motion (1150-1240) and the eastward drifting 'inverted Ω ' band (1405-1416 UT). All these features are so typical that there is little ambiguity about their identification. In this case, too, it must be concluded that auroral substorms were progressing during the 'growth phase'.

The lower half of Figure 13 shows the AE, AU, AL and D_{st} indices (Cape Wellen, College, Byrd, Baker Lake, Cape Chelyuskin, Murmansk, Tixie Bay and Dixon) on May 30, 1960. The period indicated by the letter B fits well the description of the growth phase defined by Kokubun (1971); in particular, note that $AU > AL$ and the D_{st} index shows a slight depression. However, a poleward motion of auroras was observed at Byrd (68.6°S CGL) and subsequently at South Pole (74.7°S CGL) during this period (Figure 14). The poleward motion began about 0415 UT, and auroras crossed the zenith of Byrd about 0532 UT and of the South Pole about 0625 UT. From 0630 UT to about 0700 UT the poleward boundary of the instantaneous auroral oval moved equatorward approximately four degrees of latitude. As the

growth of AL continued, the aurora again moved poleward, crossing the South Pole zenith about 0706 UT and eventually reached the poleward horizon of the South Pole Station ($\sim 79^{\circ}\text{S}$ CGL). Thus period B cannot be the growth phase of the substorm with the sharp onset negative bay about 0830 UT.

There is also another example in which the growth phase is not clearly defined. Figure 16 shows the H component magnetic records from College, Barrow and Cape Wellen on February 13, 1968. Aubry and McPherron (1970) determined the onset of the expansion phase to be 1230 UT. In spite of the bright moon and foggy condition, all-sky photographs from all the Alaskan stations (Fort Yukon, Bettles, Eagle and College) showed considerable auroral activity after 0800 UT. This activity can be seen clearly in the magnetic records from College and Barrow. The last intensification of auroral activity began about 1215 UT, or even earlier, in Alaska which was located in the early morning sector; the Cape Wellen record shows the onset of a negative bay at 1145 UT. Aubry and McPherron (1971) determined also the onset time of the expansion phase for the second substorm to be 1610 UT. However, the auroral substorm activity began at 1559 UT or earlier in Alaska (the last morning sector). Their determination of the onset time of the expansion phase was partly based on a decrease of the magnetic field intensity in the distant tail which is usually associated with the expansion of the plasma sheet (cf. Meng et al., 1971). However, simultaneous

observations of the expansion by two satellites indicate that the times when the expanding plasma sheet reaches satellites are a complicated function of location of satellites in the distant tail (cf. Meng *et al.*, 1970).

The preceding discussion shows clearly that it is difficult to define the growth phase on the basis of magnetic records alone. The identification of a growth phase from the magnetic records for any of the substorm examples discussed in this paper is incorrect. It is concluded that until geomagnetic field variations during an early phase of magnetospheric substorms are well established, the growth phase should not be defined on the basis of auroral zone magnetic records alone.

It should be noted in this connection that the AE index should not be considered to be proportional to the total current intensity of the auroral electrojet because of the lack of accurate knowledge of the growth pattern of the electrojet during the early phase of magnetospheric substorms. It is also unlikely that all initial slow growths can be attributed to the expansion effect of the oval associated with successive substorms. A similar pattern occurs also in the vicinity of the path of westward traveling surges (Akasofu 1968, p. 43).

Akasofu (1950) noted that rapid motions of the auroral electrojet make it difficult to assume that an observed negative bay represents time variations of the total intensity of the electrojet. A very rapid growth of the negative bay could be either or both a rapid growth and a rapid motion of the

electrojet toward the observer. This is quite common near the poleward expanding bulge. Similarly, a rapid decay of negative bays could be either or both a rapid decay and a rapid motion of the electrojet away from the observer.

It is also clear that the absence of auroral displays over an auroral zone station in the midnight sector does not necessarily indicate the absence of auroral substorms. An auroral substorm may occur almost beyond the field of view of a typical auroral zone station. One must also be careful in interpreting an equatorward motion of auroras, since there are several causes which are not related to the growth phase (Akasofu, Kimball and Meng 1966c). In particular, a slight equatorward motion of the oval a little before the arrival of westward traveling surges or eastward drift motions (Akasofu 1968, Figure 17) should not be identified with the growth phase feature.

In brief, extreme care is needed to identify the growth phase without a close network of magnetic or all-sky stations, in particular a meridian chain of stations. The AE index is a good index for substorms, but it is too crude to identify the growth phase.

Thus far the theme of this section has been to illustrate the prior and incorrect identifications of magnetospheric substorm growth phases. One may attribute the inadequacies of the determinations to an insufficient and possibly inappropriate data base.

Hones et al. (1971) have shown that the auroral brightening, immediately prior to the poleward expansion, to be a good indicator of substorm onset. The brightening occurs within the temporal uncertainty (several minutes) of the onsets of other magnetospheric substorm phenomena, i.e. plasma sheet thinning, auroral zone negative bay, and low latitude positive bay. Since the auroral substorm onset is often unambiguously defined and apparently an indicator of the onset of all substorm phenomena, it is natural to ask if there are any other auroral characteristics that might help to identify the growth phase. As mentioned previously, several workers have suggested or observed that midnight sector equatorward auroral motions precede the expansive phase of magnetospheric substorms. However, a large uncertainty must exist in these unqualified statements because equatorward auroral motions are common throughout the night sector (cf. Davis and Kimball, 1960).

An inspection of Figures 4-8 seems to show that there are interesting and pronounced meridional motions prior to the substorm expansive phase. Of the five days analyzed, auroral substorms occurred near midnight on December 5, 1969 and January 5 and 8, 1970 that exhibited well defined expansive phases and that were not preceded by any unusual magnetic activity that would confuse the auroral situation during the possible growth phase. These cases should be ideal for the study of pre-expansive phase auroral activity. Several interesting characteristics may be noted.

First, up to 60 - 120 minutes prior to the expansive phase onset, the equatorward drift rate of auroral forms increases. Møzer (1971) suggested that such an increased equatorward speed arises from an increasing westward electric field during this period. Second, the poleward sky is relatively free of auroras just prior to the expansive phase. That is, the auroral oval in the midnight sector is reduced to one, or possibly several, equatorward auroral arcs prior to the activation and the expansive phase. Notice that this equatorward thinning of the midnight auroral belt occurs during the relative magnetic quiet prior to the sudden onset negative bay of the expansive phase. Notice also that the equatorward 'spread' of the expansive phase is minor relative to the equatorward drifts that precede the expansive phase. This means that in the midnight sector the auroral belt moved and thinned equatorward prior to the substorm and relatively little equatorward motion was associated with the expansive phase of these substorms. On December 5, 1969 two substorms occurred within approximately one hour (~ 1040 and ~ 1130 UT). Notice that in the second substorm the midnight auroras drifted and thinned equatorward prior to the weak intensity but significant poleward expansion. This is in contrast to the January 5, 1970 double substorm structure (~ 1000 and ~ 1045 UT) where the equatorward recovery of the poleward boundary of the auroras was interrupted by the second substorm and poleward expansion. From these limited examples, it appears that the evening, midnight and possibly the early morning auroras shift equatorward prior to an 'isolated' magnetospheric substorm; whereas in the midday

sector, the auroras shift equatorward during the substorm (Akasofu, 1972a, b).

It is thus of great interest to examine interplanetary magnetic field conditions during the equatorward motions prior to the expansive phase. A preliminary study of Explorer 33 and 35 satellite data indicates that on both December 5, 1969 and January 8, 1970, there was no clear indication of the expected relationship, while on January 5, 1970, the situation was more or less as expected. It is thus necessary to examine many more events before being able to identify the equatorward motion to be a true manifestation of the growth phase. It should be noted in this connection that the equatorward motion does not occur concurrently with the thinning of the plasma sheet. Hones et al. (1971) showed that the thinning begins at the onset time of the expansive phase.

The possibility of a depression of the H component in low-latitudes during the equatorward motion was also examined. Kokubun (1971) suggested this possible magnetogram characteristic to be a manifestation of the growth phase. There were, however, no such indications on any of the days studied.

McPherron (1970) noted that there is a slow growth of the AL index prior to the expansive phase. The data examined do not show any consistent indication of such a slow growth. This was discussed in detail in previous paragraphs.

2.3.3.2 Poleward Motions and the Expansive Phase

The most spectacular of the meridional motions is the poleward expansive motion of the midnight sector of the auroral

oval associated with the polar magnetic substorm (cf. Akasofu, 1968). Poleward expansive motions within an hour of local magnetic midnight were observed on December 5, 1969, January 5 and 8, 1970 and February 14, 1970. The January 5 (~1000 UT) and 8 (~1020 UT) events are the clearest and appear to be free of the complications of other superimposed substorm activity. However, in both of these cases, the expansion was not purely poleward but had a significant westward component (see Figure 19 for photographs of the January 8, 1970 event). The westward component indicates that the auroral substorm may have begun slightly east of the Alaskan meridian and that the observed motion was composed of a poleward expansion and a westward traveling surge. During a poleward expansion, the location of the northern boundary of the expanding oval can be easily defined but the auroral motions within the poleward 'bulge' are often too violent to be studied in detail from the all-sky camera photographs (Akasofu et al., 1966a). In the cases where it was possible to define the meridional motions of the forms within the poleward 'bulge', equatorward motions were observed prior to the time that the expansion had reached its most poleward point, e.g. 1200 UT December 5, 1969 and 1030 - 1130 UT January 5, 1970. This is another situation that undoubtedly adds to the dominance of night sector equatorward motions (Davis and Kimball, 1960).

From figures 4-8 one can see that in general the poleward motion of a night sector auroral form was normally associated with or followed an increase in auroral zone magnetic activity. An obvious exception to this statement occurred at 0700 UT on

February 14, 1970 when a rapid poleward motion was observed following a decrease in auroral zone magnetic activity. However, the inspection of the Mould Bay magnetic data shows that a negative bay of approximately 60 gammas occurred in the Y component record. This weak bay was nearly coincident with the poleward motion of the aurora. As discussed previously, the AE index may not be proportional, in certain situations, to the total intensity of the auroral electrojet. This study suggests that poleward auroral motions in the night sector are a sensitive indicator of magnetospheric activity; whereas, with the exception of the apparent morning poleward drift, equatorward motions dominate the quiet night sector auroral oval.

The equatorward motion of irregular auroral bands during a substorm has been described by Akasofu et al. (1966c). Examples of these meridional motions are illustrated in relation to the other meridional motions by noting the equatorward expansion of the southern boundary of the auroras in Figures 4 (~1130-1200 UT), 5 (~1000 UT), 6 (~1120-1230 UT), 7 (~1020 UT), and 8 (~1100-1115 UT). It is noted that this substorm associated equatorward 'spread' is relatively minor, several degrees of latitude, while the poleward expansion often occurs over ten degrees of latitude.

Another characteristic difference between the poleward and the equatorward auroras during a substorm is that much lower intensity auroras comprise the equatorward-most region of auroral luminosity. The irregular bands and the diffuse auroras are weak compared to the discrete auroras that advance poleward and that occupy the poleward 'bulge' during the auroral substorm.

The equatorward diffuse auroras show little meridional motion compared to the rapid, generally eastward, latitudinal drift that is easily seen in the cine projection of the all-sky camera films.

2.3.3.3 Recovery Phase

Equatorward auroral motions during the recovery phase of substorms have been discussed by Akasofu et al. (1966c). They found that the characteristic equatorward recovery speed was slower than the poleward expansive speed, and that the equatorward recovery may be interrupted by a new substorm that will renew the poleward motion.

From the analysis here, it is apparent that equatorward motions, following the advent of the expansive phase of the auroral substorm, begin before the poleward expansion is complete or before the poleward envelopes begin to contract equatorward. It is not readily apparent from the case histories presented in these examples that the equatorward recovery speeds are less than the poleward expansive speeds. When the poleward envelope of the auroras is considered, then the comparative statement about the speeds is correct for the situations studied. Further, it may be pertinent to ask what is the recovery phase of the auroral substorm? Is it the reappearance of a significant equatorward-component of motion within the poleward 'bulge' or the subsequent equatorward recovery of the auroral form that defines the poleward boundary of the 'bulge'?

The January 5, 1970 data (Figure 5) show an excellent example

of an interruption of the equatorward auroral motions of the recovery phase by the onset of a second poleward expansion at about 1045 UT. Note that the AL index, constructed from the auroral zone magnetic records, shows only a gradual onset negative bay and no definite hint of successive substorms; whereas, the Inuvik magnetogram shows clearly the double bay structure that follows closely the poleward motion of the auroras. This is another example that illustrates the inadequacy of the AE index for use in detailed studies of auroral and magnetospheric dynamics. It also points toward the importance of magnetic meridian chains of observatories for the detailed study and monitoring of high latitude magnetospheric substorm phenomena.

2.3.4. Summary

Both all-sky and magnetic records from the Alaskan meridian chain of stations have provided and clarified several important features of auroral morphology.

A. Although the daily 'scanning' by the chain stations reveals the general pattern of the auroral oval, there are at many times considerable departures from the pattern suggested by the earth rotating beneath a quasi-stationary auroral oval.

B. Regardless of the local time in the night sector, individual auroral forms drift generally equatorward within the band of latitudes where auroras are observed most frequently, i.e. the statistical auroral oval. The exception to the equatorward drift occurs during brief periods of the expansive phase of auroral substorms or in association with less well defined

increases in auroral oval magnetic activity. The dominance of the equatorward drift motions throughout the night is in agreement with a statistical study by Davis and Kimball (1960).

C. Poleward auroral motions, within the night sector, appear to be a sensitive indicator of magnetospheric substorm activity.

D. There seems to be an enhanced equatorward drift of auroral forms 60 - 120 minutes prior to the onset of the expansive phase of an auroral substorm. The equatorward drift (Pudovkin et al., 1968; Feldstein, 1971; Kelly et al., 1971; and Mozer, 1971) and the 'clearing' of the poleward sky result in an equatorward thinning of the auroral oval. However, since the equatorward drift motion of auroras is a common feature, another independent phenomenon is needed to define definitely the growth phase. From the examples considered, there does not appear to be any unambiguous characteristic of the AU or the AL indices that can be associated with the enhanced equatorward drift of auroras prior to the onset of an auroral substorm in the midnight sector. A preliminary examination of the corresponding interplanetary conditions at about the onset of the enhanced equatorward drift is inconclusive. There is also no consistent relationship between the claimed manifestations of the growth phase and the equatorward motion.

E. During an auroral substorm, equatorward motions of auroral forms may occur within the expanding 'bulge' before the poleward boundary of the 'bulge' reaches its highest latitude.

F. The speed of the equatorward auroral motions may be, at times, of the same magnitude or even greater than the speed of the poleward expansive motions of the auroral substorm.

G. All-sky camera data analyses illustrate, by case study, the contraction of the auroral oval associated with a decrease in solar activity.

2.4 AURORAL SUBFORMS ON THE CONTRACTED AURORAL OVAL

2.4.1 Introduction

Several workers have noted that the auroral oval contracts poleward during periods of magnetoquiet. Stringer et al. (1965) have shown specific examples that during IQSY periods of zero and very weak magnetic disturbance that the midnight sector auroras contract poleward to near 75° dipole latitude. The work of Feldstein and Starkov (1967) and Starkov and Feldstein (1967b) has shown the equatorward boundary of the midnight sector $Q = 0$ statistical auroral oval to be located near 70° latitude (CGL) during both the IGY and the IQSY. For $D_{st} \gtrsim -30$ gammas (more positive) and $Q = 3$, the equatorward boundary of the midnight sector of the auroral oval shifts to near 65° CGL (Feldstein and Starkov, 1967; Starkov and Feldstein, 1968; Starkov and Feldstein, 1967). The upper limit of the magnetic disturbance amplitude for $Q = 3$ is 80 gammas (Bartels, 1957). This suggests that an auroral zone station, such as College, Alaska (64.9°N, CGL) would be statistically just equatorward of or even beneath the midnight sector auroras for all associated polar magnetic substorms with a disturbance amplitude greater

than or equal to 80 gammas.

It should be noted that the midnight sector Q indices, referred to by the Russian workers, are those reduced to the value of the Q index for 64.5°N CGL (Feldstein and Starkov, 1967). With this fact, there remains the possibility that auroral and polar magnetic substorms do occur on the contracted oval; yet, the associated magnetic disturbance at ~65° latitude (CGL) is relatively minor (less than ~100 gammas). The purpose of this section is to present observational evidence from the Alaskan meridian chain that intense auroral and polar magnetic substorms do occur on the contracted oval with only minor indications at a typical auroral zone latitude station such as College.

Two such substorms will be discussed that were observed near local midnight by the Alaskan meridian chain on January 5 and 8, 1970.

2.4.2 January 5, 1970 Auroral Substorm

On January 5, 1970 the equatorward migration of auroras, discussed in previous section as a possible pre-expansive phase, culminated in the 0917 UT appearance of a new auroral arc about 120 kilometers poleward of Fort Yukon (Figure 5). At 0923 UT this arc brightened for a short time and drifted slightly poleward -- possibly in association with the slight negative bay (~70 gammas) in the AL index. At 0954 UT this same arc suddenly brightened, and at 0957 UT the expansive phase of the auroral substorm began. The poleward moving auroras crossed the Inuvik zenith about 1000 UT, and a very sharp onset negative bay of about 350 gammas

began at Inuvik just a few minutes prior to the poleward motion of the auroras through the Inuvik zenith (Figure 5). After 1004 UT the equatorward moving arc of the auroral substorm disintegrated into patches that prevailed for about 10 minutes in a position poleward of $\sim 66.7^\circ\text{N}$ CGL. A reintensification of the substorm phenomena after 1030 UT resulted in the poleward 'bulge' expanding poleward to approximately 77.5°N CGL by 1145 UT; however, there were no auroras observed equatorward of $\sim 68.5^\circ\text{N}$ CGL.

It is important to note several aspects of this disturbance. All auroras associated with this intense substorm occurred poleward of 66.7°N CGL. Only a minor, ~ 50 gamma, positive bay was observed at College (64.9°N CGL) whereas Inuvik recorded an intense, 350 gamma, negative bay (Figure 17).

2.4.3 January 8, 1970 Auroral Substorm

The substorm of January 8, 1970 was similar in many respects to the January 5, 1970 substorm. The auroral substorm occurred poleward of 66.9°N CGL. The magnetic 'signature' of the substorm at College was a minor, generally positive, perturbation compared to the 270 gamma negative bay recorded at Inuvik (Figure 18). The expansive phase of this substorm was also preceded by an equatorward 'thinning' of the auroral oval at about 69°N CGL (Figure 7). This thinning began almost two hours prior to the expansive phase. These pre-substorm auroral forms were at times bright and active bands (e.g. 0900-0930 UT). At 0920 UT and 1001 UT the equatorward-most arc brightened transiently and drifted poleward. From 1017 to 1020 UT the auroral oval

narrowed to a single arc that brightened from east to west; the expansive phase of the auroral substorm followed immediately. The poleward 'bulge' auroral forms were very bright and active with no organized internal motion discernable in cine projection of the all-sky camera data. The poleward expansion can be recognized easily by comparing the simultaneous photographs from Sachs Harbour and Inuvik (Figure 19).

2.4.4 Discussion

From Figures 5, 7, 17, 18 and 19, it is easily seen that auroral and polar magnetic substorms do occur on the contracted auroral oval. The features of these substorms are identical, with the exception of the latitude of occurrence, to those that occur at typical auroral zone latitudes. It is also easily seen that the magnetic and auroral records from auroral zone latitudes give little hint of the occurrence of substorms on the contracted oval. Therefore without a meridian chain of observatories, that extends to about 75° CGL, it is not possible to monitor substorm activity during quiet periods such as discussed for January 5 and 8, 1970.

2.5 CONTINUOUS AURORAL OBSERVATIONS

2.5.1 Limiting Factors for Continuous Auroral Observations

As discussed in the previous sections of this chapter, the magnetic meridian observing chain is the most efficient way to monitor the auroral oval. The meridian chain may be compared to an azimuth scan radar that 'scans' the auroral oval once per day. The Alaskan meridian chain is ideal for

the systematic monitoring of the night sector auroras; however, sunlight precludes day-sector observations except for possibly near the winter solstice. Since upper atmospheric lighting conditions are a strong governing factor for any type of optical auroral measurement, the following paragraph will outline the major limitations in the northern hemisphere. The discussion will ignore tropospheric weather conditions.

For the highest potential of observing auroras any day of the year near magnetic midnight, one requires a ground station with a relatively low geographic latitude for a corresponding geomagnetic latitude of approximately 65 to 70° CGL. In the northern hemisphere, this region is located in the eastern Hudson Bay area of Canada.

For the highest potential of observing auroras for a full 24 hour period near the winter solstice, one requires a ground station with relatively high geographic latitude for a corresponding geomagnetic latitude of approximately 73 to 78° CGL. The most favorable land areas in the northern hemisphere are northeastern Greenland, Svalbard, Franz Josef Land, and Severnaya Zemlya.

Figure 20 will help to illustrate the preceding, and several following, considerations. The geographic outlines of the major land areas for high latitudes in the northern hemisphere are shown as transformed into the corrected geomagnetic coordinate system (Whalen, 1970). The 50 kilometer shadow height at local solar noon is shown for various dates. Also shown are several constant geomagnetic latitude (CGL) circles.

To observe auroras from a ground based observatory or even a jet aircraft, the upper atmosphere cannot be sunlit below 50 kilometers, at the absolute lowest, and preferably not below 100 kilometers. These shadow heights correspond to solar depression angles of seven and ten degrees respectively. If sunlight illuminates the atmosphere below 50 kilometers, the scattered sunlight will prevent optical observations of aurora.

Another limiting factor is moonlight. Moonlight interferes with most optical auroral observations - especially those of the fainter auroral forms that comprise the midday sector of the auroral oval. Moonlight can become a significant problem when one considers that at high geographic latitudes that the winter moon may be continuously above the horizon for several days about the time of the full moon.

It should be pointed out that the advances in lighting technology are also important to consider. The installation of mercury and sodium vapor exterior lighting at remote arctic stations has been detrimental to the quality of the all-sky camera data -- especially under blowing snow conditions. This fact is clearly illustrated when the excellent data taken at Mould Bay in the early 1960s (without high intensity exterior lighting) are compared to those data from the recent past (with high intensity exterior lighting).

2.5.2 A Southern Hemisphere Auroral Observing Chain

From the title of this section and the previous discussion,

it may be inferred that there are certain advantages in auroral data acquired in the southern hemisphere. South Pole Station (Amundsen-Scott) is located at 90°S geographic and has a favorable geomagnetic latitude (74.7°S CGL) for auroral observations. South Pole is complimented by Byrd Station located at 80°S geographic latitude and at 68.6°S CGL. Davis and DeWitt (1963) demonstrated the value of the Byrd data in the determination of characteristic auroral motions. Simultaneous data from both stations become more interesting when one notes that these two stations are separated by only 25.6° in geomagnetic longitude (approximately 1 hour 40 minutes in geomagnetic time, CGLT). This means that Byrd and South Pole form a two station 'quasi-meridian' observing chain.

2.5.3 Continuous Auroral Observations for May 30, 1960

All-sky camera films were reviewed for both stations for approximately one observing season to find a day with clear skies and auroras at both stations. May 30, 1960, a day also considered by Davis and DeWitt (1963), was selected for investigation. The meridional position and character (diffuse or discrete) of each auroral form was determined, and the results are shown in Figure 13 in a similar format to the Alaskan meridian figures. Since the stations are separated by almost two hours in geomagnetic time, the poleward and the equatorward boundaries of the $Q = 3$ statistical auroral oval were defined separately by the distances from South Pole and Byrd respectively. Since ground projection position data are uncertain for large zenith angles, auroral forms for $Z > 80^{\circ}$ have been grouped into two categories (poleward

and equatorward of each station) and are displayed in Figure 13 by dashed lines. No attempt has been made to smooth the data because of the latitudinal and the temporal separations of the stations.

The geomagnetic field was moderately disturbed on May 30, 1960. The lower half of Figure 13 shows that several polar magnetic substorms occurred and that the equatorial D_{st} index decreased to a minimum of -49 gammas at 1700 UT (Sugiura and Poros, 1970). K_p ranged from 2o to 4+ and ΣK_p for the day was 25- (Solar-Geophysical Data, July, 1960).

As before, with the Alaskan meridian chain, the 'scanning' speed around the auroral oval is too slow to depict the instantaneous azimuthal display of the oval. Yet, the two station chain data reveal that a gross oval pattern does emerge from the complete 24 hour 'scan' (Figure 13).

Since ΣK_p was greater than 10 for May 30, 1960, one would expect to find a continuous band of auroras around the geomagnetic pole (Buchau et al., 1970); with minor exceptions, this was the situation found. Discrete auroras were not observed continuously for two periods: ~0015 to 0105 UT and ~1000 to 1030 UT. During the earlier period the auroras disappeared and reappeared at similar latitudes. This suggests that the first 'gap' in the auroral oval may have been temporal rather than spatial and possibly related to the lower threshold auroral intensity that could have been recorded by an all-sky camera in 1960. The second period was not an absence of auroral forms. Rather, there was an absence of discrete auroral forms during a substorm

that began at about 0945 UT. Diffuse auroral forms covered the entire field-of-view of the Byrd camera (Figure 14). No definitive statements can be made about the presence of discrete auroras for the period in question.

The slow, two station 'scan' of the auroral oval for May 30, 1960 supports the concept of a continuous auroral oval without any spatial gaps. There is no indication of a latitude discontinuity between the day and night sector auroras as has been suggested by Mishin et al. (1970) and reported by Lassen (1972) from visual auroral observations in Greenland.

In Section 4.2, midday auroral patches are discussed for northern hemisphere observations. As mentioned earlier, the northern hemisphere lighting conditions are not the most favorable for midday auroral observations. The 'discovery' of midday auroral patches in auroral data from the northern hemisphere prompted an examination of Byrd films for the same phenomena. Diffuse patchy midday auroras observed on May 30, 1960 are typical of occurrences on other days. Figure 15 shows remarkable examples of intense diffuse patchy auroras from 1300 to 1700 UT. After the later time, twilight interference became too great for good photographic reproduction; however, cine projection revealed that the patches continued through 1800 UT (\sim 1240 hours CGLT).

With the exception of an approximate 75 minute period (\sim 1130 to 1245 UT), auroral patches were observed continuously from 0940 UT to midday twilight at 1800 UT. These diffuse auroral displays are morphologically related to the series

of magnetospheric substorms that occurred prior to 1600 UT; the extension of the patchy auroras from the early morning sector, where their occurrence has been well documented (cf. Akasofu et al., 1966b) into the day sector is established.

An equatorward 'thinning' of the auroral oval is indicated prior to the midnight sector substorm (Figures 13,14). This 'thinning' is in agreement with the results found for the substorms studied with the Alaskan meridian data. Equatorward 'thinning' of the auroral oval prior to subsequent substorms is not clearly indicated -- possibly because of the increased disturbance level and the location of the stations in the morning sector.

Data from both Byrd and South Pole indicate the equatorward motion and the subsequent retreat poleward of the day-sector auroras associated with the development and recovery of the largest polar magnetic substorm (~1330 to 1500 UT) (Figures 13, 15). Notice also for this same time period, the occurrence of auroral patches equatorward of the discrete auroras (Figures 13, 15).

Following the substorm recovery motion of the day-sector auroras and during a period of relatively constant AE index, numerous auroral forms were observed to appear equatorward of the South Pole zenith, drift poleward through the zenith, and subsequently disappear while continuing poleward. Shortly after 2100 UT (1800-1900 hours CGLT) the dominant meridional auroral motions became equatorward.

2.5.4 Day-Sector Meridional Auroral Motions

It is not clear exactly what the motions of auroras indicate.

Two plausible possibilities are: magnetospheric convection patterns (Davis, 1971) or motion of primary auroral electron sources through the magnetosphere. If the first possibility is correct, the dominance of poleward auroral motions observed between 1700 and 2100 UT on May 30, 1960 may indicate the steady state convection pattern similar to that suggested by Dungey (1961). A survey of South Pole all-sky camera films revealed that the occurrence of poleward drifting auroral forms varies from day to day. For this reason no absolute statement can be made as to whether the pattern of May 30, 1960 is representative of the general meridional motions of day-sector auroras.

Nine eight-hour periods (1200-2000 UT) during days in 1962 were selected for additional study (May 31, June 1, 7, 28, 29 and 30, and July 1, 5, and 6, 1962). Figure 21 presents the meridional distributions of the day sector discrete auroras that were observed during the nine additional periods. Of the total of ten days studied, there were four extended periods in which the day-sector 'migrating' poleward auroral motions were observed (May 30, 1960, 1800-2000 UT; May 31, 1962, 1430-1530 UT; July 1, 1962, 1145-1400 UT and July 6, 1962, 1145-1415 UT). From this limited investigation it appears that the frequent successive birth, poleward migration, and disappearance of the day-sector auroras are not uncommon phenomena, but not necessarily representative of all day-sector auroras.

A statistical approach was undertaken to gain further insight into the data sample. The number of auroral forms was

determined that passed through or that disappeared in the South Pole zenith as the forms drifted poleward or equatorward. The resulting distribution for the ten eight-hour periods is:

Poleward motion crossings of the South Pole zenith: 44

Equatorward motion crossings of the South Pole zenith: 17

If one makes the a priori assumption that day-sector auroral motions through the South Pole zenith are equally probable in either direction, the probability of achieving the observed distribution is less than one percent.

Another approach used was to determine the number of auroral forms that disappeared poleward or equatorward of their position of first observation. This question removes bias that may have been introduced in the first distribution as a result of the position of the station relative to those auroral forms that passed through the station latitude. The results for the second distribution are:

Poleward disappearances: 103

Equatorward disappearances: 50

Again if both disappearances are equally probable, the probability of achieving at least 103 poleward disappearances out of 153 is much less than one percent.

This limited study demonstrates that poleward auroral motions are more likely than equatorward motions within the day-sector auroral oval. This is in obvious contrast to the night-sector where equatorward motions are more frequent than poleward motions (Davis and Kimball, 1960).

TABLE 1
Alaskan Sector Observatories (1969-1970)

<u>Station</u>	<u>Geographic</u>		<u>Corrected Geomagnetic</u>		<u>Instruments Operated</u>		
	<u>Lat.</u>	<u>Long.</u>	<u>Lat.</u>	<u>Long.</u>	<u>All-Sky Camera</u>	<u>Magnetometer</u>	<u>Riometer</u>
Mould Bay	76.2°N	119.4°W	80.9°N	96.0°W	X	X	
Sachs Harbour	72.0	125.3	76.3	89.2	X	X	X
Inuvik	68.6	133.0	71.1	91.2	X	X	X
Bar-I	69.2	143.7	69.9	100.3		X	X
Barrow	71.3	156.8	69.7	113.0		X	
Fort Yukon	66.9	145.3	67.1	99.3	X	X	X
College	64.9	147.8	64.9	99.7	X	X	X
Anchorage	61.2	149.9	60.8	98.7		X	X

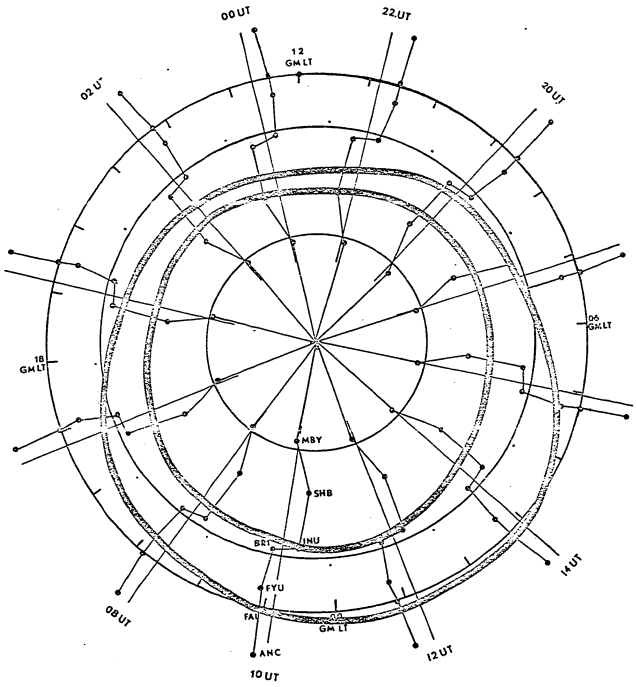


Fig. 1

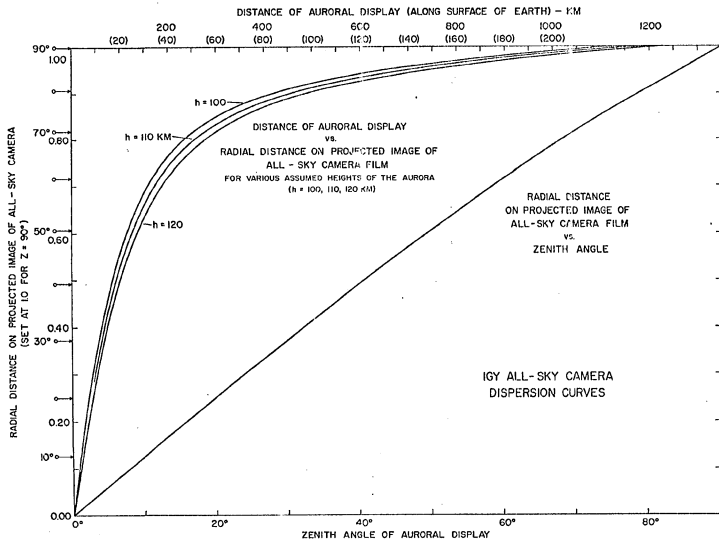


Fig. 2

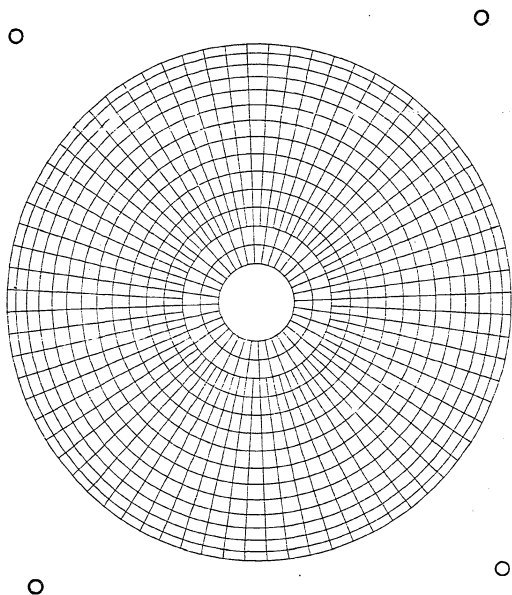


Fig. 3

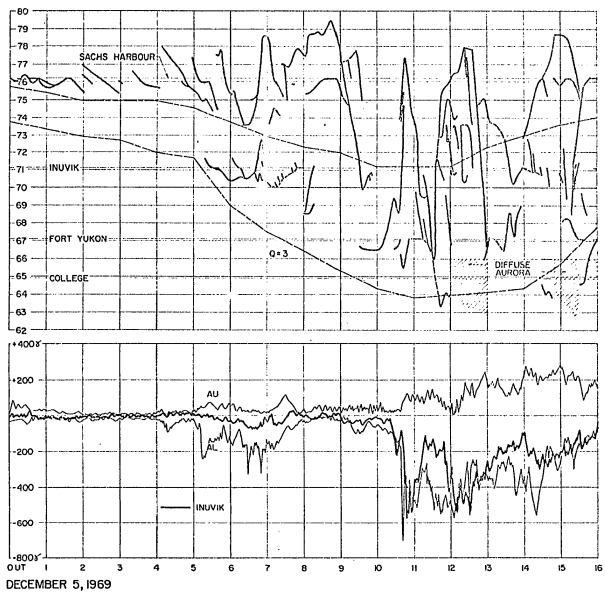


Fig. 4

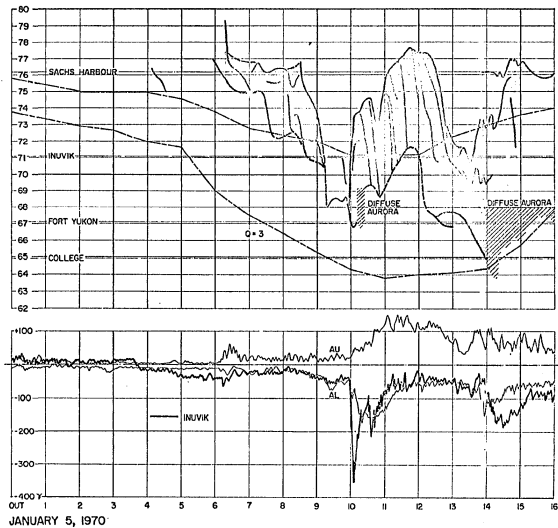


Fig. 5

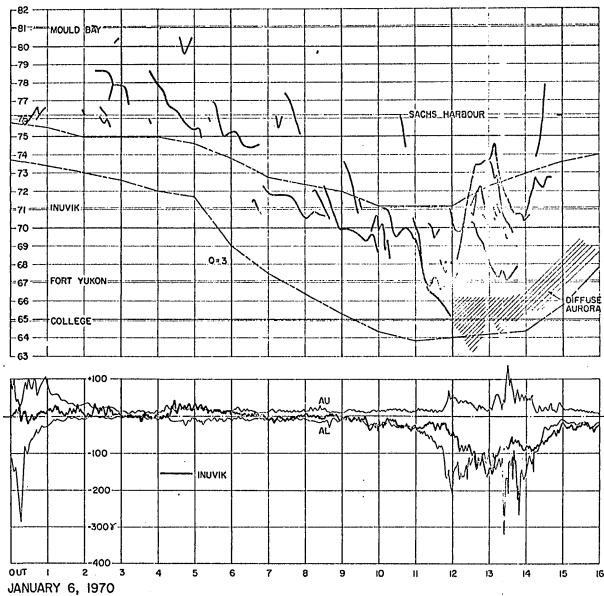


Fig. 6

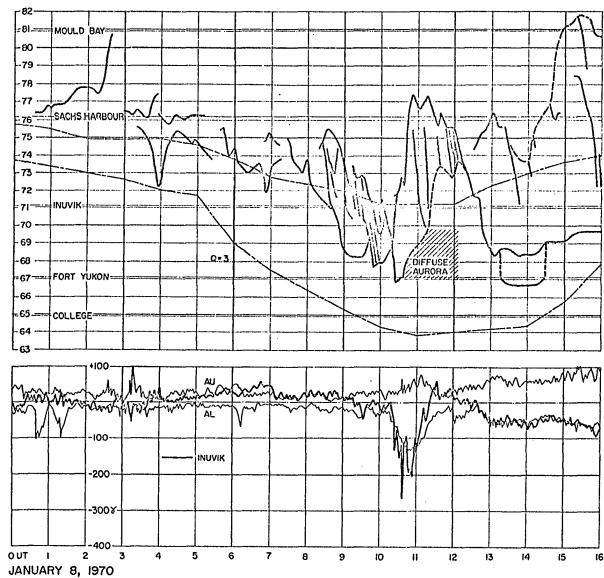


Fig. 7

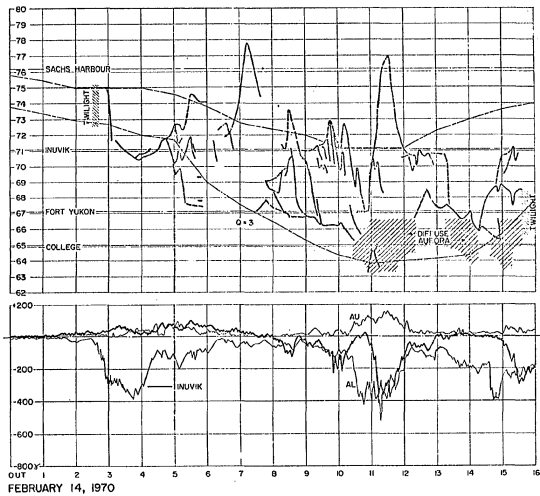


Fig. 8

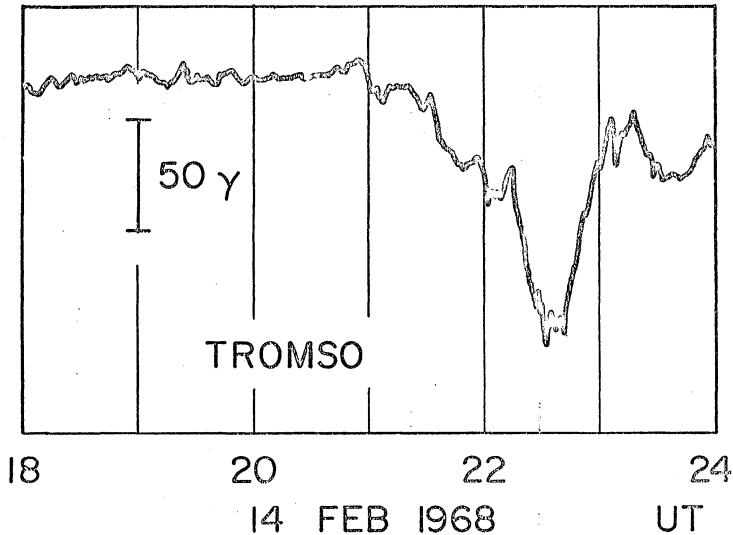
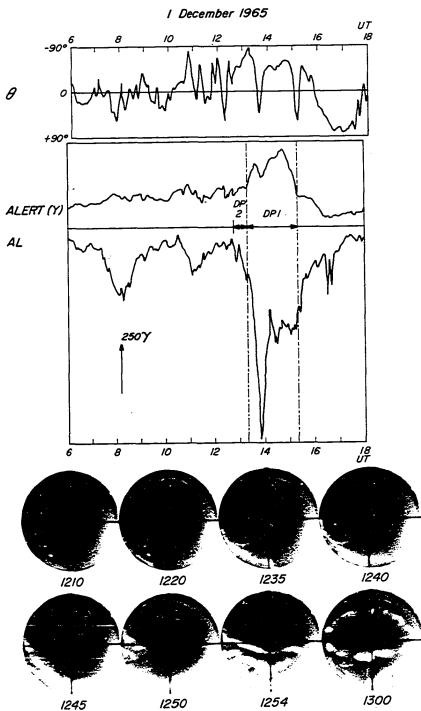


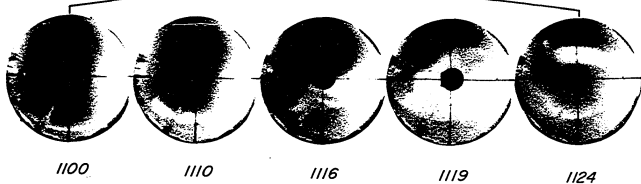
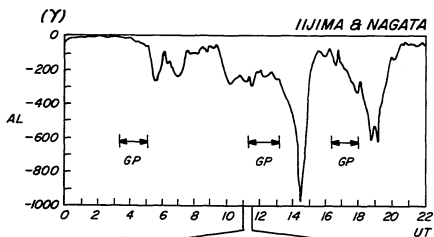
Fig. 9



MOULD BAY ALL-SKY PHOTOGRAPHS

Fig. 10

22 December 1967



FORT YUKON ALL-SKY PHOTOGRAPHS

Fig. 11

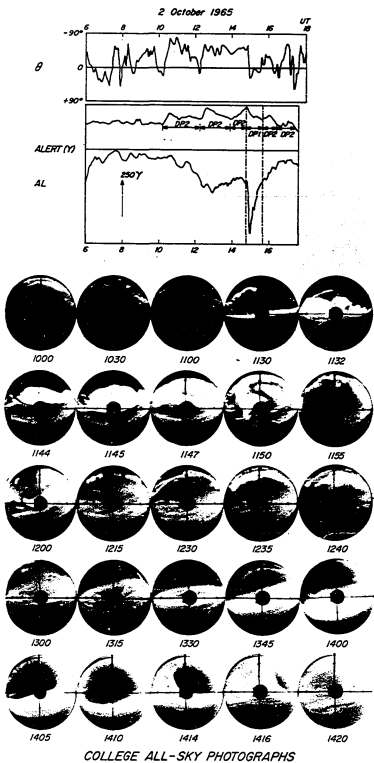


Fig. 12

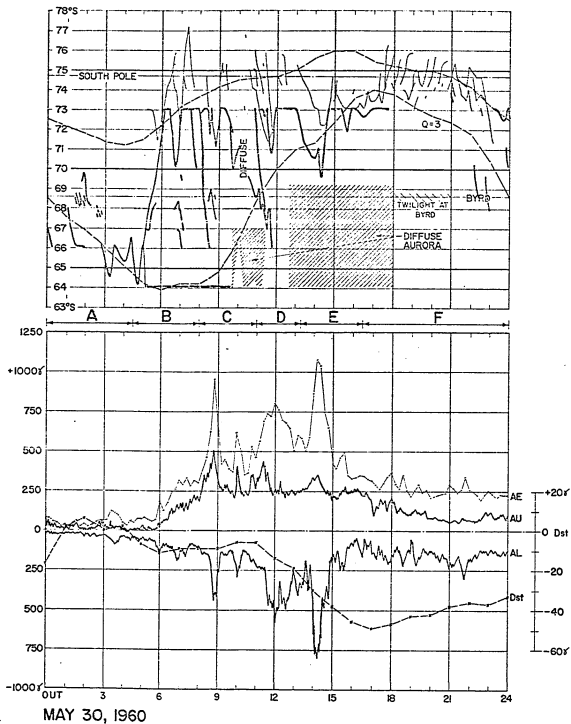


Fig. 13

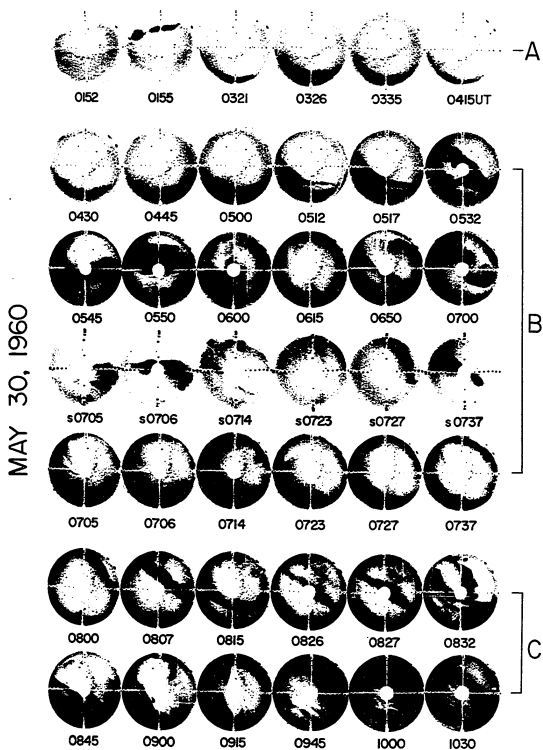


Fig. 14

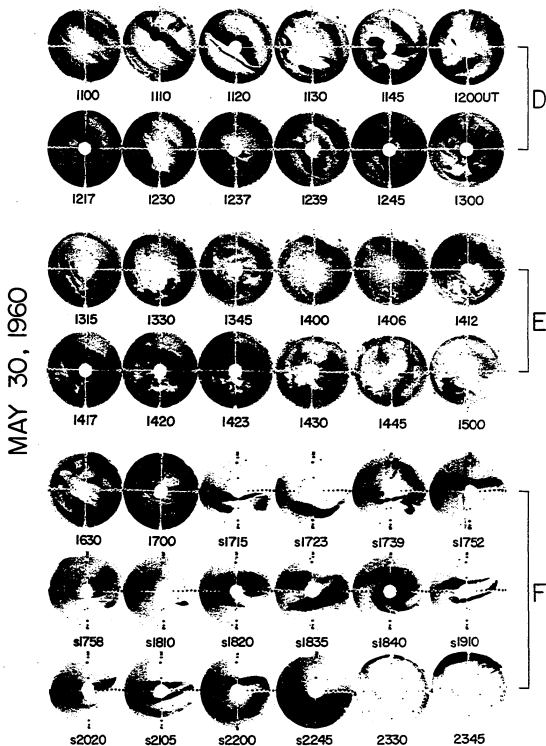


Fig. 15

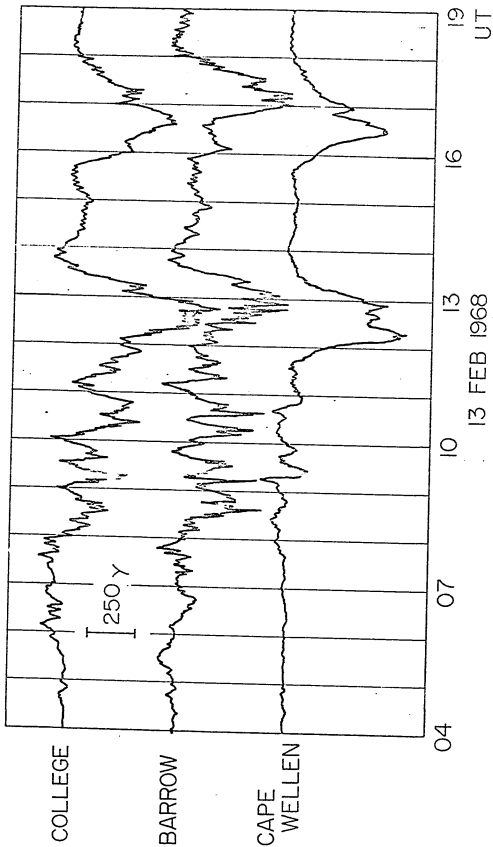


Fig. 16

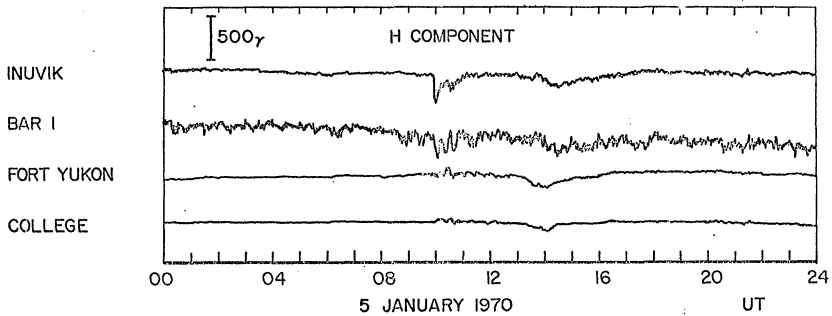


Fig. 17

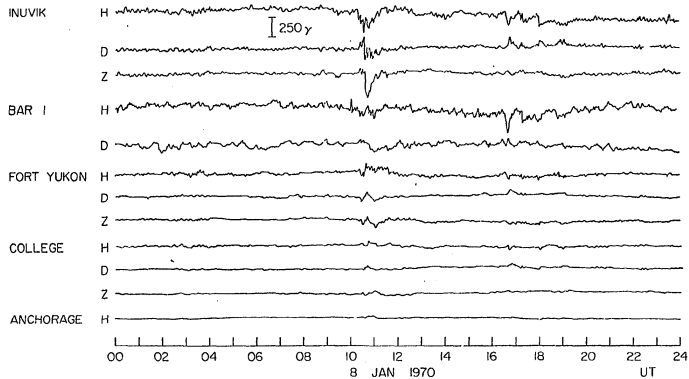


Fig. 18

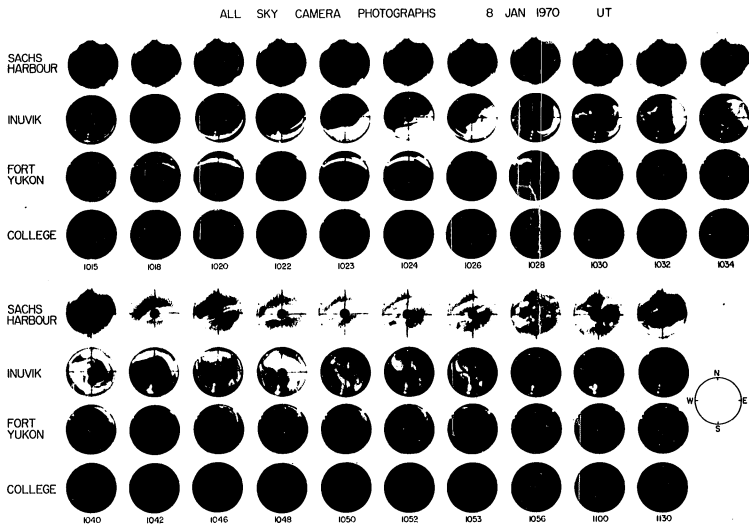


Fig. 19

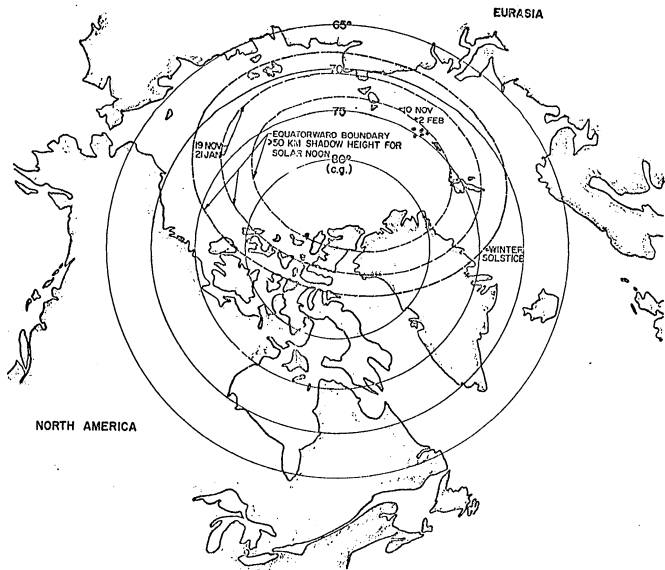


Fig. 20

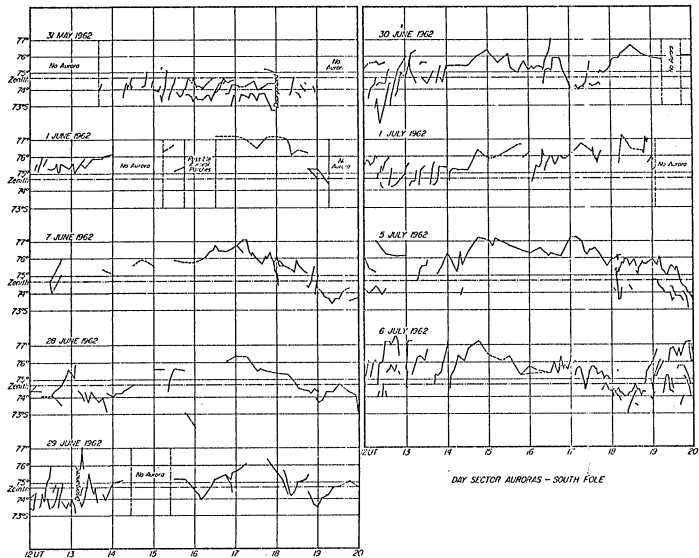


Fig. 21

CHAPTER 3

THE HIGH LATITUDE IONOSPHERE DURING MAGNETOQUIET

A thorough investigation of ionospheric disturbances depends upon a detailed knowledge of the characteristics of the quiet ionosphere. Prior investigations of the quiet ionosphere have generally been restricted to mesoscale features, or the results have been generalized from the collation of data greatly smoothed in time and space. In this chapter, ionospheric data, obtained from airborne surveys and from ground based ionosondes, are combined, with limited smoothing, to deduce the macroscale patterns of the magnetoquiet high latitude ionospheric E-region and the F₂-layer. The results are presented and discussed in sections 3.2.1.2 and 3.3.

3.1 INTRODUCTION

Recent studies (e.g. Buchau et al., 1972 and Whalen et al., 1971) have established the importance of considering high latitude ionospheric phenomena in the context of the auroral oval. The position of an observing station relative to the instantaneous auroral oval is a significant parameter for understanding high latitude ionospheric data.

Many of the problems that previous workers have encountered in ordering ground acquired high latitude ionospheric data have arisen because of this fact. Due to the eccentricity of the auroral oval and the shift of the 'auroral pole' toward the night sector, the data from a single station are often representative of several data types. On the average, a station between 65° and 72° CGL

'scans' the subauroral ionosphere during the day, but at night the same station rotates beneath the auroral oval; a station between 75° and 80° CGL is beneath the auroral oval during the day and becomes a polar cap station at night; a station between 72° and 75° CGL is positioned to observe at different local times all three high latitude ionospheric zones: subauroral (main trough), auroral oval and polar cap.

This simple spatial pattern is subject to temporal variations. This means that a station's transition times from one zone to another are not fixed but vary in association with the geomagnetic disturbance level. During disturbed conditions, a station normally beneath the auroral oval may become a polar cap station. During magnetoquiet the same station may observe the subauroral ionosphere. These temporal considerations coupled with the prior absence of a known ionospheric synoptic pattern have resulted in a seemingly inconsistent body of ionospheric data that has been difficult to understand. Before considering the temporal variations of the high latitude ionosphere, it is important to establish the prevailing ionospheric conditions during extremely quiet periods. Disturbances may be considered or defined to be deviations from the magnetoquiet characteristics. The data are not available to determine the instantaneous high latitude ionospheric patterns. Two indirect approaches have been used to establish the magnetoquiet characteristics. The first used the ionospheric data obtained from airborne surveys of the high latitude ionosphere conducted by the Air Force

Cambridge Research Laboratories. The second approach used data from the Alaskan ground ionosonde stations to study the magnetoquiet F2-layer between 60° and 70°N CGL.

3.2 AIRBORNE SURVEYS

The jet aircraft borne ionospheric observatory has several advantages for detailed studies of the high latitude ionosphere. When compared to the satellite, the aircraft can be flown in a variety of flight track modes that are impossible for a satellite. Flight paths may be chosen that permit a latitude scan while maintaining or accelerating local time. A meridian flight path may be flown so that the aircraft drifts in local time with the meridian. The aircraft borne ionosonde can observe the lower ionosphere up to the height of the peak electron density. The airborne observatory can also probe the ionosphere above remote areas that are not suitable for ground observations.

Five airborne surveys have been made during magnetoquiet and hours of darkness. Table 2 is a tabulation of the dates, flight times and the corresponding K_p indices. Figures 22-24 present the auroral zone H (or X) component magnetograms for three of the five flights for which the ionospheric E and F-region data were investigated. Note that the most significant auroral zone magnetic perturbations were generally less than 50 gammas, of short duration and confined to narrow local time sectors. Figure 25a shows the flight tracks in corrected geomagnetic latitude and local time coordinates. Note that the night sector was fairly well covered equatorward of 80°N CGL whereas only

a single flight occurred in the noon and the early afternoon sectors. There have been no magnetoquiet airborne surveys into the late morning sector.

The analysis of the airborne survey data was subdivided into data for the E region heights ($\approx 95 - 150$ kilometers) and the F2 layer. The results of these analyses are shown in Figures 25b and 26. The first three flights occurred in the Alaskan longitude sector. Because of the F2-layer variations with longitude, discussed in a following section, data from only the first three flights were used in the F2-layer analysis.

3.2.1 High latitude Ionospheric E-Region

3.2.1.1 Ionogram Interpretation

Ionograms have provided the data base for the study of the high latitude E-region. A brief review follows that gives the ionogram characteristics that were used to determine the presence of the following phenomena: auroral E-layer, retarded type sporadic E (Es-r) and non-retarded types of sporadic E (Es).

Hanson, Hagg and Fowle (1953) (see also King, 1962) described the auroral E-layer (night E) ionogram echoes by five characteristics:

1. There is a definite cusp on both the E and the F2-layer traces defining the critical frequency.
2. There is complete blanketing of the F2-layer up to the critical frequency and complete penetration of the ordinary wave beyond it unless sporadic E is present.
3. The extraordinary trace appears frequently and the Z trace is also commonly seen.

4. There is generally more spread near the critical frequency than is the case with the normal E-layer.

5. The critical frequency often varies rapidly; changes of 1.0 MHz or more in a few minutes sometimes occur. Values of foE may be anywhere from 1.0 to 4.5 MHz or more.

Beynon and Brown (1957) define retarded type sporadic E as non-blanketing sporadic E with group retardation at the high frequency end but no group retardation on the F2 trace at the corresponding frequency.

The definitions and the photographic examples presented by the referenced authors as well as those shown in Figure 27 lead to the belief that auroral E and retarded type sporadic E are mutually exclusive phenomena. However, the recommendation of the URSI/STP Seminar on the Interpretation of High Latitude Ionograms, held in Leningrad in May 1970, proposed that auroral E and retarded type sporadic E be classified together. The resolution of this dichotomy of views could be possible through the study of ionogram sequences obtained from low interference high quality data down to approximately one-half megahertz. Such high quality data would simplify the ionogram scaling in the inherently complex two megahertz frequency band centered on the gyrofrequency (cf. Ratcliffe, 1962).

The airborne acquired ionospheric data are not good for such a study. The low frequency limit of the aircraft ionosonde is two megahertz. Due to this low frequency cutoff, it is possible that a retarded E region echo, observed on the ionograms

without a corresponding F-layer cusp, is the extraordinary component of the auroral E layer with a critical frequency below two megahertz. The difficulties in observing the rapid temporal variations of the auroral E-layer (Hanson et al., 1953) are compounded by the nominal 14 kilometer per minute speed of the aircraft; spatial variations are thus integrated with the temporal variations. It is felt that a meaningful distinction cannot be reliably made between auroral E and retarded type sporadic E for the data acquired from the airborne ionosonde. For this reason only, all retarded E-region echoes recorded by the airborne ionosonde have been considered as a single phenomenon.

Beynon and Brown (1957) define and illustrate six types of non-retarded sporadic E that may be observed on high latitude ionograms. These types are low, cusp, high, flat, slant and auroral. A seventh type of non-retarded type sporadic E is Es-d (Oleson and Wright, 1961). The occurrence of Es-d is normally ignored in routine ionogram scaling. A typical example of non retarded Es is shown in Figure 26. No attempts were made to investigate the space-time distribution of the various types of sporadic E. Figure 25b shows the occurrence of non-retarded sporadic E regardless of type. The only Es data requirements for inclusion in Figure 25b were that the virtual heights be between 95 and 150 kilometers and that the echoes be continuous over a frequency range of about one megahertz. These requirements have filtered out the most oblique occurrences of sporadic E

and have also served to reject weak fragmented echoes, ground reflections and possible occurrences of Es-d.

3.2.1.2 Results

Figure 25b shows the location of the discrete auroras, the location along the flight track of the non-retarded types of sporadic E, indicated by dotted lines, and the location of auroral E and/or retarded sporadic E, indicated by heavy solid lines.

Whalen et al., (1971) have shown that the auroral E layer is caused by particle precipitation. The background intensity of the auroral emission of N_2^+ (4278A) is proportional to the ambient ion (electron) production rate (Whalen et al., 1971); they have quantified the relationship between the background intensity of the N_2^+ emission (I_{min}) and the critical frequency of the auroral E layer (foE):

$$I_{min}(N_2^+) = 0.55(foE)^4$$

I_{min} is given in Rayleighs and foE in megahertz.

The determination that such a relationship is valid for the auroral E-layer means that this layer is in equilibrium, i.e. the electron production rate equals the loss rate which for the E region is proportional to N_e^2 which in turn is proportional to $(foE)^4$.

Figure 25b shows for magnetoquiet that the auroral E-layer and retarded type sporadic E occur, with one exception, equatorward of the latitude of the discrete auroras; the polar cap is almost a complete void for the occurrence of thick E-layers required to

produce retarded type E-region ionogram echoes. Whalen et al. (1971) conclude that the auroral E-layer is produced by electron precipitation with energies of several keV. Frank and Ackerson (1971) show that the polar cap is a void for the precipitation of electrons with such energies; they further show that the poleward boundary of the auroral precipitation zone is normally well defined. It would then be surprising to find a particle precipitation produced E-layer within the polar cap.

The exception occurred on December 1, 1970 near local magnetic midnight and 80°N CGL. This occurrence was a clear case of retarded type sporadic E. Note the lack of a corresponding retardation in the F-layer trace even though both the ordinary and the extraordinary magnetoionic components of the E-region echoes are clearly recorded on the ionogram (December 1, 1970, 1133 UT, Figure 27).

A review of E-region data recorded during other flights into the polar cap reveals that this area, with minor exceptions such as described, is a void for the occurrence of auroral E and Es-r. It is noted that the geomagnetic field was moderately disturbed during the other flights into the polar cap. The conclusion may be generalized to state that the polar cap is a void for particle precipitation produced E-layers.

Note also in Figure 25b that the low latitude boundary for the magnetoquiet occurrence of auroral E and Es-r is between 68° and 70° CGL for all the local hours investigated. It also appears that these E-region phenomena occur in a circumpolar

band of five to eight degrees in latitudinal width that is positioned slightly equatorward of the instantaneous position of the discrete auroras.

Wagner and Pike (1971) have found good agreement between auroral type sporadic E parameters and the occurrence of visual auroras. Pittenger and Gassmann (1971) in a survey and reordering of past investigations of sporadic E concluded that there exist occurrence patterns of Es that are related to the occurrence patterns for visual auroras. They further conclude that the occurrence of Es in the polar cap appears to be more 'sporadic' in the time and the location of occurrence and negatively correlated with increasing geomagnetic activity.

The occurrence of non-retarded sporadic E shown in Figure 25b generally follows the characteristics previously determined. Note the equatorward-most occurrence of Es. One can visualize a bounding circle or oval that is displaced toward the night sector. This spatial characteristic is suggestive of the auroral oval equatorward boundary configuration. Minor exceptions to this generalization were observed in the midnight sector. Because of the short, several minute, temporal span during which the exceptions were observed, it is concluded that the magnetoquiet occurrences of Es between 58° and 62° CGL represent short-lived temporal occurrences and are not part of a large scale spatial pattern.

From this limited data sample, there appears to be no consistent polar cap pattern for the spatial and the temporal

occurrence of Es. During the November 30, 1970 flight to approximately 90°N CGL, only infrequent and short-lived occurrences of Es were observed (Figure 25b). However, one day later Es was observed well poleward of the discrete auroras during the midnight sector polar cap penetration. The blanketing frequencies of the polar cap Es were almost always below the ionosonde's two megahertz low frequency cutoff. These low values of the blanketing frequencies are in agreement with the review work of Pittenger and Gassmann (1971).

As mentioned earlier, the polar cap appears to be a void for particle precipitation of sufficient energies to ionize the atmospheric constituents at E-region heights (Frank and Ackerson, 1971). This combined with the normally low blanketing frequencies of polar cap Es suggests that partial reflections from electron density gradients or scattering from Es irregularities (Reddy, 1968) may be responsible for the high top frequencies of polar cap Es relative to the blanketing frequencies. A review of the ionospheric data from several additional flights into the polar cap, during moderately disturbed geomagnetic conditions, shows variable polar cap Es occurrences such as those found for the magnetoquiet flights.

In summary the occurrence of non-retarded sporadic E during magnetoquiet appears to have a low latitude boundary that is positioned at most only several degrees of latitude equatorward of the instantaneous position of the discrete auroras. Non-retarded sporadic E normally occurs poleward of auroral E and retarded type

sporadic E. The polar cap is not a void for the occurrence of non-retarded sporadic E; this means that the poleward boundary for the occurrence of such Es is ill-defined. Polar cap Es is normally non-blanketing above two megahertz. Polar cap Es is not the result of particle precipitation but may be due to partial reflections from electron density gradients or scattering from Es irregularities as Reddy (1968) has suggested for mid-latitude sporadic E.

3.2.2 High Latitude Ionospheric F2-Layer

The magnetoquiet synoptic pattern of the F2-layer critical frequencies has been investigated by using data from two Alaskan magnetic meridian flights and a third flight into the local noon sector. This third flight originated from and returned to the Alaskan sector. Figure 26 shows the flight path schematics in the corrected geomagnetic latitude and local time coordinate system.

Notice that two additional flights used to study the magnetoquiet E-region were not included in the F2-layer study. The F2-layer is subject to geographic as well as geomagnetic influences. There exist pronounced longitude sector differences among F2-layer characteristics that are ordered geomagnetically without regard for the geographic considerations. For this reason, the F2-layer has been studied with the Alaskan sector data, and the data from other longitude sector flights have not been considered. A portion of the data from the noon sector flight was also not considered. Part of this flight occurred near

135°E geographic longitude where the solar depression angles (geographic latitudes) are greater than those for the same geomagnetic latitudes in the Alaskan sector. The effect of this difference was seen equatorward of the aurora where, in the Siberian sector, the F2-layer critical frequencies were approximately one-half of the critical frequencies at the same geomagnetic latitude and local time (CSLT) in the Alaskan sector. The synoptic pattern of the F2-layer (Figure 26) is valid in detail for the Alaskan sector only. If the longitude sector were changed, the general local time-latitude pattern would remain, but the pattern would be adjusted according to the geographic influences. If an instantaneous hemispheric pattern were available for the F2-layer, the general pattern shown in Figure 26 would change to accommodate the geographic longitude sector variations.

Critical frequencies of the F2-layer were determined for College, Alaska at 15 minute intervals and added to the data base for November 30 and December 1, 1970. College ionograms were not available to supplement the airborne ionogram data for December 13-14, 1969. The College data provided for lower latitude continuity in the final analysis and also extended the night sector data below the two megahertz low frequency limit of the airborne ionosonde.

While portions of the three flights took place poleward of the instantaneous positions of the discrete auroras, an analysis of the F2-layer data has not been included in Figure 26. A

circumpolar band called the F-layer irregularity zone (plasma ring in the topside nomenclature) extends nominally poleward for three to five degrees from near the equatorward boundary of the discrete auroras. The F-layer irregularity zone (FLIZ) ionograms are generally not amenable to a critical frequency determination; see Figure 32 for examples of such ionograms. Because of the uncertain critical frequencies, the F-layer irregularity zone data were not included in Figure 26. The polar cavity, poleward of the FLIZ, was observed on only two of the four scans above 80°N CGL. Critical frequencies of four to six megahertz were observed near the geomagnetic pole and within the polar cap on the equatorward leg of the November 30, 1970 flight. It is concluded that sufficient data are not available for a valid analysis of the polar cap F2-layer critical frequencies. Thus, Figure 26 presents only the synoptic pattern of the subauroral winter F2-layer as deduced from Alaskan sector ionospheric data.

The contours of the F2-layer critical frequencies shown in Figure 26 represent the data closely. There were no major discrepancies where multiple data were available. The contours have not been smoothed in areas of data to reduce irregularities. Obviously the contours have been subjectively extended across areas without data.

Since the analysis presented in Figure 26 does not reveal any sharp discontinuities and very little indication of a patchy synoptic pattern, it is concluded that the magnetoquiet subauroral

Ionospheric F2-layer, poleward of approximately 60°N CGL, exhibits a quasi-stationary pattern fixed with respect to the earth-sun line. This conclusion implies that only minor temporal changes occur within a local time sector.

Several features of the main trough are evident from Figure 26. The trough is most pronounced in the early morning hours; this is in agreement with the work of Tulunay and Sayers (1971). The F2-layer critical frequencies equatorward of 65° CGL drop to their lowest values between midnight and 0400 hours CGLT while the poleward trough wall F2-layer critical frequencies, at approximately 70°N CGL, remain nearly constant from 2100 to 0400 hours CGLT. Sufficient data were not available to determine the pattern of the main trough in the day sector. However, the F2-layer critical frequencies decrease poleward to the position of the midday auroras before increasing to attain higher values near and several degrees poleward of the midday auroras. This limited data sample suggests that the lowest electron densities in the midday F2-layer occur near or slightly equatorward of the midday auroras.

The poleward trough wall is very evident in the data recorded on the meridional flight paths that occurred in the local time sector of 1800 to 0400 hours CGLT. In the night sector, this wall was consistently observed to be near 67° CGL with a quasi-plateau of F2-layer critical frequencies extending poleward to the auroral position. The single flight into the 1800 hours CGLT sector observed the poleward trough wall to

be near 72°N CGL. If these observations are representative of the average magnetoquiet positions, it appears that the poleward trough wall in the night sector is approximately three degrees of latitude equatorward of the average auroral position given by the $Q = 0$ auroral oval (Feldstein and Starkov, 1967).

Figure 27 shows a typical ionogram sequence through the trough wall recorded on December 14, 1969. The 0845 UT ionogram, recorded at approximately 68°N CGL and 2120 hours CGLT shows a weak multiple of the F2-layer and an oblique E-region echo. Ten minutes later at approximately 67.5°N CGL and 2140 hours CGLT the multiple of the F2-layer and the E-region echo were both gone. Notice also that the virtual height of the F2-layer echo had increased between 0845 and 0855 UT. During the next 15 minutes (0855-0910 UT) the F2-layer echo became very weak and increased in virtual range, and finally the F2-layer echo disappeared at 0912 UT at a latitude of approximately 66°N CGL and a local time of 2155 hours CGLT. Similar ionogram sequences were observed on the flights of November 30 and December 1, 1970. For equatorward flight paths, the disappearance of the F2-layer multiple, the weakening of the ionogram echoes, the increase in the virtual range of the F2-layer echoes, the final disappearance of the F2-layer echoes from the ionogram and the less than two megahertz F2-layer critical frequency recorded at College combine to provide evidence that the poleward wall of the main trough is a well defined feature of the magnetoquiet, night sector, bottomside, high latitude ionosphere. (Data for

poleward flight paths are similar, but the sequence is reversed).

3.3 F2-LAYER SYNOPTIC PATTERN DEDUCED FROM GROUND IONOSONDES

The purpose of this section is to show that during magnetoquiet that ground acquired ionosonde data can provide a similar synoptic pattern of the F2-layer critical frequencies as was deduced from airborne survey data. This analysis will also serve to illustrate that a meridian chain of ground ionosondes can provide during magnetoquiet a reasonable meridional cross-section of the ionospheric F2-layer.

Data from three ionosondes that were operated in Alaska during September 1964 provided the data used for this investigation. September 1964 ionosonde data for Barrow were scanned to learn the character of the ionograms recorded at $\sim 70^{\circ}\text{N}$ CGL compared to those recorded at College at $\sim 65^{\circ}\text{N}$ CGL. A quiet 24-hour period was found (September 14, 1000 UT to September 15, 1000 UT) during which F2-layer data were available continuously except for a brief period of blanketing sporadic E near magnetic midnight. Good quality ionosonde data were found to exist for College and Anchorage with the exception of a 3 hour 45 minute period at Anchorage. Data for the following 24-hour period were substituted for the missing Anchorage data as the data for the two days on either side of the missing data period agreed closely.

Worldwide magnetic conditions were quiet for this 24-hour period. K_p was 0+ except for 1- for the periods September 14, 2100 to 2400 UT and September 15, 0600 to 0900 UT,

respectively. D_{st} ranged from +2 to +16 gammas (Sugiura and Poros, 1971). Figure 28 presents the auroral zone magnetograms for the September 14-15, 1964 period. Three rather well defined but short duration negative bays occurred during the 24-hour period. These less than 100 gamma negative bays occurred at about 1900 UT and 2300 UT on September 14 (Dixon and Leirvogur) and at about 0500 UT on September 15 (Fort Churchill). These bays were the most notable magnetic substorm activity of the 24-hour period.

The F2-layer critical frequencies for the three stations were scaled for 15 minute intervals and were plotted in the corrected geomagnetic latitude and local time coordinate system. Contours at one-half megahertz intervals were hand drawn, and the results are shown in Figure 29. Again the contours represent the data closely.

Several features are apparent. The slow 24-hour scan of the three station ionospheric observing chain beneath the auroral zone ionospheric F2-layer has produced a synoptic pattern essentially like that deduced in the previous section from the airborne ionosonde data. The only local time sector where a 'patchy' contour pattern exists is in the afternoon sector. One notes that this breakdown in the smooth contour pattern occurred after the first two negative bays and during the third bay mentioned earlier. However, such a connection may be fortuitous. Data poleward of 70°N CGL are needed to better define the contour pattern in the afternoon time sector (CGLT) and to determine if

F2-layer effects occurred in association with the weak negative bays. F2-layer conditions associated with magnetospheric substorms will be treated in the next chapter.

The characteristics of the night sector main trough are very similar to those found from the aircraft data. The poleward trough wall is not as well resolved, as data were only available at $\sim 65^{\circ}\text{N}$ and $\sim 70^{\circ}\text{N}$ latitude CGL. It is interesting to note that in the night sector between 60° and 65°N CGL that there was essentially no meridional gradient in the F2-layer critical frequency.

Winter night F2-layer data will be used from Allakaket (65.6°N CGL), College and Anchorage to study the F2-layer substorm time variations. It is therefore reasonable to ask if the magnetoquiet winter pattern of F2-layer critical frequencies at approximately 65°N CGL follows the character found for the period studied in September, 1964 and deduced from the airborne ionosonde data. Reference to Stanley (1966, figure 5) shows that the F2-layer critical frequencies at College and Allakaket, during four magnetoquiet days in January 1966 follow the same general pattern deduced in this and the previous sections (Figures 26 and 29).

It has been shown that the data from a meridian chain of ionosondes are useful for the study of the ionospheric F2-layer between 60° and 70°N CGL. Data combined from one 24-hour period during a magnetoquiet period have produced a latitude local time pattern (Figure 29) consistent with topside sounder satellite

data smoothed over many passes as well as consistent with the pattern deduced from three magnetoquiet airborne surveys of the high latitude ionosphere (Figure 26).

TABLE 2

Airborne Surveys of the High Latitude Ionosphere during Magnetoquiet

<u>Date</u>	<u>Flight Times (UT)</u>		<u>K_p</u>	<u>K_p Periods</u>
	<u>Takeoff</u>	<u>Land</u>		
December 13-14, 1969	13/2353	14/0928	0o 1- 0+ 0+ 1+	21 - 09 UT
November 30, 1970	30/0400	30/1315	0+ 0o 0o 0+	03 - 15 UT
December 1, 1970	01/0820	01/1800	0o 0o 0o 0+ 0+	06 - 21 UT
January 8, 1971	08/0055	08/0923	0o 0o 0o 0o	00 - 12 UT
November 16-17, 1971	16/2208	17/0600	0+ 0o 0o 0o	21 - 09 UT

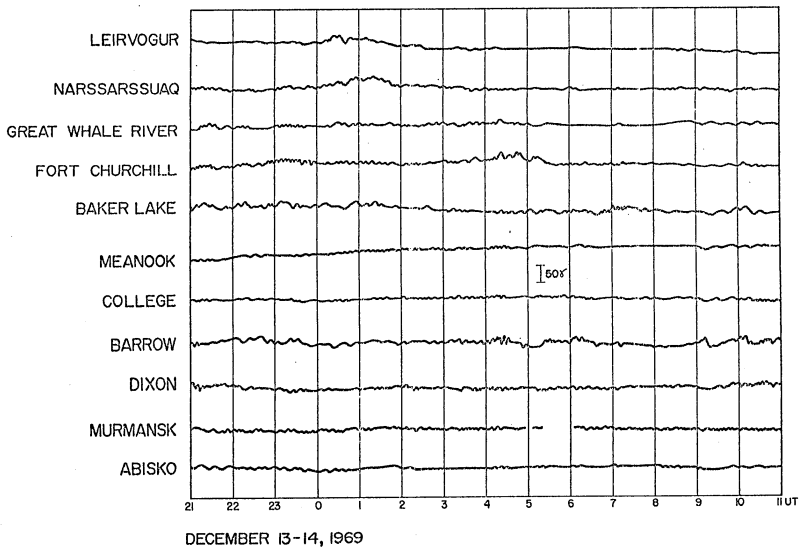


Fig. 22

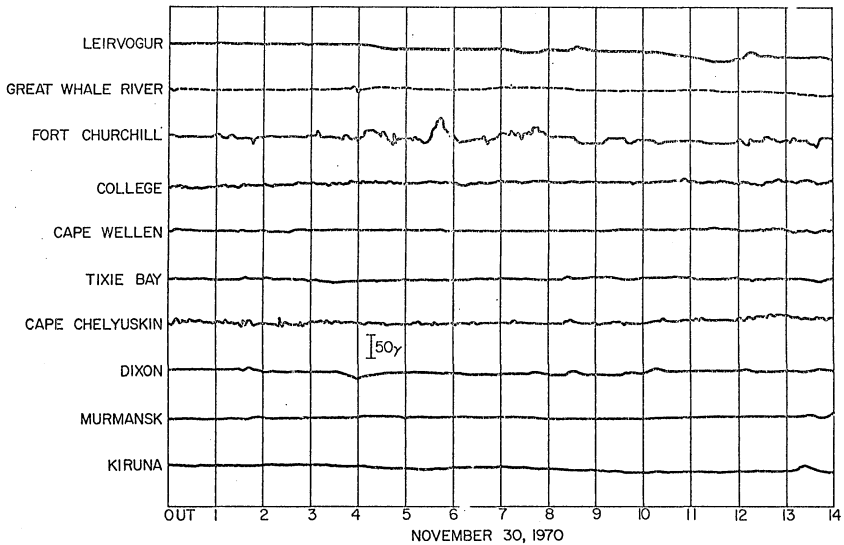


Fig. 23

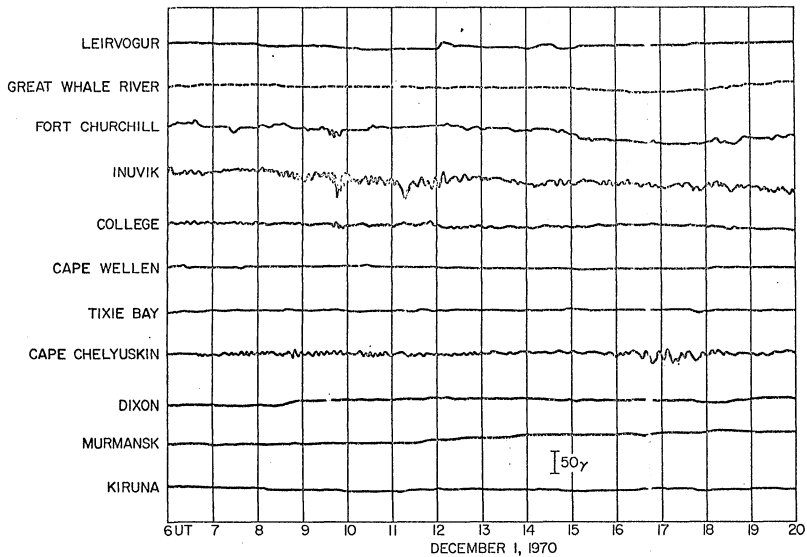


Fig. 24

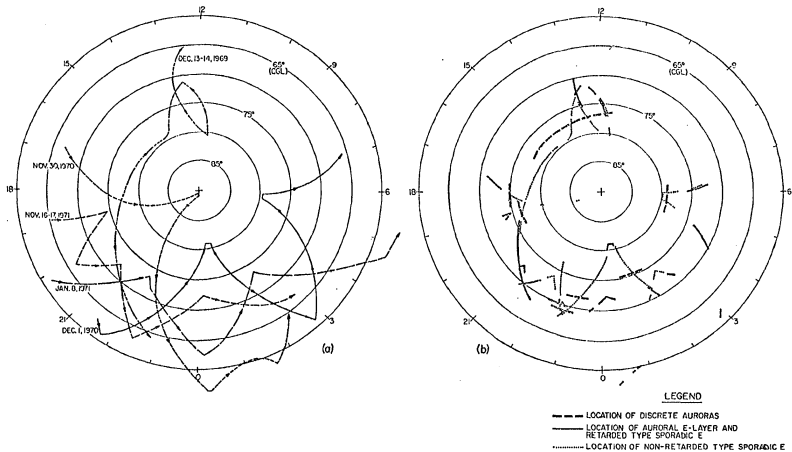
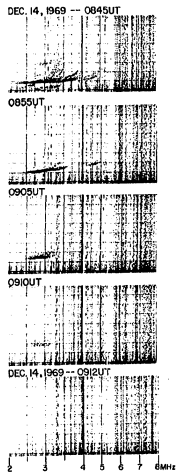
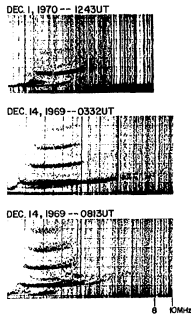


Fig. 25

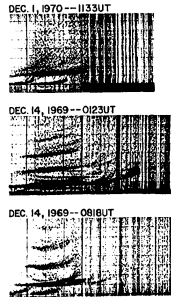
POLEWARD TROUGH WALL



AURORAL E-LAYER



RETARDED TYPE Es



NON-RETARDED TYPE Es



ALL HEIGHT MARKERS ARE AT 150 KM. INTERVALS

Fig. 27

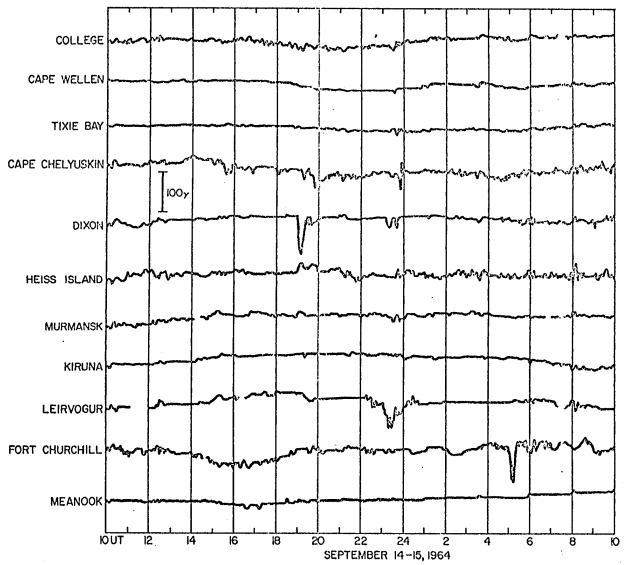
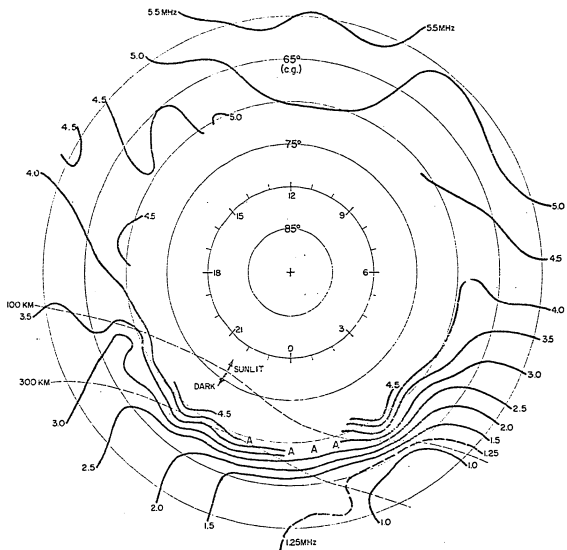


Fig. 28



SEPTEMBER, 1964
14/1000UT -- 15/1000UT

Fig. 29

CHAPTER 4

THE HIGH LATITUDE IONOSPHERE DURING MAGNETOSPHERIC SUBSTORMS

Various workers have noted that high latitude ionospheric and magnetic disturbances are closely related. However, the relationships have not been investigated within the concepts of the magnetospheric substorm. The purpose of this chapter is to identify and consider several substorm variations of the high latitude ionosphere. The results of these investigations are summarized in sections 4.1.7, 4.2 and 4.3.4

4.1 THE DAY SECTOR F-LAYER DURING A MAGNETOSPHERIC SUBSTORM

4.1.1 Introduction

Chapter 3 considered the general magnetoquiet pattern of the F2-layer equatorward of the discrete auroras. With this background, the first section of this chapter will consider in more detail the day sector features of the F-layer and their variations during a magnetospheric substorm. The 'F2-layer' nomenclature will be dropped in favor of 'F-layer' for the remainder of this section. Layering of the F-region occurs infrequently at geographic latitudes poleward of approximately 70° in the winter hemisphere.

Satellite studies provided the initial impetus for an increased understanding of the high latitude ionospheric F-layer (cf. Petrie, 1966; Muldrew, 1965; Andrews and Thomas, 1969; and Thomas and Andrews, 1969). However, Oguti and Marubashi (1966), in a study of bottomside ionograms recorded in the noon CGLT sector, identified that a localized enhancement in the F2-layer electron density existed near 75° CGL. Later

Feldstein and Starkov (1967) showed that the noon CGLT sector of the $Q = 3$ statistical auroral oval also occurred near 75° CGL.

Until recently however, a relationship between the ionosphere and the auroras in the day sector could only be inferred. The Air Force Cambridge Research Laboratories, using a jet aircraft as an observing platform for high latitude ionospheric and auroral research, have now directly studied this relationship (Whalen et al., 1971; Pike, 1971b; Buchau et al., 1972). Their observations show that the day-sector F-layer electron density enhancement, herein called the F-layer irregularity zone (FLIZ), is co-located with a band of enhanced 6300A emission within which discrete visual auroras appear. Pike (1971) has also shown that the topside 'plasma ring' and the bottomside FLIZ are the same feature and that the F-layer polar cavity is a feature common to both observations. In addition, Wagner and Pike (1972) have observed that the equatorward boundary of the FLIZ coincides closely with the presence of aurora in the zenith in the late evening sector. If this latter observation is representative of the relationship between the FLIZ and the entire auroral oval, statistical auroral studies (e.g. Feldstein and Starkov, 1967), can be used to infer the synoptic distribution of the equatorward boundary of the FLIZ.

Numerous authors (Akasofu and Chapman, 1963; Feldstein and Starkov, 1967; Feldstein, 1969; Stringer et al., 1965; Stringer and Belon, 1967; and Chubb and Hicks, 1970) have shown that changes in the shape and the size of the auroral oval

correspond to changes in magnetic activity. Akasofu (1972a, 1972b) has shown that day-sector auroras typically move equatorward with the development of a magnetospheric substorm, and, as the substorm recovers, the day-sector auroras retreat poleward. If the close spatial relationship between the FLIZ and auroras is substantiative, then the FLIZ is expected to exhibit meridional motions similar to those of the auroras. It is the purpose of this section to present observational evidence that such a relationship does exist during a magnetospheric substorm.

4.1.2 Aircraft Instrumentation and Flight Track

In December 1969 the flying ionospheric laboratory, a NKC-135 jet aircraft of the Air Force Cambridge Research Laboratories, investigated the midday sector of the auroral oval under conditions of darkness. The aircraft is instrumented with a Granger vertical incidence ionosonde (30 kw pulse peak power), an all-sky camera, and several photometers. The aircraft flight path on December 5-6, 1969 is depicted in CGL and CGLT coordinates in Figure 30. The position of the aircraft at various universal times has been indicated next to the flight path. Figure 31b depicts in greater detail than Figure 30 the midday portion of the flight path. Of major interest here is the period from 0230 to 0630 UT.

4.1.3 Magnetic Activity

Magnetic activity during the ten hour flight was moderately disturbed (K_p ranged from 3- to 4+). Negative D_{st} values, (Sugiura and Poros, 1971) which ranged from -7 to -37 gammas,

indicated that a significant ring current was present during the flight. Figure 31a shows the AE, AU, AL and the D_{st} magnetic indices for the flight. The AE, AU and AL indices were derived from the superposition of the H or X component magnetograms from 11 observatories which are identified in the Figure caption. An examination of the data presented in Figure 31a shows that two magnetic substorms occurred during the flight. The magnetic activity from about 0400 to 0600 UT is of prime interest for our discussion. The increase in the AE and the AL indices began shortly after 0330 UT (Figure 31a). However, as pointed out in Chapter 2, the onset of a magnetospheric substorm is difficult to determine from magnetic records alone. The Alaskan meridian chain of auroral all-sky cameras, which was located in the later afternoon and early evening sector, recorded the sudden appearance and brightening of an auroral arc just south of Inuvik (71.1° CGL) between 0405 and 0410 UT which was then followed by typical night sector substorm auroras (Akasofu *et al.*, 1971). Since the Alaskan magnetic meridian was in the pre-midnight sector, it is likely that the substorm onset time was prior to 0400 UT. For the purposes of our consideration the precise onset time is not essential. For convenience, the magnetic disturbance of prime interest will be termed the '0400 UT substorm'. The maximum development of the '0400 UT substorm' occurred near 0530 UT. All-sky camera data, taken at stations along the Alaskan magnetic meridian, show that the 0400 UT substorm

ended at about 0600 UT and that another disturbance began at about 0630 UT (Akasofu et al., 1971).

4.1.4 Auroral Activity

Due to fortuitous circumstances midday auroras were near the zenith of the aircraft from about 0130 to 0500 UT, even though the aircraft scanned over a six degree wide latitude band. Representative positions of the day-sector auroras observed in the aircraft are shown schematically in Figure 31b by the symbol X. Akasofu (1972a) has shown that midday auroras shift equatorward during magnetospheric substorms, and Akasofu (1972b) has also shown that a close relationship exists between the magnitude of the equatorward shift and the intensity of the auroral electrojet. On the flight of December 5-6, 1969, the equatorward shift and the poleward recovery of the midday auroras during two substorms could be followed (Figure 31b). The first substorm (~0200 UT) had an AL index of approximately -650 gammas as compared to about -450 gammas for the 0400 UT substorm. The symbol X for the aurora in Figure 31b shows that the long duration negative bay associated with the 0400 UT substorm resulted in a greater equatorward shift of the midday auroras than the first substorm (~0200 UT). This relationship has been indirectly suggested by Akasofu (1972b).

4.1.5 Ionogram Interpretation

Pike (1971b), Wagner and Pike (1971), and Buchau et al. (1972) have discussed the character of ionograms recorded during numerous aircraft latitude scans beneath the midday sector of the auroral oval.

The subauroral F-layer, equatorward of the auroral oval, is characterized by relatively simple ionograms with little spreadiness and with identifiable critical frequencies. A similar type of ionogram is also recorded from the polar cavity F-layer.

In contrast to such simpler ionograms from the F-layers equatorward and well poleward of the aurora, the F-layer irregularity zone (FLIZ) is characterized by ionograms that are difficult to interpret in the sense of virtual heights and critical frequencies. Spreadiness dominates the FLIZ ionograms and often there is no significant critical frequency retardation.

In this section an attempt will be made to identify what sector of the high latitude ionosphere is represented by each F-layer ionogram. These three sectors are: the subauroral F-layer (SF) equatorward of the aurora, the F-layer irregularity zone (FLIZ) near and extending characteristically four degrees of latitude poleward of the aurora (Pike, 1971b), and the polar cavity F-layer (PC) poleward of the FLIZ.

Figure 32 shows representative ionograms and all-sky camera photographs selected from the recorded sequences. The sector of the high latitude ionosphere characterized by each F-layer ionogram is shown in Figure 32. Each F-layer echo in Figure 32 is also identified by a corresponding number. A brief discussion follows of the essential ionogram characteristics.

For the period of prime interest, the aircraft was equatorward of the midday auroras from 0215 to 0239 UT and from 0421 to 0448 UT (Figure 31b). The low levels of spreadiness and the retarded

F-layer echoes shown on the 0230 and the 0440 UT ionograms are characteristic of the subauroral F-layer (Figures 32a and 32g). The 0430 UT frame (Figure 32f) shows a transition ionogram with echoes from both the FLIZ and the subauroral F-layer. After 0430 UT the FLIZ echo increased in virtual range while the range of the subauroral F-layer echo decreased.

The ionograms between 0241 and 0420 UT were recorded with aurora in the zenith or slightly equatorward of the aircraft position (Figure 31b). These ionograms are representative, with minor exceptions, of the FLIZ. The F-layer echoes on the 0241 UT transition ionogram by 0244 UT had evolved to be very characteristic of the FLIZ.

Note the clear differences between the ionograms recorded poleward of the auroras (Figures 32c and 32d) compared to those recorded well equatorward of the aurora (Figure 32a and 32g).

On the final poleward leg, aurora was observed in the zenith at 0449 UT. The majority of the ionograms on this flight leg were recorded with aurora well equatorward of the aircraft (Figure 31b).

The 0455 UT ionogram (Figure 32h) represents a transition ionogram. After 0455 UT the echo from the subauroral F-layer increased rapidly in virtual range, became spread and disappeared. The FLIZ echo, slightly below 300km, developed rapidly as the plane continued poleward. The 0524 UT ionogram is representative of the FLIZ. However, about this time the FLIZ echo began to increase in virtual range. This increase in range indicated the departure of the aircraft from the area where the FLIZ

was located.

The 0535 UT ionogram shows clearly an echo with a different character. The low critical frequency and the decreased spreadness combined with the fact that the aircraft was deep within the polar cap leads to the conclusion that the new F-layer echo was from the equatorward portion of the polar cavity F-layer. A comparison of the ionograms in Figures 32c and 32j shows the lack of a polar cavity-like echo at 0324 UT even though the aircraft was more poleward of the statistical auroral oval than at 0535 UT (Figure 31b).

The FLIZ is recognized on the 0535 UT ionogram (Figure 32j) as the spread non-retarded F-layer echo. The FLIZ echo continued to increase in virtual range until 0558 UT and then decreased steadily in virtual range through 0615 UT. During this period prior to 0558 UT, the polar cavity F-layer echo was dominant. Following 0558 UT, as the FLIZ echo decreased in virtual range, the clear dominance of one echo over the other was not clear in the transition zone between the polar cavity F-layer and the FLIZ.

By 0616 UT the FLIZ echo had returned to a virtual height of about 290 kilometers. The polar cavity F-layer echo, just prior to this time, had become spread and had partially merged with the FLIZ. These ionogram features are interpreted to indicate that the FLIZ had replaced the polar cavity as the dominant F-layer at the aircraft position.

4.1.6 Discussion

From the data discussed in the sections on magnetic and

auroral activity and ionogram interpretation, several relationships can be established between the aurora and the high latitude F-layer.

Even though the aurora exhibited rather large latitude shifts, associated with two magnetospheric substorms (Figure 31b), the equatorward boundary of the FLIZ occurred within a fraction of a degree of the position of the midday auroras. This relationship was observed on each of the five midday aurora encounters. The preservation of this close relationship in a dynamical situation, such as that which occurred during the period of this flight, implies that the equatorward boundary of the FLIZ moves in conjunction with the meridional motions of the aurora.

On the second poleward flight leg, the aircraft passed beneath the aurora and the equatorward boundary of the FLIZ near 73°N CGL. The flight continued poleward for approximately five degrees, but the polar cavity F-layer was not observed. However, the aurora moved poleward at a comparable speed to that of the aircraft and was only 1.5° of latitude (CGL) equatorward of the aircraft at the flight leg's terminus. These observations are interpreted to mean that the aircraft remained beneath the FLIZ as it shifted poleward in phase with the poleward motion of the aurora. The close relationship between the FLIZ and auroral motions is supported also by the data for the second equatorward flight leg; the FLIZ remained above the aircraft until the plane passed equatorward of the aurora.

During the final poleward flight leg, the aurora was initially moving equatorward (Figure 31b). After 0500 UT these separative

motions of the aircraft and the aurora resulted in the aircraft being located well within the polar cap. When the aircraft was six or more degrees of latitude (c.g.) poleward of the aurora, the polar cavity F-layer was observed (0535 UT, Figure 32j). This observation is interpreted to mean that the FLIZ had moved equatorward with the aurora and was six or more degrees of latitude (CGL) in width near the time of the maximum development of the 0400 UT magnetospheric substorm.

During the recovery phase of the substorm, the midday auroras retreated poleward with the decrease in the $|AL|$ index (Figures 31a and 31b). Following the turn to the east at 0545 UT, the aircraft remained at a constant latitude (CGL) for 15 minutes then drifted slowly equatorward. During this period the aurora was moving poleward. By about 0616 UT the FLIZ had replaced the polar cavity as the dominant F-layer. This means that the FLIZ had recovered poleward in conjunction with the aurora during the recovery phase of the substorm. Note also that the poleward boundary of the FLIZ was then four degrees of latitude (CGL) poleward of the aurora. It is inferred from this observation that the FLIZ contracted in latitudinal width as it retreated poleward during the recovery phase of the substorm.

Figure 33 summarizes the preceding discussion by illustrating in schematic the relationship between the F-layer Irregularity zone and the midday auroras during a magnetospheric substorm.

Oguti and Marubashi (1966) suggested that the midday F-layer near 75° CGL was due to ionization by particle precipitation

through the magnetic neutral points that arise in mathematical models of the boundary surface of the magnetosphere. Frank (1971) has shown that the neutral points are in fact bands that he designated 'polar cusps' through which the magnetosheath plasma has direct access to the inner magnetosphere. Winningham and Pike (1972) have shown excellent agreement between precipitating particle measurements through the polar cusp and the day-sector FLIZ characteristics. There appears to be little doubt that the winter day-sector FLIZ is maintained by ionization from particle precipitation through the polar cusps.

Frank (1971) has suggested that during relative magnetic disturbance that the polar cusp moves to lower latitude and is not accompanied by a large increase in cusp width (less than or equal to a factor of approximately two). Polar cusp data from Ogo 5 were reported by Russell et al. (1971) for the great world-wide magnetic storm of November 1, 1968. Their data show that the polar cusp moved equatorward to about 66° invariant latitude during a very large substorm (2500 gamma negative bay at College). The ionospheric data discussed in this section indirectly confirm Frank's (1971) observations and extend further the work of Russell et al. (1971) to suggest a close relationship between polar cusp motions and width and magnetospheric substorm phase.

4.1.7 Summary

High latitude ionospheric data from an aircraft borne ionosonde have been combined with auroral and magnetic records to arrive at

the following conclusions:

1. During a magnetospheric substorm, the winter day-sector F-layer disturbance zone (FLIZ) exhibits meridional motions in close association with those of the day-sector auroras. The FLIZ moves equatorward during the expansive phase of the substorm and poleward during the recovery phase.

2. The equatorward boundary of the day-sector FLIZ corresponds to that of the day-sector auroras to within a fraction of a degree of latitude independent of auroral motions or substorm phase.

3. The width of the day-sector FLIZ increases by several degrees of latitude during the expansive phase of a magnetospheric substorm.

4. The spatial characteristics of the FLIZ during a magnetospheric substorm suggests that a close relationship ought to exist between polar cusp motions and widths and substorm phase.

5. Also illustrated are the advantages of considering ionospheric data jointly with auroral and magnetic data for the proper interpretation and understanding of high latitude F-layer phenomena.

4.2 MIDDAY AURORAL PATCHES AND RELATED IONOSPHERIC PHENOMENA

Auroral displays during auroral substorms have now been well documented in the night sector (cf. Akasofu 1968), but not in the day sector, particularly in the midday sector. Feldstein and Starkov (1967) reported that auroras along the auroral oval are activated about half an hour after the onset of an auroral

substorm in the midnight sector. Akasofu (1972a, b) reported that the midday part of the oval shifts equatorward during an early phase of substorms and returns to the pre-substorm location during a later phase of substorms.

Riometer studies of auroral substorms show that an intense precipitation zone develops along the morning side of the auroral zone from the midnight sector toward the day sector (cf. Hartz and Brice, 1967). In the dark sector, this precipitation zone coincides with the region where patchy auroral forms develop and drift eastward.

It is known that this intense precipitation zone extends to the midday sector and even beyond. It is thus of great interest to examine whether auroral patches can be observed in the midday sector during auroral substorms. In the northern hemisphere, such an observation can be made from only a very limited region of the polar region, since daylight tends to obscure midday auroral displays (cf. Figure 20).

Fortunately, the formation of the patchy auroral structure well equatorward of the oval in the midday sector was confirmed by an aircraft observation on December 9, 1969. An airborne ionospheric sounder and Asian sector riometer data indicated the simultaneous absorption event, substantiating the precipitation and the associated ionization in the lower ionosphere. In the following, the observations will be described.

During December 1969 the Flying Ionospheric Laboratory, an NKC-135 jet aircraft of the Air Force Cambridge Research Laboratories, made a series of flights to examine the midday

auroral oval. During the flight of December 9, a single polar magnetic substorm occurred during an otherwise magnetically quiet period (Figure 34). The aircraft, instrumented with an all-sky camera, an ionosonde, and several photometers, passed beneath the midday auroral oval during the early expansive and the late recovery phases of the polar magnetic substorms that began about 0230 UT (Figure 35).

Diffuse auroral patches were observed well equatorward of the discrete auroral oval from about 0420 to 0600 UT (Figure 26). Twilight prevented definitive observations during the period 0510 to 0530 UT. The presence of auroral patches near the southern horizon can be inferred both before and after 0420 and 0600 UT respectively; however, precise interpretation from a single all-sky camera photograph is difficult because of the great distance to these auroras.

A detailed examination of the all-sky camera photographs from the other midday oval flights reveals that the auroral patches occur only in association with polar magnetic substorms. Auroral zone magnetograms from the night sector for the 0230 UT substorm on December 9 show that the substorm ended about 0400 UT (Figure 34). The character of the discrete auroras of the midday oval at the 0406 UT crossing is consistent with the Feldstein and Starkov (1967) schematic of the recovery phase of the midday auroral substorm. Nevertheless, at the 0406 UT crossing a luminous glow was present on the southern horizon. This glow cannot be totally twilight as the earth's shadow height at the all-sky camera horizon was about 170 kilometers.

By 0420 UT the aircraft had approached close enough to the glow to observe that the luminosity was due to diffuse auroral patches.

By 0435 UT the aspect sensitive auroral patches were observed on all horizons, and by 0500 UT the patches covered the entire sky. The patches appeared in the zenith near 73° corrected geomagnetic latitude and three to five degrees of latitude south of the midday auroral oval. On the southbound leg of the flight, twilight interfered with the observations after 0510 UT. After the aircraft turned to a poleward heading at 0519 UT, the sequence of observations seen on the southbound leg was repeated in reverse. Figure 37 presents photographic evidence of the midday auroral patches observed at 0445 UT. A photograph from the magnetically quiet flight of December 14, 1969 is shown for comparison so that the patches of auroral luminosity can be more easily recognized. The comparative photograph from December 14 was taken at approximately the same local magnetic time and with the same zenith shadow height.

Riometer data from the Russian day-sector and from the aircraft ionosonde indicate conclusively that the auroral patches occurred within the hard precipitation zone equatorward of the discrete midday auroras. Figure 38 shows the relations, in latitude, Universal time, and local magnetic time (CGLT) between the correlative data that pertain to the observations of the midday auroral patches. Notice that the riometer absorption was minimal in the early afternoon sector poleward of the discrete midday auroras. However, in an approximate ten degree wide

band equatorward of the auroral oval, significant riometer absorption was observed in the morning and the midday sectors. Figure 39 is a plot of the minimum frequency (f_{\min}) 0400 and 0615 UT. The general increased value of f_{\min} and the occasional total blackouts indicate absorption and correspond to the time period during which the auroral patches were observed. Since the ionosonde and the riometer observe a large portion of the sky, the variations in f_{\min} and the riometer absorption are evidence for a temporal variation in the particle precipitation into the hard zone.

Berkey (1971) documents photometrically, from College, Alaska data, several occurrences of mid-afternoon twilight pulsations in N_2^+ , 4278Å, and relates these pulsations to intense afternoon absorption events as observed by riometer. Of the three events studied by Berkey, all-sky camera photographs were available for one event; weak equatorward drifting arc segments were observed and Berkey concluded that these auroral forms were similar to the dusk sector patches seen by Montbriand (1969).

It is quite likely that the formation of patchy auroras in the midday sector is associated with the drift motion of energetic electrons (cf. Lezniak and Winckler, 1970) and their subsequent precipitation (cf. Hoffman and Berko, 1971).

4.3 THE NIGHT SECTOR IONOSPHERE DURING MAGNETOSPHERIC SUBSTORMS

4.3.1 Introduction

As noted in the introductory section of Chapter 3, there have been difficulties in ordering high latitude ionospheric data obtained from ground ionosondes. During the past decade,

satellite and aircraft-borne ionospheric observatories have provided the necessary data to identify macroscale ionospheric patterns and to demonstrate the validity of ordering high latitude ionospheric data relative to the auroral oval (see for example Thomas and Andrews, 1969 and Buchau et al., 1972). These recent advances combined with the magnetoquiet investigations presented in Chapter 3, as well as previous studies such as those of Burkard (1948), Meek (1953, 1954), Bellchambers et al. (1962), Stanley (1966) and Bowman (1969), provide a base of knowledge for a reconsideration of ground ionosonde data.

The main purpose of this section is to present observational evidence to indicate that a better understanding of high latitude ionospheric phenomena in the winter night sector results from a study of ground ionosonde data within the framework of the magnetospheric substorm.

The ionospheric data base for these studies included copies of the original ionograms recorded at Allakaket (65.6°N CGL), College (64.9°N CGL), and Anchorage (60.8°N CGL) during the fall and winter of 1965 - 1966. Four nights were selected for detailed investigation: December 5, 1965, January 2 and 18 and March 3, 1966. Data for the three ionosonde stations were available for only December 4, 1965.

These four nights were selected because the F-layer ionogram data illustrated clearly the 'replacement-layer' (equatorward displacement of the poleward trough wall) phenomenon noted by Bellchambers et al. (1962) as well as in earlier studies

by Burkard (1948) and Meek (1953, 1954). There were also interesting E-region characteristics that represent significant departures from the magnetoquiet patterns illustrated in Figure 25b.

For the purposes of this discussion, disturbances are defined as deviations from the quiet conditions. The major magnetoquiet features of the night sector subauroral ionosphere will be reviewed as they pertain to the substorm-time variations to be discussed later.

An examination of Figure 25b reveals for the magnetoquiet night sector, at latitudes of $\sim 60^\circ$ to 65° CGL, that few E-region ionogram echoes were observed above the two megahertz low frequency cutoff of the airborne ionosonde. Thus E-region echoes above two megahertz would indicate a departure from magnetoquiet conditions.

The F2-layer data presented for magnetoquiet conditions (Figures 26 and 28) show that a station at a latitude of $\sim 60^\circ$ to 65° CGL is beneath the main trough for most of the night sector period. F-layer critical frequencies at these latitudes in the night sector are typically one to two megahertz during magnetoquiet periods. Yet note that the poleward trough wall with higher critical frequencies occurs during magnetoquiet at approximately 67° CGL. Thus a small equatorward displacement of the poleward trough wall would result in an increase in the F-layer critical frequencies at Allakaket and College and indicate a departure from magnetoquiet conditions.

4.3.2 Data Presentation

The ionospheric data have been scaled and are presented

in Figures 40, 43, 45 and 47 as partial f-plots (see Beynon and Brown, 1957, p. 132 for a discussion of f-plots). The type of sporadic E is not indicated on the f-plot results. If there are data for both the E and the F-regions at comparable frequencies and times, letters are used (E and F) to identify on the f-plot the ionospheric region that particular data refer to.

Integral parts of the total data base are the correlative magnetic, auroral and riometer absorption data that form the basis for the discussion of the high latitude ionospheric disturbances within the concept of the magnetospheric substorm. Representative, rather than comprehensive, correlative data are presented. Riometer data, representative ionograms, and corresponding all-sky camera photographs are presented for the December 4, 1965 disturbance to illustrate by example the relationships that exist between the various data types. Even though auroral zone magnetograms have limitations for the detailed study of certain substorm phenomena (see Chapter 2), the magnetic records form a reliable and readily available data base for the determination of substorm occurrences. For this reason, the magnetic H component records for the night sector auroral zone observatories are presented for each period studied.

4.3.3 Discussion of the Observed Ionospheric Variations

The purpose of this section is to consider the observed ionospheric variations jointly with data that are accepted as defining the occurrence of magnetospheric substorms. Each night studied will be discussed separately in a following subsection.

Each subsection will first identify the substorm occurrences and will then discuss the related ionospheric variations.

4.3.3.1 December 4, 1965

Reference to Figures 40 and 41 reveals that two major polar magnetic substorms occurred during the period studied. The first substorm attained a maximum development at approximately 1250 UT and the second at approximately 1625 UT. The period from 0700 UT to approximately 1030 UT was a time of general magnetoquiet. It is noted that while no significant magnetic activity was recorded in the Alaskan (midnight) sector prior to 1115 UT, a weak negative bay was observed to begin at 1030 UT in the morning sector (Fort Churchill, Figure 41). Positive bays were also observed to begin about the same time at Cape Chelyuskin, Dixon and Heiss Island in the late afternoon sector (Figure 41).

A survey of all-sky camera data revealed that the night sector auroral oval was contracted far poleward during this magnetoquiet period. Oval aligned auroral arcs were observed near the Mould Bay zenith (80.9°N CGL) between approximately 0715 and 0900 UT. Between 1055 and 1115 UT an equatorward moving arc crossed the Mould Bay zenith. Auroras were not observed within the College field-of-view until 1030 UT when an auroral arc was also observed moving equatorward through the Barrow zenith. The onset of the auroral substorm was observed to occur in the Alaskan sector at 1115 UT as the sudden brightening of a rayed arc (Figure 42).

The College ionosonde was operated at a reduced gain for this entire night. Numerous blackout conditions observed at College were not confirmed by the higher quality Allakaket ionosonde data. For this reason, only the Allakaket f-plot is shown in Figure 40; however, Figure 42 shows that when College ionosonde data were available they were comparable in character to the higher gain ionograms from Allakaket.

Note from the Allakaket f-plot (Figure 40) that the top frequency of sporadic E increased above two megahertz at about 1045 UT - some 30 minutes before the Alaskan sector onset of the auroral substorm. In fact, the blanketing frequency of sporadic E (fbEs) began to increase at approximately 0930 UT - almost one hour prior to any magnetogram indication of substorm activity (Figures 40 and 41). The blanketing frequency of sporadic E is the lowest frequency at which ionosonde echoes from higher layers are received through the Es layer. (See Reddy (1968) for a discussion of the physical significance of fbEs).

Also during this 'pre-substorm' period the critical frequency of the auroral E-layer increased slightly prior to complete blanketing after 1000 UT by the lower virtual height Es. Figure 42b shows that sporadic E of greater than two megahertz top frequency developed at Anchorage prior to the substorm as well as at Allakaket and College. The latter two stations showed retarded type Es while a non-retarded type was observed at Anchorage.

At 1130 UT the first evidence for the 'replacement-layer' echo was observed on the Allakaket ionograms. This echo showed a critical frequency of five megahertz but was amidst another F-region echo that was not seen on prior or following ionograms. It is important to note that the Allakaket F-layer critical frequencies during the early phase of the substorm were representative not of the main trough but rather of the plateau in the F-layer critical frequencies north of the poleward trough wall. The 1205 UT Allakaket ionogram shows a multiple of the new higher critical frequency F-layer (Figure 42). The Anchorage ionogram for 1200 UT recorded an oblique F-layer echo near 400 kilometers and between three and four megahertz top frequency. The decrease in the virtual range of the Anchorage F-layer echo to 300 kilometers at 1400 UT combined with the higher critical frequency F-layers observed at Allakaket and College lead to the conclusion that the poleward trough wall was displaced equatorward from $\sim 67^\circ$ CGL to $\sim 62^\circ$ CGL during the early phase of the substorm. Between 1400 and 1500 UT, the weak poleward trough wall echo, observed at Anchorage, increased in virtual range as the auroras retreated poleward (Figures 42f, g and h). During the same period, both the Allakaket and the College ionograms indicated a slow decay of the F-layer critical frequencies (Figures 40 and 42f, g and h).

The next major substorm was accompanied by an intense display of auroral patches and increased D-region non-deviative absorption (Figures 40 and 42k). During this second substorm,

the Anchorage and College ionosondes recorded no ionospheric echoes while the Allakaket ionograms showed rather clear examples of Es-d (Figure 40k). With twilight and the recovery of the substorm by 1900 UT, the normal solar produced F-layer was observed at all three stations.

4.3.3.2 January 2, 1966

Two polar magnetic substorms occurred during the period of 0700 to 1700 UT. The first substorm is seen best in the Fort Churchill magnetogram (Figure 44) which recorded a sharp onset negative bay of ~ 100 gammas at about 0810 UT; however, note that the Great Whale River magnetic record shows a gradual onset bay that began about 0730 UT. A second extended period of polar magnetic substorm activity began about 1300 UT. (Figures 43 and 44).

The ionospheric parameters prior to the first substorm were typical of the $\sim 65^\circ$ CGL magnetoquiet ionosphere (Figure 43). The F-layer critical frequencies were approximately one megahertz at both College and Allakaket, and the blanketing frequencies of sporadic E were near or below one megahertz.

With the very early development of the first polar magnetic substorm, fbEs was observed to increase at Allakaket. The top frequency of the completely blanketing sporadic E increased through two megahertz near the time of the sharp onset negative bay observed at Fort Churchill.

After 0830 UT a new higher critical frequency F-layer was observed at both College and Allakaket. An auroral E-layer,

with a critical frequency of approximately 1.0 to 1.5 MHz, was observed at both stations after ~0915 UT (Figure 43). After ~0930 UT multiples of the new F-layer were also observed at both stations.

As the blanketing frequency of Es decreased, the main trough ionogram echo was observed at College and later at Allakaket (Figure 43). With the reappearance of the main trough echo, the virtual range of the 'replacement-layer' increased and the multiple of this layer disappeared. These occurrences are interpreted to mean that the poleward trough wall had moved slightly northward to about 66° CGL.

The onset of the second magnetic substorm was well defined in the Asian sector (Figure 44). Again about 30 minutes prior to the onset of the polar magnetic substorm in the Asian sector, the Allakaket blanketing frequency of sporadic E began to increase (Figure 43). Yet at College there were only minor indications of this effect until some 15 minutes after the substorm onset. The Allakaket fbEs reached two megahertz near the magnetic substorm onset time, whereas the College fbEs exceeded two megahertz about 45 minutes later. After approximately 1430 UT, the F-layer was observed again. The post-substorm F-layer electron densities were approximately four times the pre-substorm values at both Allakaket and College. These higher post-substorm values are characteristic of the plateau in the F-layer critical frequencies found north of the poleward trough wall.

4.3.3.3 January 18, 1966

The night sector magnetograms reveal that a rather slow

onset \sim 100 gamma negative bay occurred at about 0800 UT (Fort Churchill, Figure 46). A second, better defined, polar magnetic substorm occurred with its maximum development between 1530 and 1630 UT. The earliest auroral zone magnetogram indication of the second substorm was at approximately 1400 UT. The 0800 UT magnetic activity was confined to a narrow local time sector at auroral zone latitudes; the only definitive indication of a possible substorm was at Fort Churchill.

The ionospheric data for Allakaket and College reveal no significant variations in the characteristics of the overhead ionosphere during the 0800 UT magnetic activity. Typical values of fbEs were less than one megahertz, and the critical frequencies of the F-layer were consistently near 1.2 megahertz at both stations. However, during the period from 0800 to 0900 UT, the poleward trough wall was displaced equatorward to near 66° CGL. This was deduced from the Allakaket data that revealed an oblique F-layer echo that decreased in virtual range from 500 to 370 kilometers during the period of 0815 to 0900 UT. This echo maintained a nearly constant virtual range through \sim 1345 UT when the echo could no longer be observed because of blanketing sporadic E. Except for a slightly greater range (50 to 100 kilometers), oblique F-layer echoes were observed to vary in a similar manner on the College ionograms compared to those recorded at Allakaket. The difference in range can be attributed to the more southerly latitude of College compared to Allakaket.

As mentioned previously, the earliest auroral zone magnetogram indication of the second substorm was at ~ 1400 UT. However, both Allakaket and College recorded increasing fbEs shortly after 1300 UT, and the two megahertz value of fbEs was reached at both stations at ~ 1330 UT. With the reduction of the top frequency of the sporadic E (fEs), associated with the substorm, an overhead F-layer with higher critical frequencies was observed at both Allakaket and College. This F-layer is again interpreted to be characteristic of the plateau in critical frequencies north of the poleward trough wall.

4.3.3.4 March 3, 1966

A large polar magnetic substorm occurred between approximately 0900 and 1100 UT. With the exception of this period, the auroral zone magnetograms indicated magnetoquiet conditions. The earliest indications of the onset of the polar magnetic substorm occurred at about 0800 UT (Great Whale River and Cape Chelyuskin, Figure 48).

In this case there were no early indications of the substorm in the College ionosonde data (Figure 47). Allakaket ionosonde data were not available. However, shortly after 0900 UT the top frequency of the sporadic E increased dramatically to over seven megahertz and blanketed the F-region (Figure 47). Note that the College magnetogram revealed only a slight ~ 20 gamma position perturbation during this same time period of increasing Es. With the sharply defined onset of the negative bay at College the top frequency of Es decreased slightly.

After 1100 UT, the blanketing frequency of sporadic E decreased, and a new overhead F-layer was observed with a critical frequency of four to five megahertz. The critical frequency of this layer increased through 1230 UT and then decreased systematically until ~1545 UT when the F-layer electron density began to increase following about 90 minutes the time of sunrise at 300 kilometers above College. Strong multiples (generally two or three) of the F-layer echoes were observed after 1130 UT indicating that the post-substorm 'replacement-layer' was overhead. Even though the blanketing frequency of sporadic E was approximately one megahertz, there were no post-substorm indications of ionogram echoes from the main trough that was the overhead F-layer prior to the substorm. The post-substorm F-layer is again interpreted to be characteristic of the plateau in the critical frequencies found north of the poleward trough wall.

4.3.4 Summary and Discussion of Results

From these limited studies it appears that an ionosonde located at approximately 65° CGL is a sensitive night sector detector for the occurrence of magnetospheric substorms. The onset of auroral substorms and other known magnetospheric substorm phenomena (cf Akasofu, 1968) usually occurs in the local midnight time sector. Nevertheless, the time sector location of the ionosonde does not appear to be important for the detection of significant ionospheric variations that occur simultaneously and at times precede the earliest onsets of proven substorm phenomena.

It is apparent, from the four periods studied, that certain

relationships exist between winter night sector ionospheric variations at 60° to 65° CGL and the occurrence of magnetospheric substorms:

1). Sporadic E with blanketing frequencies equal to or greater than two megahertz occurs in conjunction with magnetospheric substorms; further, on three of the four nights studied, there were systematic increases in the blanketing frequency of sporadic E, 30 to 60 minutes prior to the earliest substorm onset times determined from auroral zone magnetograms. On the fourth night considered, the onset of high top frequency sporadic E occurred in the evening sector several minutes before the local sharp onset of an intense negative bay.

2). The F-layer poleward trough wall is displaced equatorward during a magnetospheric substorm. Sporadic E, which completely blankets the F-layer, often interferes with the determination of when this displacement occurs relative to the onset of the substorm; however, it appears from these limited investigations that the displacement occurs during the expansive phase of the auroral substorm - possibly in association with the equatorward 'spread' of irregular auroral bands discussed in Chapter 2. It appears that the poleward trough wall in the early morning sector is displaced equatorward to approximately 61° CGL with the occurrence of a magnetospheric substorm with an AL index of approximately -400 gammas (December 4, 1965).

3). Normally once the poleward trough wall is displaced equatorward, it remains equatorward of its magnetoquiet position for the remainder of the night. The post-substorm F-layer at

approximately 65° CGL remains representative of the plateau in the critical frequencies found north of the poleward trough wall. This situation normally exists even though only a single substorm occurs during an otherwise magnetoquiet night (e.g. March 3, 1966).

Recent studies have shown that particle precipitation is an important mechanism for the maintenance of the winter polar F-layer (cf. Thomas and Andrews, 1969 and Pike, 1971a, b). The calculations of Rees (1964) show that the precipitation of electrons with energies less than about 500eV produces the maximum ionization rates at F-region heights. Frank and Ackerson (1971) have reported very detailed measurements of particle precipitation into the auroral zone; they conclude that the dominant contribution to the particle precipitation intensities and energy fluxes in the early morning sector is provided by electrons with energies equal to or less than 300 eV. Such primary electron energies are efficient for producing F-region ionization (Rees, 1964). Frank and Ackerson (1971) also summarize the features of electron precipitation in the late morning sector as being generally more diffuse and less intense compared to the patterns observed in the evening sector. They also show, for both local time sectors, that electron precipitation occurs at lower latitudes with increasing K_p . A survey of the Frank and Ackerson (1971) (E-t) spectrograms reveals that the auroral precipitation region boundaries are normally well defined.

Hoffmann (1969) presents examples of satellite recordings of 700eV detector responses to precipitating electrons at auroral latitudes: he concludes that electron precipitation in the morning sector is characterized by relatively structureless precipitation 'bands' near and equatorward of 'bursts' that have a short temporal duration or a small spatial extent. The 'bands' and 'bursts' observed by Hoffmann (1969) correspond to the enhanced background levels and the structured precipitation events observed by Frank and Ackerson (1971).

The general morphology of the F-layer phenomena studied for latitudes of 60° to 70° CGL is consistent with the satellite observations of precipitating electrons into the same latitude zone. The F-layer poleward trough wall corresponds to the equatorward edge of the auroral precipitation region. The plateau in the F-layer critical frequencies north of the poleward trough wall corresponds to the enhanced background level in the particle precipitation. It is also likely that the night sector F-layer irregularity zone corresponds to the location of the particle precipitation 'bursts' (Hoffmann, 1969) and the structured particle precipitation events (Frank and Ackerson, 1971). The equatorward shift of the poleward trough wall in association with magnetospheric substorms can only be inferred from the satellite observations; however, the satellite data do show that the particle precipitation region extends to lower latitudes in association with an increased geomagnetic disturbance level (K_p).

There is uncertainty as to the physical significance of sporadic E parameters; however, it is likely that the blanketing frequency of sporadic E (fbEs) corresponds to the maximum plasma frequency in the Es layer (Reddy and Rao 1968 and Reddy, 1968). If this relationship is valid, then the maximum Es-layer electron densities may be determined from the values of fbEs.

In Chapter 3 it was concluded that sporadic E, either blanketing or non-blanketing with top frequencies above two megahertz, normally does not occur during magnetoquiet at latitudes equatorward of $\sim 68^\circ$ CGL. Further, the examples considered for this section reveal that fbEs values, during magnetoquiet, are normally less than one megahertz.

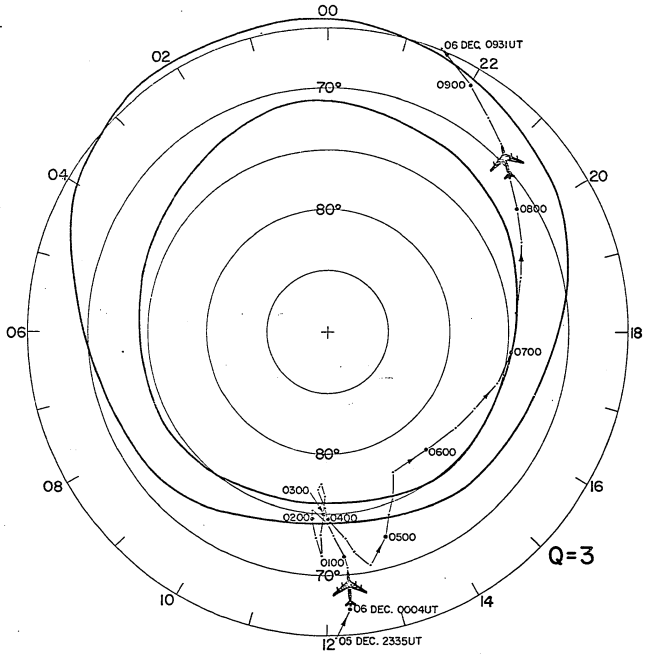
The early increase, at auroral zone latitudes, in the blanketing frequency of sporadic E prior to magnetospheric substorms indicates an increase in the electron density at Es heights -- assuming that fbEs is related to the electron density. It would be of great interest to examine auroral electron precipitation data for such latitudes prior to substorms to determine if the intensity of the 10 keV precipitating electrons shows a 'pre-substorm' increase that could account for the increased Es ionization. The absence of an increase in the precipitation of 10 keV electrons prior to substorms would be equally interesting, as this would point toward a local mechanism for the production of the 'pre-substorm' increases in the blanketing frequency of sporadic E.

The results of this chapter illustrate the potential value in establishing an ionosonde network to systematically observe

the high latitude ionosphere.

The synoptic pattern of the high latitude ionosphere is characterized by pronounced circumpolar features that are closely associated with the auroral oval. For this reason a magnetic meridian chain of ionosondes; established in association with a chain of geophysical observatories such as now exists in Alaska, would provide the data to further relate the F-region ionospheric structure to the dynamics of the auroral oval and magnetospheric substorms. E-region data from such a high quality geophysical observing chain would permit a detailed study of the auroral E-layer and retarded type sporadic E. The E-region data would also permit a comprehensive investigation of the relationships between sporadic E, auroras and magnetospheric substorm phenomena.

The high latitude ionosphere forms the base of the outer magnetosphere. The ionosonde is not only an instrument for ionospheric studies but is in a much broader sense a simple and powerful instrument for monitoring the temporal changes in the large scale magnetospheric structure. The ionosonde, recognized in this realm, is capable of providing essential data for the continued interdisciplinary study of ionospheric and magnetospheric phenomena.



DECEMBER 5-6, 1969

Fig. 30

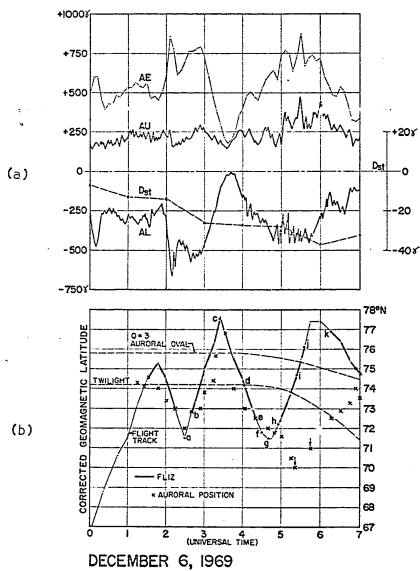
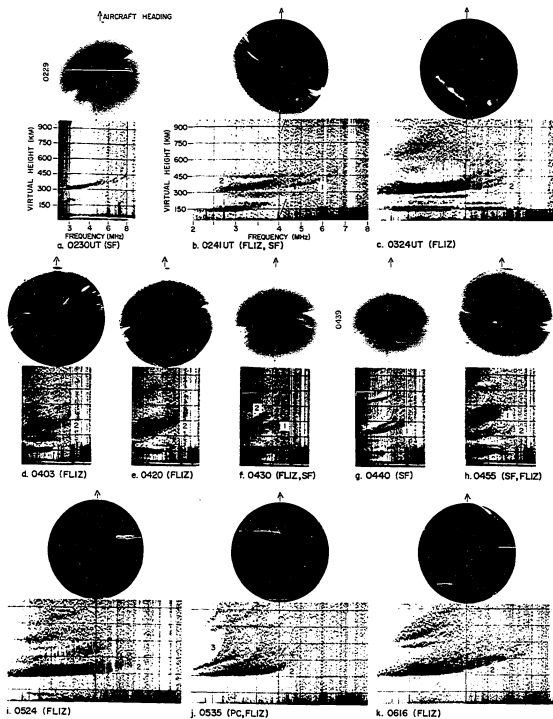


Fig. 31



DECEMBER 6, 1969

Fig. 32

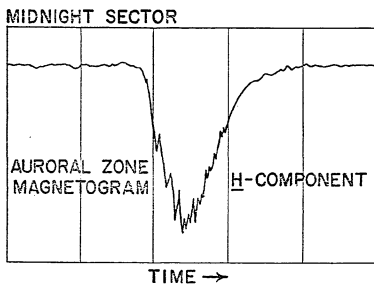
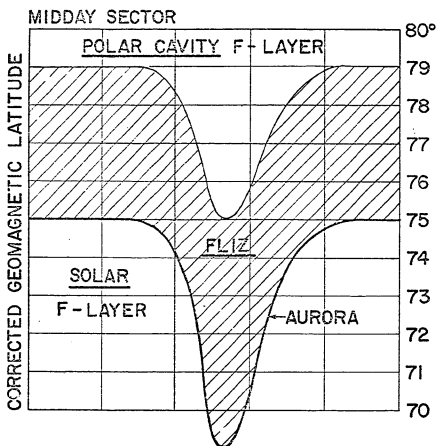


Fig. 33

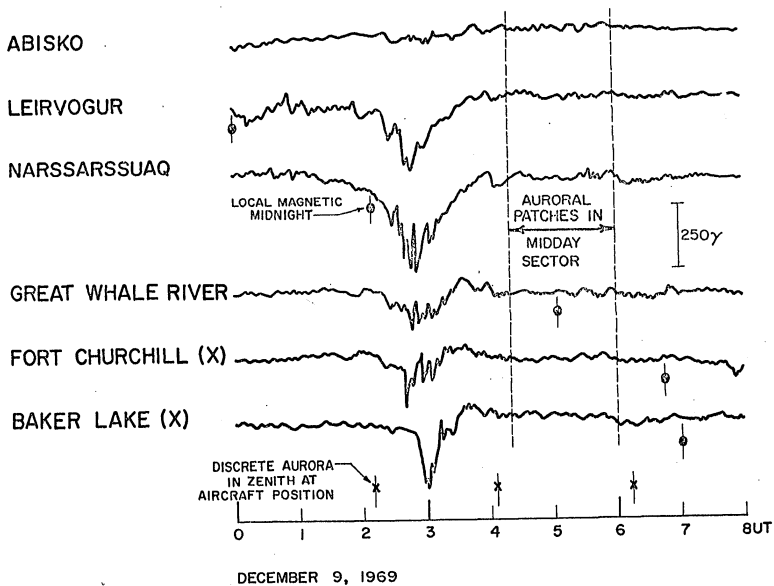


Fig. 34

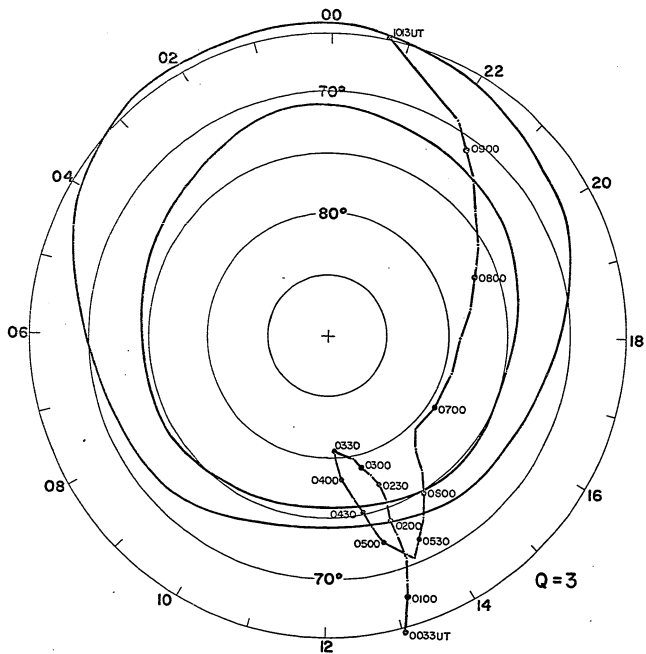


Fig. 35

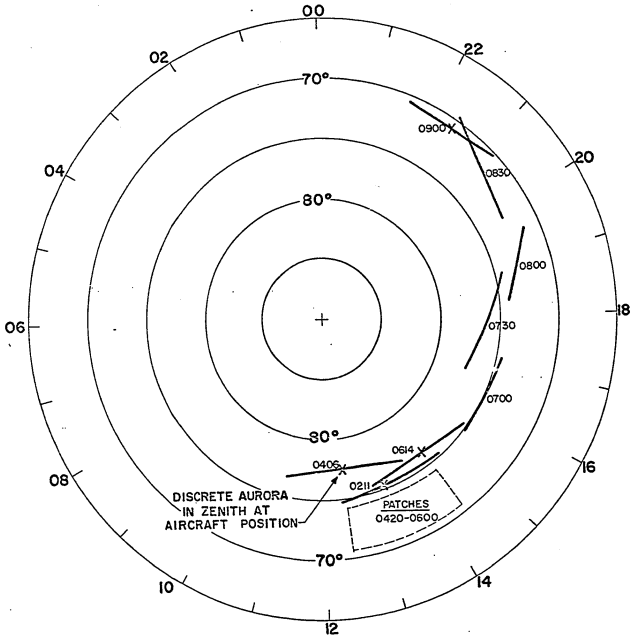


Fig. 36

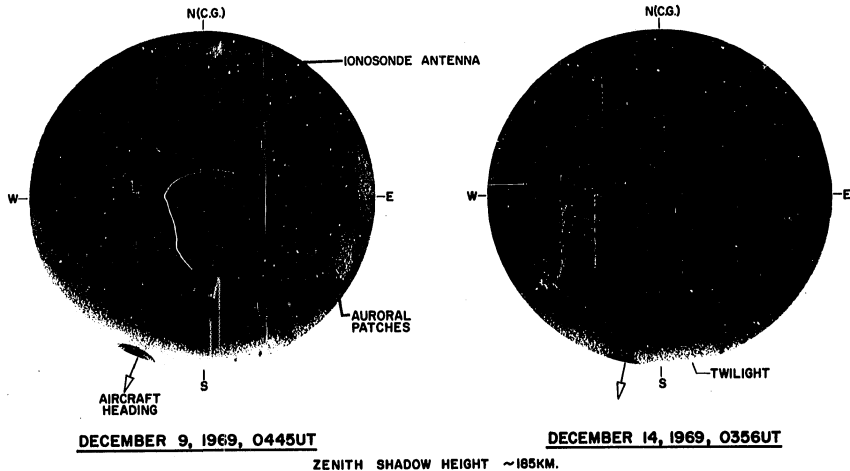


Fig. 37

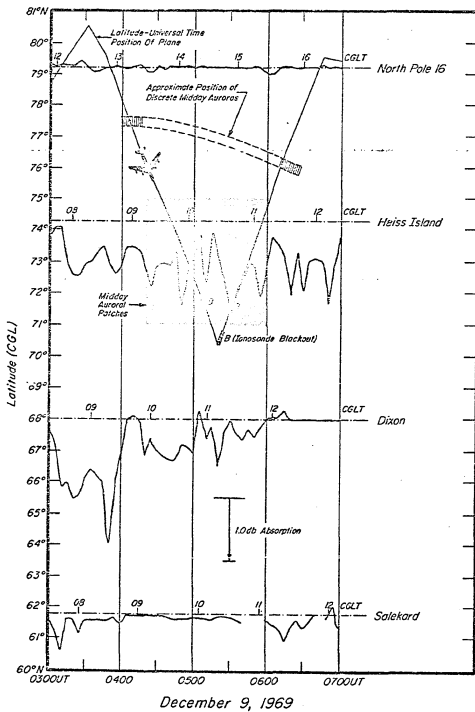


Fig. 38

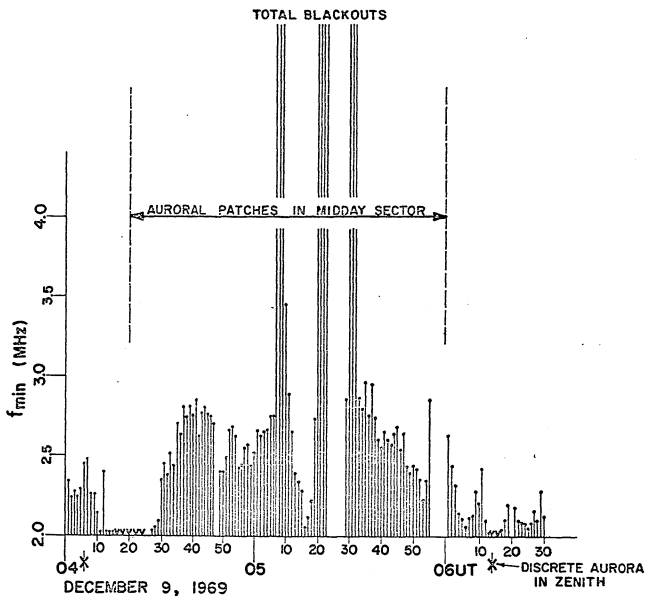


Fig. 39

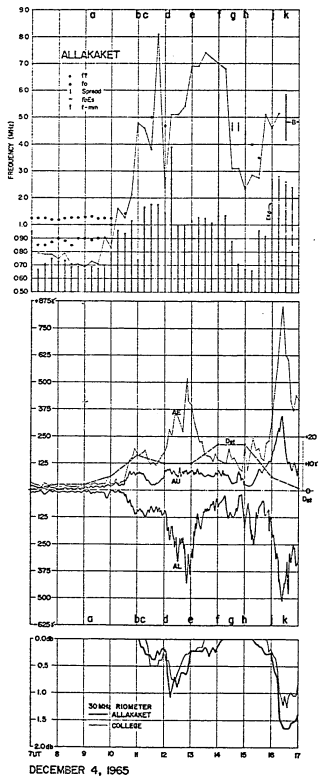


Fig. 40

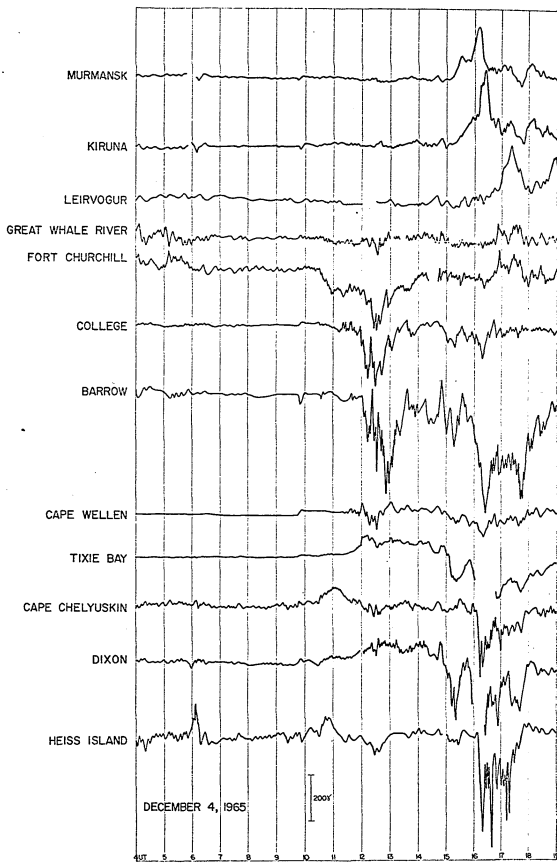


Fig. 41

DECEMBER 4, 1965

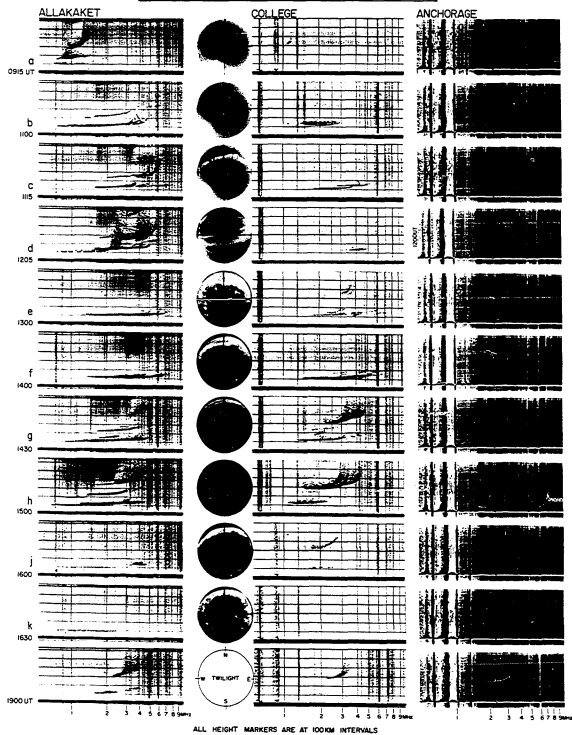


Fig. 42

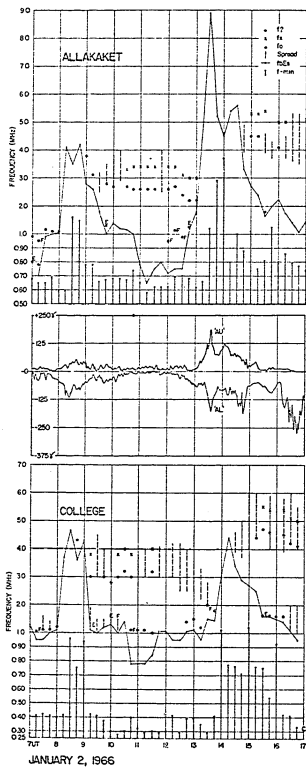


Fig. 43

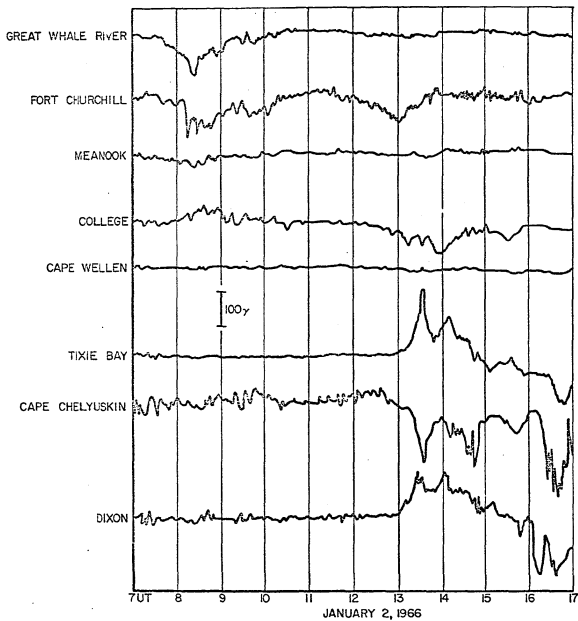


Fig. 44

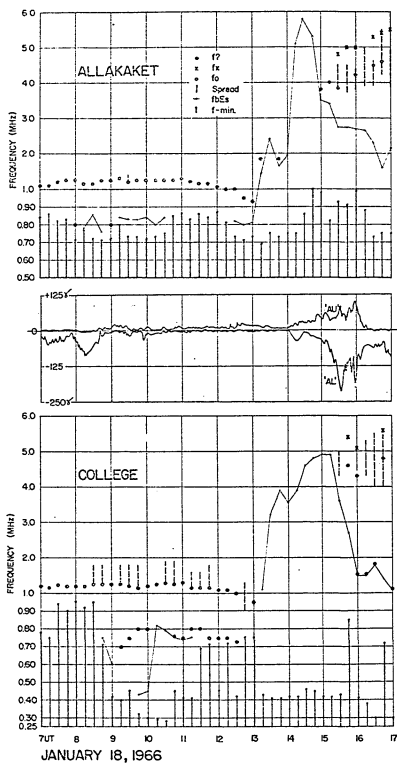


Fig. 45

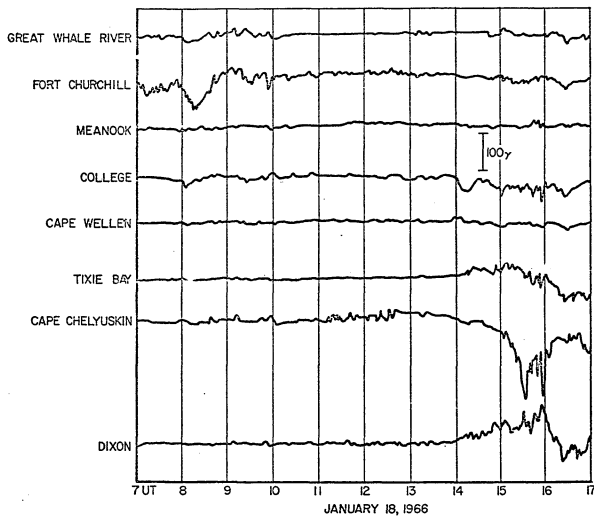


Fig. 46

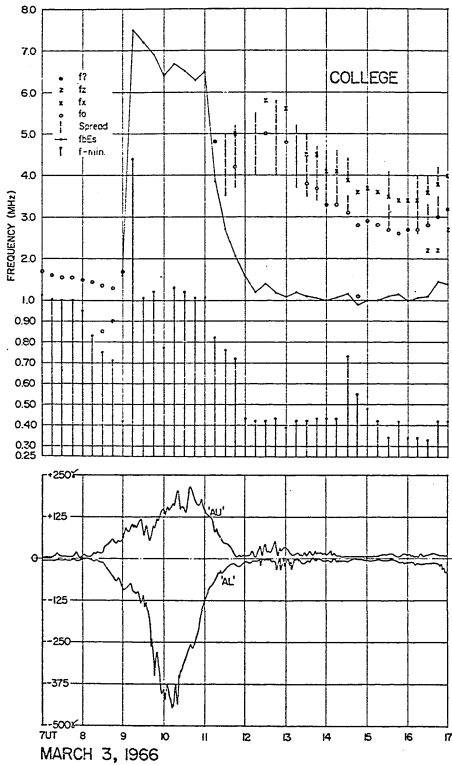


Fig. 47

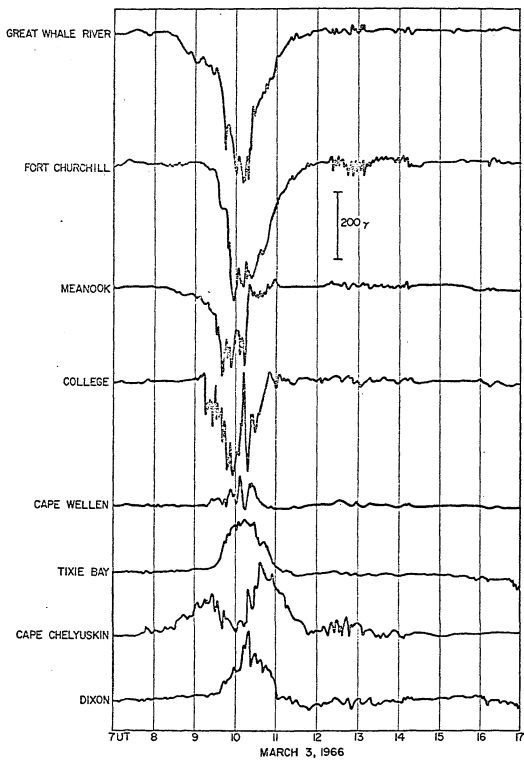


Fig. 48

CHAPTER 5

SUMMARY

The main purpose of this thesis has been to examine the morphology of the high latitude ionosphere during magnetospheric substorms. The approach adopted here differs from many of the earlier morphological studies which confined their attention to the mid-latitude ionospheric variations during worldwide magnetic disturbances (e.g. Matsushita, 1959; King, 1961 and Thomas and Venables, 1966). Because of the complexity of high latitude ionospheric phenomena, there have been relatively few detailed studies of large-scale ionospheric disturbances that occur in the polar regions. Notable exceptions include the earlier investigations of Burkard (1948), Meek (1953, 1954) and Bellchambers et al. (1962) who each observed that the F-region variations at latitudes of approximately 61° to 67° CGL are closely related to the local magnetic disturbance level; however, because of the lack of a known synoptic pattern or frame of reference for high latitude ionospheric parameters, the significance of these investigations was not fully understood.

During the past decade, aircraft and satellite borne ionosondes have provided the data to identify the large-scale circumpolar features of the high latitude ionosphere and to show a close association between these features and the auroral oval (e.g. Thomas and Andrews, 1969 and Buchau et al., 1972). Based upon these recent developments, it was hypothesized and proved that variations of the large-scale features of the high latitude

ionosphere are related to the dynamics of the auroral oval during magnetospheric substorms.

5.1 THE AURORAL OVAL AND AURORAL SUBSTORMS

All-sky camera data from the Alaskan meridian chain of observatories were studied to determine the meridional distributions and motions of auroras that comprise the auroral oval. This study provided a background for the evaluation of ionospheric variations in relation to the auroral oval during magnetospheric substorms. A magnetic meridian chain of observatories is analogous to an azimuth-scan radar that systematically 'scans' the auroral oval once per day. The results of this investigation have revealed several new morphological features of the auroral substorm.

An enhanced equatorward drift of auroral forms and the 'clearing' of the poleward sky result in an equatorward 'thinning' of the auroral oval prior to the onset of the expansive phase of the substorm. These phenomena may possibly indicate the growth phase of a magnetospheric substorm.

Because of the current interest in the early phase of magnetospheric substorms, growth phases defined by other workers were investigated on the basis of all-sky camera photographs. It is concluded that until the geomagnetic field variations during the early phase of magnetospheric substorms are well established, the growth phase should not be defined from auroral zone magnetic records alone.

During worldwide magnetoquiet, intense auroral substorms can occur on the contracted auroral oval. Such substorms may

occur beyond the poleward horizon of an auroral zone observatory; except for the difference in the latitude of occurrence they are similar in character to those substorms observed at typical auroral zone observatories; such as College or Fort Yukon. Without a meridian chain of observatories extending to approximately 75° CGL, such substorms would not be detected. This fact emphasizes the importance of a meridian observing chain for morphological studies of auroras.

Auroral motions may be a visible indicator of the magnetospheric convection pattern (cf. Davis, 1971). Accepting this premise, night sector equatorward motions correspond to the earthward convection of magnetic flux tubes in the magnetotail, while the poleward motions of day sector auroras correspond to the non-midnight meridian convection pattern into and across the polar cap (cf. Axford, 1969). All-sky camera data from the Alaskan meridian chain confirm the earlier statistical results that concluded that night sector equatorward auroral motions are more frequent than poleward motions. Sunlight precludes comprehensive day sector observations by the Alaskan meridian chain. For this reason southern hemisphere all-sky camera data were used to determine that poleward motions of day sector auroras occur statistically more frequently than equatorward motions. Thus, the characteristic meridional motions of night and day sector auroras support the concept of the 'open' magnetosphere with a steady convection driven as a result of the reconnection of interplanetary and geomagnetic field lines (Dungey, 1961).

The concept of the continuous auroral oval is supported by the auroral studies undertaken for this dissertation. 'Gaps' were observed during magnetoquiet, such as those reported by Buchau *et al.* (1970). However the gaps were not associated with spatial discontinuities of the type reported by Lassen (1972).

5.2 THE HIGH LATITUDE IONOSPHERE DURING MAGNETOQUIET

An investigation of ionospheric disturbances depends upon a detailed knowledge of the behavior of the ionosphere during magnetoquiet periods. Data from airborne and ground based ionosondes were combined to deduce the macroscale patterns of the magnetoquiet high latitude ionospheric E-region and the F2-layer. During such periods the auroral E-layer and retarded type sporadic E occur in a circumpolar band bounded by approximately 68° and 75° CGL; non-retarded type sporadic E, with top frequencies above two megahertz does not occur equatorward of approximately 68° CGL. The magnetoquiet night sector F2-layer is characterized by the main trough, with critical frequencies of approximately one megahertz; the main trough is bounded on the poleward side ($\sim 67^\circ$ CGL) by a well-defined wall and plateau of F-region ionization that extends poleward to the instantaneous auroral oval.

While many factors may contribute to the maintenance of the high latitude winter ionosphere (*cf.* Rishbeth, 1968 and Rishbeth and Garriott, 1969), particle precipitation into the circumpolar ring bounded by the main trough and the polar cavity must be a prime consideration. Whalen *et al.* (1971) show a close correspondence between the characteristics of the auroral E-layer and the ion production rate deduced from measurements of the auroral N_2^+ emission.

The meridional profiles of lower energy particle precipitation (≈ 700 eV), reported by Frank and Ackerson (1971) and Hoffmann (1969), agree qualitatively with deduced positions of the poleward trough wall of the night sector F-layer. Winningham and Pike (1972) have shown excellent quantitative agreement between the day sector characteristics of the F-layer irregularity zone and the low energy particle precipitation through the polar cusp.

5.3. THE HIGH LATITUDE IONOSPHERE DURING MAGNETOSPHERIC SUBSTORMS

Night sector ionospheric disturbances are closely associated with the occurrence of magnetospheric substorms. At approximately 65° CGL in the night sector, sporadic E with top frequencies greater than two megahertz occurs in conjunction with substorms. The top frequency of sporadic E decreases below two megahertz during the recovery phase of the substorm. At times the blanketing frequency of sporadic E increases prior to the onset of accepted substorm phenomena.

There is uncertainty as to the physical significance of the top frequency or the critical frequency of sporadic E as scaled from ionograms; however, it is likely that the blanketing frequency of sporadic E corresponds to the maximum plasma frequency in the sporadic E layer. Accepting this likelihood, then the early increase in the blanketing frequency of sporadic E, prior to magnetospheric substorms and at latitudes of approximately 65° CGL, indicates an increase in the electron density at sporadic E heights. Such a finding, if properly verified by independent data, could be important in the studies of the growth of the

auroral electrojet during the growth and early expansive phases of magnetospheric substorms.

The poleward trough wall in the night sector is displaced equatorward during the development of a substorm. From limited examples, it appears that the displacement occurs during the expansive phase of the auroral substorm. Normally once the poleward trough wall is displaced equatorward, it remains equatorward of its magnetoquiet position for the remainder of the night.

The equatorward shift of the poleward trough wall in association with magnetospheric substorms can only be inferred from the reported satellite observations of low energy particle precipitation. The satellite data do show that the precipitation zone extends to lower latitudes with an increased geomagnetic disturbance level (K_p) (Frank and Ackerson, 1971). Limited observations indicate that the poleward trough wall is displaced equatorward five or more degrees of latitude with the development of a moderate polar magnetic substorms (ALV-400 gammas). It is concluded that the displacement of the poleward trough wall of the night sector F-layer is associated with a similar displacement of the equatorward boundary of the auroral precipitation zone.

Buchau et al. (1972) show that the day sector of the auroral oval is co-located with a band of enhanced 6300 Å emission and the day sector F-layer irregularity zone; they further show that both features result from the precipitation of low energy electrons through the polar cusp. This suggests that the F-layer irregularity zone is an excellent indicator of the intersection of the polar cusp with the ionosphere. The meridional motions of the F-layer

irregularity zone can thus be interpreted to indicate large-scale motions of the polar cusp. Day sector disturbances are recognized by ionospheric characteristics closely associated with auroral phenomena. The day sector F-layer irregularity zone and the discrete auroras move equatorward and subsequently poleward with the development and decay of a magnetospheric substorm.

Increased non-deviative ionospheric absorption of high frequency radio waves is associated with the formation of midday auroral patches that occur in conjunction with magnetospheric substorms. This is further evidence that indicates the circumpolar nature of the hard particle precipitation zone associated with magnetospheric substorms (Hartz and Brice, 1967). Midday auroral patches must also be an integral part of the substorm morphology of midday auroras.

5.4 HIGH LATITUDE IONOGRAM INTERPRETATION

Earlier studies of ionospheric variations emphasized the investigation of 'scaled' ionogram parameters, such as critical frequencies and heights. However, for the studies presented here, the scaled ionogram parameters have been used only to illustrate differences in ionogram character that in turn identify with known large-scale ionospheric features. This 'characterization' of complex high latitude ionograms often relates more information than do the scaled data. The application of the current international guidelines (Piggott and Rawer, 1961) for the interpretation and scaling of high latitude ionograms often requires arbitrary decisions by the scaler and does not require a consideration of additional significant

information recorded on many high latitude ionograms. Any revision of the international guidelines for the interpretation and scaling of high latitude ionograms should consider the demonstrated significance of ionogram characterization.

5.5 A MAGNETIC MERIDIAN OBSERVING CHAIN FOR CONTINUED STUDIES

This work illustrates the advantages of an interdisciplinary study of the high latitude ionosphere. It also demonstrates the need for a meridian chain of geophysical observatories equipped with ionosondes, as well as all-sky cameras, magnetometers and riometers. On the basis of the studies presented here, it is recommended that ionosondes be installed along a meridian chain of observatories as well as the standard monitoring equipment. Such an interdisciplinary and systematic observing approach would provide the data necessary for refinement of the studies presented here and for examination of the possibilities of providing warning for the occurrence of magnetospheric substorms.

Several results of this dissertation suggest that the growth phase of magnetospheric substorms may be observed in auroral and ionospheric data. The pursuit of these suggestions to a definitive conclusion is important for a better understanding of magnetospheric phenomena. In addition, such studies would extend the understanding of the ionospheric environment and its effect upon the communication of information via or through the polar ionosphere.

APPENDIX I

Dates Studied	Phenomena		Section
	Auroral	Ionospheric	
May 30, 1960	X		2.3, 2.5
May 31, 1962	X		2.5
June 1,7,28,29,30, 1962	X		2.5
July 1,5,6, 1962	X		2.5
September 14,15, 1964		X	3.3
October 2, 1965	X		2.3
December 1, 1965	X		2.3
December 4, 1965	X	X	4.3
January 2,18, 1966		X	4.3
March 3, 1966		X	4.3
December 22, 1967	X		2.3
February 13, 1968	X		2.3
December 5, 1969	X		2.3
December 6, 1969	X	X	4.1
December 9, 1969	X	X	4.2
December 13,14, 1969		X	3.2
January 5,6,8, 1970	X		2.3, 2.4
February 14, 1970	X		2.3
November 30, 1970		X	3.2
December 1, 1970		X	3.2
January 8, 1971		X	3.2
November 16,17, 1971		X	3.2

REFERENCES

- Akasofu, S.-I., Large-scale auroral motions and polar magnetic disturbances - I., A polar disturbance at about 1100 hours on 23 September 1957, *J. Atmosph. Terr. Phys.*, 19, 10, 1960.
- Akasofu, S.-I., The development of the auroral substorm, *Planet. Space Sci.*, 12, 273, 1964.
- Akasofu, S.-I., Dynamic morphology of auroras, *Space Sci. Rev.*, 4, 498, 1965.
- Akasofu, S.-I., Electrodynamics of the magnetosphere, geomagnetic storms, *Space Sci. Rev.*, 6, 21, 1966.
- Akasofu, S.-I., Polar and Magnetospheric Substorms, D. Reidel Pub. Co., Dordrecht, Holland, 1968.
- Akasofu, S.-I., The ionosphere as a base of the magnetosphere, *Annals of IQSY*, Vol. 5, 167, 1969, ed. by A.C. Stickland, MIT Press, Cambridge, Mass.
- Akasofu, S.-I., Midday auroras and magnetospheric substorms, *J. Geophys. Res.*, 77, 244, 1972a.
- Akasofu, S.-I., Midday auroras at the South Pole during magnetospheric substorms, (submitted to *J. Geophys. Res.*), 1972.
- Akasofu, S.-I. Chapman, S., The lower limit of latitude (US sector) of northern quiet auroral arcs, and its relation to $D_{st}(H)$, *J. Atmos. Terr. Phys.*, 25, 9, 1963.
- Akasofu, S.-I., Kimball, D.S., and Meng, C.-I., Dynamics of the aurora - II, Westward traveling surges, *J. Atmos. Terr. Phys.*, 27, 173, 1965.
- Akasofu, S.-I., Kimball, D.S. and Meng, C.-I., Dynamics of the aurora - V, poleward motions, *J. Atmos. Terr. Phys.*, 28, 497, 1966a.
- Akasofu, S.-I., Meng, C.-I., and Kimball, D.S., Dynamics of the aurora - VI, formation of patches and their eastward motion, *J. Atmos. Terr. Phys.*, 28, 505, 1966b.
- Akasofu, S.-I., Kimball, D.S. and Meng, C.-I., Dynamics of the aurora, VII, Equatorward motions and the multiplicity of auroral arcs, *J. Atmos. Terr. Phys.*, 28, 627, 1966c.
- Akasofu, S.-I., Kimball, D.S., Buchau, J., and Gowell, R.W., The alignment of auroral arcs, *J. Geophys. Res.*, (in press) 1972.
- Akasofu, S.-I., Wilson, C.R., Snyder, A.L., and Perreault, P.D., Results from a meridian chain of observatories in the Alaskan sector (I), *Planet. Space Sci.*, 19, 477, 1971.

- Allen, C.W., Astrophysical Quantities, Athlone Press, London, 1955.
- Andrews, H.K. and Thomas, J.O., Electron density distribution above the winter pole, Nature, 221, 223, 1969.
- Aubry, M.P. and McPherron, R.L., Magnetotail changes in relation to the solar wind magnetic field and magnetospheric substorms, J. Geophys. Res., 76, 4381, 1971.
- Axford, W.I., Magnetospheric convection, Rev. Geophys., 7, 421, 1969.
- Bartels, J., II - The technique of scaling indices K and Q of geomagnetic activity, Annals of IGY, 4, 215, 1957.
- Bates, H.F., A proposed polar auroral radar system, J. Atmos. Terr. Phys., 28, 903, 1966.
- Bates, H.F., Private communication, University of Alaska, 1972.
- Bates, H.F., Belon, A.E., Romick, G.J., and Stringer, W.J., On the correlation of optical and radio auroras, J. Atmos. Terr. Phys., 28, 439, 1966.
- Bates, H.F., Sharp, R.D., Belon, A.E., and Boyd, J.S., Spatial relationships between HF radar aurora, optical aurora and electron precipitation, Planet. Space Sci., 17, 93, 1969.
- Bellchambers, W.H., Barclay, L.W., and Piggott, W.R., Ionospheric observations, part II, Analysis of results, in The Royal Society I.G.Y. Expeditions, Halley Bay, 1955-59, Vol II, 179, 1962.
- Belon, A.E., Private communication, University of Alaska, 1971.
- Berkey, F.T., A Study of the Auroral-Absorption Substorm, Ph.D. Thesis, University of Alaska, 1971.
- Beynon, W.J.G., and Brown, G.M., Ionospheric vertical soundings, Annals of the I.G.Y., 3, Part I, 1957.
- Bowman, G.G., Ionization troughs below the F2-layer maximum, Planet. Space Sci., 17, 777, 1969.
- Boyd, J.S., Belon, A.E., and Romick, G.J., Latitude and time variations in precipitated electron energy inferred from measurements of auroral heights, J. Geophys. Res., 76, 7694, 1971.
- Buchau, J., Gassmann, G.J., Pike, C.P., Wagner, R.A., and Whalen, J.A., Precipitation patterns in the arctic ionosphere determined from airborne observations, Ann. de Geophys. (in press) 1972.
- Buchau, J., Whalen, J.A., and Akasofu, S.-I., On the continuity of the auroral oval, J. Geophys. Res., 75, 7147, 1970.
- Burkard, O., A sporadic F-layer, J. Geophys. Res., 53, 63, 1948.

- Calvert, W., Steep horizontal electron-density gradients in the topside F-layer, *J. Geophys. Res.*, 71, 3665, 1966.
- Carpenter, D. L., Whistler studies of the plasmapause in the magnetosphere, I. Temporal variations in the knee and some evidence on plasma motions near the knee, *J. Geophys. Res.*, 71, 693, 1966.
- Chubb, T. A. and Hicks, G. T., Observations of the aurora in the far ultraviolet fromOGO 4, *J. Geophys. Res.*, 75, 1290, 1970.
- Danielsen, C., Auroral observations at Thule, Danish Meteorological Institute, Geophysical Papers, R-9, 1969.
- Davis, T. N., The morphology of the auroral displays of 1957-1958, 2. Detail analyses of Alaska data and analyses of high latitude data, *J. Geophys. Res.*, 67, 75, 1962.
- Davis, T. N., Magnetospheric convection pattern inferred from magnetic disturbances and auroral motions, *J. Geophys. Res.*, 76, 5978, 1971.
- Davis, T. N. and DeWitt, R. N., Twenty-four-hour observations of aurora at the southern auroral zone, *J. Geophys. Res.*, 68, 6251, 1963.
- Davis, T. N. and Elvey, C. T., Construction of an all-sky camera, Geophysical Institute, University of Alaska Research Report No. 2, 1955.
- Davis, T. N. and Kimball, D. S., Incidence of auroras and their north-south motions in the northern auroral zone, Geophysical Institute Report, UAG R100, University of Alaska, 1960.
- Davis, T. N. and Sugiura, M., Auroral electrojet activity index AE and its Universal time variations, *J. Geophys. Res.*, 71, 785, 1966.
- Denholm, J. V., Some auroral observations inside the southern auroral zone, *J. Geophys. Res.*, 66, 2105, 1961.
- Duncan, R. A., Universal time control of the arctic and antarctic F region, *J. Geophys. Res.*, 67, 1823, 1962.
- Dungey, J. W., Interplanetary magnetic field and the auroral zones, *Phys. Rev. Letters*, 6, 47, 1961.
- Evans, S., Horizontal movements of visual auroral features, *J. Atmos. Terr. Phys.*, 16, 191, 1959.
- Evans, S., Systematic movements of aurorae at Halley Bay, *Proc. of Roy. Soc., London, A.*, 256, 234, 1960.

- Feldstein, Y. I., Geographical distribution of aurora and azimuth of auroral arcs, in Investigation of the Aurorae, Academy of Science, USSR, 4, 61, 1960.
- Feldstein, Y. I., Some problems concerning the morphology of auroras and magnetic disturbance at high latitudes, Geomag. and Aeron., (Eng. Trans.), 3, 183; 1963.
- Feldstein, Y. I., Polar aurora, polar substorms and their relationships with the dynamics of the magnetosphere, Rev. Geophys., 7, 179, 1969.
- Feldstein, Y. I., Auroras and associated phenomena, Proc. Internat. Symp. on Solar-Terrestrial Physics, Leningrad, (in press) 1971.
- Feldstein, Y. I. and Starkov, G. V., Dynamics of auroral belt and polar magnetic disturbances, Planetary and Space Science, 15, 209, 1967.
- Frank, L. A., Plasma in the earth's polar magnetosphere, J. Geophys. Res., 76, 5202, 1971.
- Frank, L. A. and Ackerson, K. L., Observations of charged particle precipitation into the auroral zone, J. Geophys. Res., 76, 3612, 1971.
- Fritz, H., Das Polarlicht, Leipzig, 1881.
- Gustafsson, G., On the orientation of auroral arcs, Planet. Space Sci., 15, 277, 1967.
- Hagg, E. L., Electron densities of 8-100 electrons cm^{-3} deduced from Alouette II high latitude ionograms, Can. J. Phys., 45, 27, 1967.
- Hanson, G. H., Hagg, E. L. and Fowle, D., The interpretation of ionospheric records, Defence Research Telecommunications Establishment Report No. R-2, 1953.
- Hakura, Y., Tables and maps of geomagnetic coordinates corrected by higher order spherical harmonic terms, Rep. Ionos. Space Res., Japan, 19, 121, 1965.
- Harang, L., The Aurorae, Wiley, New York, 1951.
- Hartz, T. R. and Brice, N. M., The general pattern of auroral particle precipitation, Planet. Space Sci., 15, 301, 1967.
- Hepner, J. P., Time sequences and spatial relations in auroral activity during magnetic bays at College, Alaska, J. Geophys. Res., 59, 329, 1954.
- Hoffmann, R. A., Low energy electron precipitation at high latitudes, J. Geophys. Res., 74, 2425, 1969.

- Hoffman, R. A. and Berko, F. W., Primary electron influx to dayside auroral oval, *J. Geophys. Res.*, 76, 2967, 1971.
- Hones, E. W., Jr., Akasofu, S.-I., Bame, S. J. and Singer, S., Poleward expansion of the auroral oval and associated phenomena in the magnetotail during auroral substorms, *J. Geophys. Res.*, 76, 8241, 1971.
- Hultqvist, B., The geomagnetic field in higher approximation, *Arkiv for Geophysik*, 3, 63, 1958.
- Iijima, T. and Nagata, T., Signatures for substorm development of the growth phase and expansion phase, *Geophys. Res. Lab. Rept.*, UT-GRL-71-03, July, 1971.
- Kelley, M. C., Starr, J. A. and Mozer, F. S., Relationship between magnetospheric electric fields and the motion of auroral forms, *J. Geophys. Res.*, 76, 5269, 1971.
- Khorosheva, O. V., The diurnal drift of the closed auroral ring, *Geomag. and Aeron.*, (Eng. Trans.), 2, 696, 1962.
- Khorosheva, O. V., The extent of the aurora arc and their orientation in space, *Geomag. and Aeron.*, (Eng. Trans.), 3, 294, 1963.
- Kim, J. S. and Currie, B. W., Horizontal movements of aurora, *Can. J. Phys.*, 36, 160, 1958.
- King, G. A. M., The night-E layer, in *Ionospheric Sporadic-E*, edited by E. R. Smith and S. Matsushita, MacMillan Co., New York, 1962.
- King, J. W., Magnetic effects in the F-region of the ionosphere, *J. Atmos. Terr. Phys.*, 21, 26, 1961.
- Kokubun, S., Polar substorm and interplanetary magnetic field, *Planet. Space Sci.*, 19, 697, 1971.
- Lassen, K., Polar cap emissions, in *Atmospheric Emissions*, ed. B. M. McCormac and A. Omholt, p. 63, Van Nostrand Reinhold New York, 1969.
- Lassen, K., Diurnal variations of auroral frequency over Greenland 1963-1966 (IQSY), Det. Danske Meteorologiske Institute, Charlottenlund, 1970.
- Lassen, K., On the classification of high latitude auroras, Danish Meteorological Institute, Geophysical Section II (Preprint), 1972.
- Lezniak, T. W. and Winckler, J. R., Experimental study of magnetospheric motions and the acceleration of energetic electrons during substorms, *J. Geophys. Res.*, 75, 7075, 1970.

- Loomis, B., On the geographical distribution of auroras in the northern hemisphere, *Amer. J. Sci. Arts*, 30, 89, 1860.
- Maehlum, B. N., Universal-time control of the low energy fluxes in the polar regions, *J. Geophys. Res.*, 73, 3459, 1968.
- Maehlum, B. N., On the high latitude Universal time controlled F layer, *J. Atmos. Terr. Phys.*, 31, 531, 1960.
- Matsushita, S., A study of the morphology of ionospheric storms, *J. Geophys. Res.*, 64, 305, 1959.
- McPherron, R. L., Growth phase of magnetospheric substorms, *J. Geophys. Res.*, 75, 5592, 1970.
- Meek, J. H., Correlation of magnetic, auroral and ionospheric variations at Saskatoon, *J. Geophys. Res.*, 58, 445, 1953.
- Meek, J. H., Correlation of magnetic, auroral and ionospheric variations at Saskatoon - Part 2, *J. Geophys. Res.*, 59, 87, 1954a.
- Meek, J. H., East-west motion of aurorae, *Astrophys. J.*, 120, 602, 1954b.
- Meinel, A. B. and Schulte, D. H., A note on auroral motions, *Astrophys. J.*, 117, 454, 1953.
- Meng, C.-I., Akasofu, S.-i., Hones, E. W., Jr. and Kawasaki, K., Magnetospheric substorms in the distant magnetotail observed by IMP 3, *J. Geophys. Res.*, 76, 7584, 1971.
- Meng, C.-I., Hones, E. W., Jr. and Akasofu, S.-i., Simultaneous observations of an energetic electron event in the magnetotail by the Vela 3A and IMP 3 satellites, I., *J. Geophys. Res.*, 75 7294, 1970.
- Mishin, V. M., Saifudinova, T. I. and Zhulin, I. A., A magnetosphere based on the two zones of precipitating energetic particles, *J. Geophys. Res.*, 75, 797, 1970.
- Montbriand, L. E. J., Morphology of auroral hydrogen emissions during auroral substorms, Ph.D. Thesis, University of Saskatoon, 1969.
- Mozer, F. S., Origin and effects of electric fields during isolated magnetospheric substorms, *J. Geophys. Res.*, 76, 7595, 1971.
- Muldrew, D. B., F-layer ionization troughs deduced from Alouette data, *J. Geophys. Res.*, 70, 2635, 1965.
- Nelms, G. L., Ionospheric results from the topside sounder satellite Alouette, *Space Research* IV, 437, 1964.

- Ness, N. F., Scearce, C. S. and Seek, J. B., Initial results of the IMP 1 magnetic field experiment, *J. Geophys. Res.*, 69, 3531, 1964.
- Nichols, B., Auroral ionization and magnetic disturbances, *Proc. of IRE*, 47, 245, 1959.
- Nishida, A., DP-2 and polar substorm, *Planet. Space Sci.*, 19, 205, 1971.
- Nishida, A. and Kokubun, S., New polar magnetic disturbances; S^P , S^Q , S^R and U^P-2 , *Rev. Geophys.*, 9, 417, 1971.
- Oguti, T. and Marubashi, K., Enhanced ionization in the ionospheric F2 region around geomagnetic noon in high latitudes, *Rep. Ionosph. Space Res. Japan*, 20, 96, 1966.
- Olesen, J. K. and Wright, J. W., The relationship of low-height ionosonde echoes to auroral zone absorption and VHF D scatter, *J. Geophys. Res.*, 66, 1127, 1961.
- Petrie, L. E., Preliminary results on mid and high latitude topside spread F, Spread F and its Effects on Radio Wave Propagation and Communication, *Agardograph*, 95, 67, 1966.
- Piggott, W. R. and Rawer, K., URSI Handbook of Ionogram Interpretation and Reduction, Elsevier Pub. Co., Amsterdam, 1961.
- Pike, C. P., A comparison of the north- and south-polar F layers, *J. Geophys. Res.*, 76, 6875, 1971a.
- Pike, C. P., A latitudinal survey of the daytime polar F layer, *J. Geophys. Res.*, 76, 7745, 1971b.
- Pittenger, E. W. and Gassmann, G. J., High latitude sporadic E, *AFRL Environmental Research Papers*, No. 347, Feb. 5, 1971.
- Pudovkin, M. I., Shumilov, O. I. and Zaitzeva, S. A., Dynamics of the zone of corpuscular precipitations, *Planet. Space Sci.*, 16, 881, 1968.
- Ratcliffe, J. W., The Magneto-ionic Theory and Its Application to the Ionosphere, University Press, Cambridge, 1959.
- Reddy, C. A., Physical significance of the Es parameters fbEs, fEs, and foEs, 2., Causes of partial reflections from Es, *J. Geophys. Res.*, 73, 5627, 1968.
- Reddy, C. A. and Rao, M. M., On the physical significance of the Es parameters fbEs, fEs and foEs, *J. Geophys. Res.*, 73, 215, 1968.

- Rees, M. H., Note on the penetration of energetic electrons into the earth's atmosphere, *Planet. Space Sci.*, 12, 722, 1964.
- Rishbeth, H., On explaining the behavior of the ionospheric F region, *Rev. of Geophys.*, 6, 33, 1968.
- Rishbeth, H. and Garriott, O. W., Introduction to Ionospheric Physics, Academic Press, New York, 1969.
- Russell, C. T., Chappell, C. H., Montgomery, M. D., Neugebauer, M. and Scarf, F. L., 030 5 observations of the polar cusp on November 1, 1968, *J. Geophys. Res.*, 76, 6743, 1971.
- Sharp, G. W., Midlatitude trough in the night ionosphere, *J. Geophys. Res.*, 71, 1345, 1966.
- Solar Geophysical Data, CRPL-F 191, Part B, p. Va, July 1960, U.S. Department of Commerce, (Boulder, Colorado 80302).
- Solar Geophysical Data, Number 329, Part 1, pp. 8-9, January 1972, U.S. Department of Commerce, (Boulder, Colorado 80302).
- Stanley, G. M., Ground based studies of the F region in the vicinity of the midlatitude trough, *J. Geophys. Res.*, 71, 5067, 1966.
- Starkov, G. V. and Feldstein, Y. I., Scheme of an elementary disturbance in auroras on the dayside of the earth, *Geomag. and Aeron.*, (Eng. Trans.), 7, 294, 1967a.
- Starkov, G. V. and Feldstein, Y. I., Aurora during the IQSY period, *Geomag. and Aeron.*, (Eng. Trans.), 7, 608, 1967b.
- Starkov, G. V. and Feldstein, Y. I., The influence of the ring current on the position of the auroral oval, *Geomag. and Aeron.*, (Eng. Trans.), 8, 854, 1968.
- Stringer, W. J. and Belon, A. E., The morphology of the IQSY auroral oval. I, interpretation of isoauroral diagrams, *J. Geophys. Res.*, 72, 4415, 1967.
- Stringer, W. J., Belon, A. E. and Akasofu, S.-I., The latitude of auroral activity during periods of zero and very weak magnetic disturbance, *J. Atmos. Terr. Phys.*, 27, 1039, 1965.
- Sugiura, M. and Poros, D. J., Hourly values of Equatorial D_{st} for the years 1957 to 1970, NASA-GSFC X-645-71-278, 1971.
- Thomas, J. O. and Dufour, S. W., Electron density in the whistler medium, *Nature*, 206, 567, 1965.
- Thomas, J. O. and Andrews, M. K., The trans-polar exospheric plasma, 3: A unified picture, *Planet. Space Sci.*, 17, 433, 1969.

- Thomas, J. O., Rycroft, M. J., Colin, L. and Chan, K. L., The topside ionosphere, II. Experimental results from the Alouette I satellite, in Electron Density Profiles in Ionosphere and Exosphere, ed, J. Friihagen, p. 322, North-Holland, Amsterdam, 1966.
- Thomas, L. and Venables, F. H., The onset of the F-region disturbance at middle latitudes during magnetic storms, *J. Atmos. Terr. Phys.*, 28, 599, 1966.
- Tulunay, Y. and Soyars, J., Characteristics of the mid-latitude trough as determined by the electron density experiment on Ariel III, *J. Atmos. Terr. Phys.*, 33, 1737, 1971.
- Vestine, E. H., The geographic incidence of aurora and magnetic disturbance, Northern Hemisphere, *Terr. Magn. Atmos. Elec.*, 49, 77, 1944.
- Wagner, R. A., Private communication, Air Force Cambridge Research Laboratories, 1971.
- Wagner, R. A. and Pike, C. P., A discussion of arctic ionograms, paper presented at AGARD Technical Meeting, Lindau/Harz, Germany, September, 1971.
- Whalen, J. A., Auroral oval plotter and nomograph for determining corrected geomagnetic local time, latitude and longitude for high latitudes in the northern hemisphere, AFCRL Environmental Research Papers, No. 327, July 27, 1970.
- Whalen, J. A., Buchau, J. and Wagner, R. A., Airborne ionospheric and optical measurements of noontime aurora, *J. Atmos. Terr. Phys.*, 33, 661, 1971.
- Winningham, J. D. and Pike, C. P., In situ observations of the effects of magnetosheath particle precipitation on the dayside ionosphere, paper presented at AGU meeting, Washington, D.C., April, 1972.